Deformative Properties of Monotropic Plastic Foams with a Pronounced Strut-Like Structure

Doctoral (PhD) Thesis
in Mechanics of Solids

by
Ilze Beverte

Institute of Polymer Mechanics,
Latvian Academy of Sciences

Riga 1996

Ilze Beverte

Deformative Properties of Monotropic Plastic Foams with a Pronounced Strut-Like Structure

Vieglu, monotropu, izteikti stieņveidīgas struktūras putuplastu deformatīvās īpašības

Inženierzinātņu doktores disertācija,
specialitāte - cietvielu mehānika

Ilze Beverte

LZA Polimēru mehānikas institūts,

Rīga, 1996.gads

Deformative Properties of Monotropic Plastic Foams with a Pronounced Strut-Like Structure

Doctoral (PhD) Thesis
in Mechanics of Solids

by
Ilze Beverte

Institute of Polymer Mechanics,
Latvian Academy of Sciences

Riga 1996

Acknowledgements

- My greatest gratitude goes to Prof., *Dr.habil.sc.ing.* Andris Krēgers, the scientific supervisor of the research performed.

- I feel much obliged to *Dr.ing.h.c.* Aivars Lagzdiņš for valuable discussions and substantial remarks in the research phase.

- I wish to thank *Dipl.Phil.* Aivars Tarvids for proof-reading the English.

- I appreciate the technical help extended by Ms. Ināra Smala.

- The research has been supported by Grant 93/171 of the Science Council of Latvia.

Ilze Beverte

Kopsavilkums

Aplūkotā zinātniskā darba mērķis ir vieglu, monotropu (robežgadījumā izotropu) putuplastu ar izteiktu stieņveida struktūru deformatīvo īpašību matemātiskā modelēšana mazu deformāciju robežās. Deformatīvo īpašību integrālai raksturošanai putuplastiem kā mikroneviendabīgiem kompozītiem materiāliem to elastiskās simetrijas asīs ir noteiktas piecas neatkarīgās un septiņas atkarīgās efektīvās elastības konstantes.

Modelējot putuplastu uzbūvi, ir piedāvāts lokālais modelis, kas sastāv no nepārtrauktas vides modeļa spriegumu noteikšanai un lokālā struktūras modeļa. Lokālais struktūras modelis ir veidots kā elipsoidāla modeļšūna ar tās iekšpusē telpiski vienmērīgi izvietotiem polimēra stieņiem. Lai izvairītos no putuplastu struktūras mākslīgas regularizācijas, stieņu sistēma tiek grozīta kā viens vesels pa visām iespējamām telpiskajām orientācijām, kuras uzdod ar Eilera leņķiem. Tādā veidā iegūst putuplastu uzbūves mikrosituāciju kopu jeb ansambli, kas ļauj ievērot putuplastu uzbūves būtisko polidispersumu un stieņu bezgalīgi daudzās telpiskās orientācijas.

Lai aprēķinātu efektīvās elastības konstantes, kas saista vidējos spriegumus un deformācijas, ir pieņemts, ka realizējas ergodiskuma nosacījums. Līdz ar to ir iespējams nomainīt vidējošanu pa tilpumu ar vidējošanu pa ansambli.

Vienasīgas spiedes/stiepes matemātiskajos modeļos ir parādīta iespēja izmantot modeļšūnas pēcdeformācijas formas variāciju analīzi un deformācijas potenciālās enerģijas minimizāciju atbildes deformācijas noteikšanai. Sprieguma aprēķināšanai, sakarā ar precīza risinājuma trūkumu elipsoīdam, ir pierādīta iespēja aizvietot modeļšūnas elipsoidālo formu ar cilindrisku. Skaitlisko aprēķinu gaitā ir konstatēts, ka aprēķināmās modeļelipsoīda pusasis ir jāsaista ar saites nosacījumu. Ir parādīta vienasīgas spiedes/stiepes modeļu savstarpējā savietojamība.

Pakļaujot modeļšūnas virsmas punktus noteiktai telpiskai transformācijai, ir parādīta iespēja adekvāti modelēt putuplastu bīdes deformāciju. Ar skaitliskiem aprēķiniem pierādīta vienasīgās spiedes/stiepes un bīdes deformācijas modeļu savstarpējā savietojamība.

Ir izpētīta aprēķināto elastības konstanšu atkarība no galvenajiem putuplastu struktūras raksturlielumiem. Salīdzinot teorētiskos rezultātus ar eksperimentu datiem, ir konstatēta apmierinoša sakritība. Tas ļauj izmantot piedāvāto matemātisko modeli un izstrādāto programmu kompleksu, lai projektētu putuplastus ar iepriekš uzdotām deformatīvajām īpašībām.

Summary

Objective of the scientific investigation proposed is a mathematical modelling of deformative properties of light-weight, monotropic (or isotropic in the boundary case) plastic foams with a pronounced strut-like structure in the region of small deformations. For integral characteristics of deformative properties of plastic foams as micro-nonhomogeneous composite materials five independent and seven dependent effective elastic constants have been determined in the axes of elastic symmetry.

In order to model the plastic foams structure a local model consisting of two parts has been proposed, that is, a model of continuous medium and a local structure model. The latter has been chosen in the shape of a rotational ellipsoid as a model cell with polymeric struts distributed spatially randomly inside it. To avoid the artificial regularization of structure, the strut system has been turned as one whole throughout all the possible spatial orientations given by Euler's angles. Thus, a cluster or an ensemble of structure microsituations has been obtained permitting to take into account the essential polydispersity of foams structure and infinitely numerous orientations of struts in foams.

When effective constants connecting the average stresses and strains were calculated the ergodic condition was assumed to realize. Therefore, it was possible to replace the averaging throughout the volume with an averaging throughout the ensemble.

The possibility to use a variational analysis of model cells post-deformation form and a minimization of deformation potential energy as a criterion for determination of this post-deformation form has been shown in the mathematical models of uniaxial compression/tension. In order to calculate stresses the ellipsoidal model cell was replaced by a cylindric one, since there is no precise solution for ellipsoids known to the author. The necessity to connect the semiaxes to be calculated by some tie condition has been stated during the numerical calculations. The mutual compatibility of uniaxial compression/tension models was proved.

Subjecting points of the model cells surface to a spatial transformation of pure shear, the possibility to model plastic foams deformation in this way has been shown. With the help of numerical calculations the compatibility of shear model and models of uniaxial loading was proved.

The dependence of calculated elastic constants on the main characteristics of plastic foams has been examined. A satisfactory agreement was found to exist between the theoretical results and the experimental data. Hence, the mathematical model proposed and the calculation programmes elaborated can be used to project plastic foams with a preassigned set of properties.

Zusammenfassung

Das Ziel der vorliegenden wissenschaftlichen Arbeit ist mathematische Modellierung der Verformungseigenschaften von leichten monotropen (im Grenzfall isotropen) Schaumstoffen mit ausgeprägter Stabstruktur in den Grenzen von Kleinverformungen. Für Integralcharakteristik der Verformungseigenschaften sind für die Schaumstoffe als mikrounhomogene Kompositmaterialien in deren Elastizitäts Symmetrieachsen fünf unabhängige und sieben abhängige effektive Elastizitätskonstanten bestimmt.

Bei der Modellierung der Schaumstoffstruktur wird das Lokalmodell vorgeschlagen, das aus einem Modell des Kontinuums für Spannungsbestimmung und einem lokalen Strukturmodell besteht. Das Lokalstrukturmodell ist als eine ellipsoide Modellzelle mit räumlich gleichmäßig angeordneten Polymerstäben im Inneren der Zelle gebildet. Um künstliche Regulierung der Schaumstoffstruktur zu vermeiden, wird das Stabsystem als ein Ganzes in allen möglichen räumlichen Orientierungen gedreht, die mit Euler-Winkeln aufgegeben werden. In dieser Weise bekommt man die Gesamtheit bzw. das Ensemble der Mikrosituationen der Schaumstoffstruktur, und dies läßt die wesentliche Polydispersität der Schaumstoffstruktur und die unendlich vielen räumlichen Orientierungen der Stäbe in Betracht ziehen.

Für die Berechnung der effektiven Elastizitätskonstanten, die die Mittelspannungen und Verformungen verbinden, wird angenommen, daß sich die Bedingungen des Ergodens verwirklicht. Hiermit ist es möglich, die Mitteneinstellung im Rauminhalt durch Mitteneinstellung im Ensemble zu ersetzen.

In den matematischen einachsigen Druck/Zug-Modellen ist die Möglichkeit für die Ausnutzung der Variationsanalyse der Nachverformungsformen der Modellzelle und die Minimisierung der potentiellen Energie der Verformung als Kriterium für die Bestimmung der Gegenverformung gezeigt. Für Spannungsberechnung ist infolge des Mangels einer genauen Lösung für einen Ellipsoiden eine Möglichkeit gezeigt, die ellipsoide Form der Modellzelle durch eine zylindrische zu ersetzen. Auf Grund von Berechnungen hat man festgestellt, daß die zu berchnenden Halbachsen eines Modellellipsoiden mit der Bedingung der Bindung zu verbinden sind. Es ist die gegenseitige Vereinigung der einachsigen Druck/Zug-Modelle gezeigt.
Bei bestimmter räumlichen Transformation von Oberflächepunkten einer Modellzelle ist die Möglichkeit gezeigt, Verschiebungsverformung der Schaumstoffe adäquat zu modellieren. Auf Grund von Berechnungen ist die gegenseitige Vereinigung der einachsigen Druck/Zug- und Verschiebungsverformungsmodelle bewiesen worden.

Für die berechneten Elastizitätskonstanten ist deren Abhängigkeit von den wichtigsten Kennwerten der Schaumstoffstruktur erforscht. Beim Vergleich der teoretischen Ergebnisse mit Experimentalangaben ist eine befriedigende Übereinstimmung festgestellt worden. Dies läßt das angebotene matematische Modell und den ausgearbeiteten Programmkomplex ausnutzen, um Schaumstoffe mit vorher aufgegebenen Verformungseigenschaften zu projektieren.

Contents:

1 Properties, Application and Mathematical Modelling of Plastic Foams. (Literature Review)

1.1 Classification and Application of Plastic Foams

Plastic foams are multiphase cellular composite materials consisting of a polymeric matrix and a mobile, usually gaseous, phase. The progress made in the technology of producing plastic foams has enlarged considerably the application sphere of these materials, to mention but consumer goods and elements of cosmic appliances [36].

Cellular materials can be obtained almost from all polymers but only some of them are suitable for industrial use. Polyurethanes (PUR), polystyrenes and polyolefines have the greatest consumption rate [20,52]. Plastic foams can be classified differently: most frequently according to their mechanical characteristics or composition and morphological properties of cells.

In view of cellular structure the plastic foams fall into open- and closed-cell foams [2,13,52]. The open-cell plastic foams can be used as filters, amortization materials (in aircraft fuel reservoirs), etc. The closed-cell plastic foams can find their application in building and fuel industry, as well as machine-building, mainly as heat and hydroisolation materials because of their low thermal conductivity and low gas and liquid permeability. The roof of restaurant "Sēnīte" covered with plastic foam "Ripors" can be given as an example of an extensive usage of the material [2].

When considering physically-mechanical properties, the plastic foams can be divided into elastic, half rigid and rigid ones. The elastic foams are used in furniture industry, machine-building and consumer goods. The half rigid plastic foams have found wide application for foot-wear and car finishing (panels, buffers, etc.). Polystyrene foams widely used as a packing material can be mentioned as an example of employment of the rigid plastic foams. The rigid PUR plastic foams are used in aviation, house, railway carriage and machine building, as well as in refrigerators [36].

According to a relative quantity of the polymer per unit volume (the space filling coefficient $P1$) the plastic foams can be divided into following groups [26]:

1) heavy	$P1 \geq 40\ \%$
2) medium	$40\ \% > P1 \geq 15\ \%$
3) light weight ,	$P1 < 15\ \%$.

In the heavy weight plastic foams mutually unconnected gaseous bubbles are dispersed in the polymeric matrix. The light-weight plastic foams are formed by polymeric struts, knots, membranes and a gaseous phase. Elements of both kinds of the structure are found in the medium-weight foams [13,26]. Particular characteristics of each group of the materials can be used in practical applications.

Depending on the foaming process, isotropic, monotropic, orthotropic or completely anisotropic plastic foams can be manufactured [52]. The specific anisotropy of physically - mechanical properties is used in various applications: filtering, heat isolation, load-bearing structural elements etc. In machine building integral plastic foams are widely used. An external, slightly porous layer with a practically constant density changes gradually into an inner, highly porous layer of almost equally constant density. In manufacturing ship bodies and wind rotor blades sandwich composites of fibreglass plastics and plastic foams are used more and more frequently.

To increase elastic moduli, compression and shear strengths, heat resistance without substantial weight growth the plastic foams can be filled with glass fibres, sand, hollow glass spheres (syntactic foams) [52].

1.2 Plastic Foams with a Pronounced Strut-Like Structure

By varying components of the composition and foaming conditions, plastic foams having prevailingly an open or closed cell structure can be obtained. According to [13,52] elastic plastic foams most often have an open-cell structure, while in rigid plastic foams the structure is closed, although many exceptions are possible. In all kinds of the plastic foams the relative quantity of open cells increases, while foams density decreases. In rigid PUR foams two maxima are observed for volume fraction of open cells when volume fraction of gas (porosity) $P2$ is the following: $1.0 \leq P2 < 0.5$ [13].

A strut-like polyhedral structure is usually characteristic for the open-cell plastic foams (absolute poroplasts). The base polymer is concentrated in struts

and knots. There are no polymer membranes in these foams or they are so thin that their participation in deformation process can be neglected. Reticulated rigid PUR foams with low density ϱ_f and the corresponding space filling coefficient $P1$ can be mentioned as an example [20]:

$$\varrho_f \leq 200 \text{ kg/m}^3 \qquad P1 = \varrho/\varrho_{pol} = \leq 0.17$$

where ϱ_{pol} is density of the base polymer.
When $P1 < 0.15$ the lengthwise dimension l_0 of a strut exceeds the crosswise dimension t. The struts are straight or slightly curved, with a practically constant cross-section along the whole strut. For the PUR plastic foams the following relationship can be observed [20,52]:

$$\text{when} \quad P1 \leq 0.10 , \quad l_0/t \geq 1.5$$

When $P1 < 0.10$ $l_0/t > 1.5$ practically for all the open-cell plastic foams and the struts may be considered as slim ones. The shape of the struts cross-section can be well described by a hypocycloid with three return points [52]. It can be approximated by an equilateral triangle with side length t. Area F of the cross-section is approximately equal for all struts.

Four to six struts usually enter a knot in the plastic foams with a uniform structure (polyurethane plastic foams). More than six struts may enter the knot in plastic foams with irregular structure [4].

The distribution of struts throughout spatial directions is uniform in isotropic foams. An additional orientation of the struts parallel to rise direction can be observed in monotropic plastic foams [15].

Open-cell plastic foams can be obtained from the closed-cell ones with the help of chemical and physical methods (reticulation) [26]. The main methods of reticulation are: hydrolysis, oxidation, high and low pressure, treatment with heat, etc. Membranes are broken or leached in these processes. With reticulation the plastic foams having a strut-like structure, a very low density and low space filling coefficient can be obtained:

$$3 \text{ kg/m}^3 \leq \varrho_f \leq 10 \text{ kg/m}^3 , \quad 0.3 \ \% \leq P1 \leq 10 \ \% .$$

1.3 Deformative Properties of Plastic Foams with a Pronounced Strut-Like Structure (Experiments and Mathematical Investigations)

1.3.1 Experimental Investigations

One of the first experimental investigations on deformative properties of plastic foams has been reported by **A.N.Gent** and **A.G.Thomas** in 1959, [9]. Young's modulus and Poisson's coefficient were determined for isotropic natural rubber foams in a wide range of $P1$ ($0.093 \leq P1 \leq 0.568$). With $P1$ increasing, the Young's modulus increased, too, while Poisson's coefficient exhibited no systematic trend.

Investigating the scatter of mechanical properties (strength and space filling coefficient $P1$) **I.G.Romanenkov** [50] found it to be great for plastic foams. The coefficient of variation for samples cut out from one moulding reached $\approx 16\%$ This should be taken into consideration when choosing the number of samples for one point measurements.

J.A.Rinde [18] made a vast study on Poisson's effect for rigid plastic foams. The Poisson's coefficient for isotropic foams was found to be greater in tension than in compression. When anisotropic foams were considered, the Poisson's coefficient was the greatest when loading was parallel to the rise direction. A similar experimental result was obtained by **A.G.Dement'yev** et al. [32]. However, no systematic experiments have been made for the dependence of Poisson's coefficients on the degree of anisotropy A (Section 2.2) of plastic foams. The conclusions about the dependence of Poisson's coefficients on $P1$ are contradictory in various publications [18,19,32] both for isotropic and anisotropic plastic foams.

Generalizing a large number of experimental data of different isotropic plastic foams, **A.G.Dement'yev** [32] concludes that the Poisson's coefficient depends on space filling coefficient $P1$ ($0.05 \leq P1 \leq 0.80$):

$$\begin{aligned} P1 &\approx 0.05 \qquad \nu = \nu_{max} \approx 0.45 \\ P1 &\approx 0.10 \qquad \nu = \nu_{min} \approx 0.25 \ ; \\ P1 &\approx 0.80 \ , \qquad \nu \approx 0.30. \end{aligned}$$

To prove this conclusion convincingly experiments should be made for dependence $\nu = \nu(P1)$ by using samples of one and the same plastic foams.

Young's modulus, Poisson's coefficient and space filling coefficient $P1$ were determined for latex foams in [15] and for foamed polystyrene in [4]. Conclusions about mutual relationships of E, ν and $P1$ were the same as in [9]. Young's modulus, $P1$ and average cell size $\bar{d}$ were determined for PUR and other plastic foams by **K.C.Rusch** [19]:

$$\text{when } 0.028 \leq P1 \leq 0.24 \text{ , } 0.2 \text{ mm} \leq \bar{d} \leq 1.3 \text{ mm}$$

With $P1$ reducing, cell dimension are increasing.

A.G.Dement'yev [33,35] has determined stress-strain curves in tension and compression. These curves are essentially different for rigid and elastic plastic foams. Axial deformation, buckling, bending and crushing of struts were evaluated as the main deformation mechanisms of a single strut. Compression tests were made on samples whose transversal dimensions were comparable with the lengthwise ones. In tension tests the lengthwise dimensions exceeded the transversal ones by several times. In such conditions all struts of a foam sample were load-carrying elements.

Investigating anisotropic PUR foams **S.V.Kanakkanatt** [11] found the difference between moduli E_1 , E_2 and E_3 was more expressed in tension than in compression. Average dimensions of the cells were also determined, since it allows to evaluate the degree of anisotropy A and dependence of moduli E_1, E_2, E_3 on A.

An extensive investigation on slightly anisotropic, light-weight PUR and polyvinylchloride (PVC) foams ($P1 \leq 0.15$) was made by **R.Renz** [20]. Qualitative foam structure photographs taken with a scanning electron microscope reveal the structure of foams. Young's moduli E_1, E_2, E_3 , shear moduli G_{13}, G_{23}, G_{12} as well as their dependence on $P1$ were determined (investigations of other authors usually have no data on shear moduli). It was found that

$$\begin{array}{llll} E_1 \approx E_2 & & E_3 \geq E_1 \text{ , } E_2 \\ G_{13} \approx G_{23} & & G_{12} \geq G_{13} \quad G_{23} \end{array}$$

Stress-strain curves in compression, tension and shear were presented.

Young's modulus, Poisson's coefficient and density were determined for PUR and PVC base polymers. These data are of great importance for a further theoretical treatment. However, no Poisson's coefficients of foams themselves as well as degree of anisotropy A were determined.

Of great practical interest are the rarely found experimental data on the relationship $E_3/E_1 = f(A)$, [52]. This relationship was investigated in compression and tension for elastic PUR foams. The same conclusion as in [11] was made: anisotropy of deformative properties is more pronounced in tension than in compression even for small deformations. Measurements of average cell diameters $\bar{d}$ in [52] provided the following range:

$$\text{when } P1 \leq 0.05 \qquad 0.01 \leq \bar{d} \leq 2.5 \text{ mm}$$

F.A.Shutov in [13] reported the existence of microcells in rigid phenolic as well as polyurethane foams. Microcells were found to be about two or three orders smaller than macrocells.

K.Cīrule [53] determined average dimensions of struts, average degree of anisotropy A and $P1$ for samples of rigid PUR foams. PUR foams with A up to $A \approx 3$ were examined. When $P1 \approx 0.03$ the length of struts exceeded their side length up to five times.

V.P.Valuiskikh and **S.A.Mavrina** [27,28,29,47] have vastly investigated the dependence of deformative and strength properties on the variational coefficient of struts dimensions. A conclusion was made that the Young's modulus and the strength could be increased several times by achieving the regularity of struts length (a reduction of the variational coefficient). A method was proposed permitting to determine the statistical characteristics of struts grid using the grids projections on coordinate planes. However, the moduli E_1, E_2, E_3 of anisotropic foams ($A \leq 1.7$) were assumed to be equal: $E_1 = E_2 = E_3 = E$. No examination of relationship $E_{1,2,3}$ $f(A)$ was made (the anisotropic foams were assumed to be quasiisotropic).

1.3.2 Empiric Relationships

The dependence of deformation mechanism on geometric parameters of cellular structure is complicated. Some knowledge about this dependence in compression can be acquired expressing the compressive stress σ as a product of compressive strain ε Young's modulus E and a function of inelastic processes $F(\varepsilon)$ (**K.C.Rusch [19]**):

$$\sigma = E\,\varepsilon\,F(\varepsilon)$$

Function $F(\varepsilon)$ can be determined empirically from stress - strain curves as well as related to deformation of a single strut [9,10]. $F(\varepsilon)$ depends greatly on geometry of cellular structure, and it is practically independent of E_0 . The dependence on $P1$ and cells dimensions is inconsiderable [19,52].

The classical expressions

$$E = K\,\varrho_f^n \qquad E = E_0\,P1^m \tag{1.1}$$

connecting deformative properties of foams with their density and $P1$ are still widely used [3,52]. Constants K , n and m are determined from experiments. It was proved that expressions in the form of Eq.(1.1) are valid in compression and tension as well as for strength properties.

Empiric constants have been used in other theoretical investigations as well. For example, in [9,15] a coefficient k is introduced denoting the fraction of knot surface covered by cross-sections of struts. The coefficient k should be determined experimentally.

1.3.3 Model Cells Shaped as Geometric Figures

The cellular structure of plastic foams can be modelled by various geometric figures. Only five of them (a cube, a hexagonal prism, a rhombic

dodecahedron, a tetragonal pillar and a cubooctahedron) can fill the space densely, without holes. Although very simple model cells shaped as geometric figures reveal the main features of deformation of structural elements.

A.N.Gent and **A.G.Thomas** [10] modelled isotropic plastic foams with a cubical grid of polymeric struts. Intersections of the struts formed undeformable knots. The struts were considered to be subjected to axial loading. Using a cubic cell, the space filling coefficient $P1$ and Young's modulus E were determined as functions of struts dimensions and E_0.

W.L.Ko [12] has proposed another kind of struts grid to study the deformative properties of open-cell elastic plastic foams. This grid was formed when the base polymer fills the holes between the closest packing of uniform spheres. Hexagonal and body centered cubic closest packings were considered. The author proved that a part of grid distinguished by a hexagonal prism could be used as a representative model cell. Struts were considered to be under combined axial, bending and shear loading. After several simplifications Poisson's coefficient ν and relative Young's modulus E/E_0 were calculated for both kinds of sphere packing.

R.Chan and **M.Nakamura** [7] proposed a space-unfilling figure: a pentagondodecahedron as a model cell. An expression for the Young's modulus of open-cell plastic foams was derived from a differential equation of struts bending for a small deflection. Initial curvature of a strut was taken into account.

In a series of investigations [31...37] **A.G.Dement'yev** used a cubooctahedron as a model cell. The shape of this figure was similar to that observed in experiments. The struts were assumed to be subjected to axial as well as transversal bending. This assumption was used in analysis of both the small and large deformations. Stress-strain curves in compression, the Young's modulus and Poisson's coefficient ν_{31} were derived from a differential equation of struts bending. It was concluded that the deformative and strength properties were independent of cell dimensions.

Although methods of orientational averaging were mainly proposed by **J.M.Lederman** in [15], the model cell shaped as a sphere was used in some stages of this investigation, too. This permits to relate deformation of a single strut to deformation of the whole material.

S.V.Kanakkanatt [11] described a model cell shaped as a parallelepiped in order to calculate the Young's modulus parallel and perpendicular to the rise direction. Small compression and small tension deformations were considered separately.

R.Renz [20] applied the method of finite elements to the model cell shaped as a cubooctahedron. Calculations were performed for one eighth of the cubooctahedron in view of its symmetry properties. The Young's modulus and Poisson's coefficients were calculated both for the closed - and open cell foams.

In order to analyse mechanical properties of light-weight plastic foams with oval microcells in a polymeric frame **A.G.Dement'yev** [37] proposed a multistage method. A cube was used for description of microcells and a pentagondodecahedron for macrocells. As a result Pl , E/E_0 and the compression strength were calculated.

In investigations of **V.P.Valuiskikh** and **S.A.Mavrina** [27,28,29,47] a stochastic simulation model was proposed as a new approach to the theoretical treatment of plastic foams. However, numerical calculations in this case could be realized only for a small number of struts. Therefore, a combined imitating model was elaborated. It consisted of regular cubooctahedrons whose structural elements were given to random deviations. In such a case advantages of geometrically determined and stochastic simulation models could be joined avoiding problems in numerical calculations.

1.3.4 Mathematical Models Based on Methods of Orientational Averaging

One of the first theoretical investigations of plastic foams by **A.N.Gent** and **A.G.Thomas** [9] was based on orientational averaging and comprised all the main assumptions of this method. The combined strut knot element deformed according to the global deformation of the specimen. The struts were distributed randomly in space. The orientational averaging of deformation energy of a single strut was used to calculate the deformative properties of the whole composite.

A.Cunningham [8] used an orientated composite structural unit consisting of a gaseous matrix and a polymeric strut as reinforcement.

Assuming a continuity of strain to exist from one strut to the next the Voigt averaged foam stiffness and compliance were calculated. Their relationship to the basic structural unit properties were found by standard fourth rank tensor transformations involving the orientation distribution function of structural units.

Small as well as large deformations of elastic foams were considered by **J.M.Lederman** in [15]. The model proposed consisted of struts of any orientation in an undeformed material. During elongation, the struts stretched and oriented in the direction of stretching. Relating the deformation of a strut to global deformation of the bulk material, stress-strain equations were derived by means of orientational averaging of the tensile stress in a strut element. As a special case the Young's modulus and the Poisson's coefficient for isotropic foams were calculated. The model predicted that a cell structure orientation parallel to the rise direction was a reasonable method for achieving a desired modulus without altering the density.

A.Zilaucs and **A.Lagzdiņš** [38] proposed a one-strut model to describe large deformations of elastic foams. Till now it is one of the most extensive investigations in methods of orientational averaging applied to plastic foams. Deformation of a strut - knot element was assumed to be equal to average deformation of foams in direction of the strut. The stress in a single strut under large deformations was calculated. Further, considering plastic foams as a continuous medium, its deformation was defined by a linear nondegenerated transformation T. Redistribution of struts in result of deformation T was taken into account. Tensor of macrostresses σ_{ij} was found by averaging the stress in a single strut element over all the possible spatial orientations. Uniform three dimensional tension and compression, simple uniaxial tension/compression, pure tension/compression and simple/pure shear were considered as particular cases of deformation T. When foams were isotropic the one-strut model provided the Young's modulus and Poisson's coefficient as follows

$$E = 1/6\ (1 - P2)\ E_0\ ,\quad \nu = 0.25$$

where porosity $P2 = 1 - P1$. These relationships are characteristic for all the theoretical treatments using the methods of spatial averaging.

1.3.5 Stochastic Simulation Models

A new theoretical approach to modelling the structure and deformation of plastic foams was proposed in [27,28,29,47] by **V.P.Valuiskikh** and **S.A.Mavrina**. These are stochastic simulation models taking into account the essential polydispersity of foams structure. *N* points are distributed randomly in a parallelepiped imitating the foams sample. This distribution is performed in such a way that the average length of struts and variational coefficient of struts lengths equal to those found in foams. Models of centres and knots were proposed. The calculations of these models were very time-consuming because of their combinatoric character. Therefore, a combined simulation model was introduced. It consisted of regular model cells shaped as cubooctahedrons. The knots of these cells were assigned to random deviations.Thus a model of plastic foams consisting of an ensemble of structural elements was obtained.

Stress - strain curves were calculated with the finite element method. It was proved that rising the regularity of struts length made it possible to improve considerably deformative as well as elastic properties of foams without changing their density. The calculations showed that the mechanical properties of foams depended not only on the average length of structural elements but also on the variational coefficient of these lengths.

1.4 Objective and Problems of the Investigation

Advances in plastic foams production are made above all by progress in the practical technology that demands a great consumption of materials and considerable funding. Therefore, theoretical investigations permitting to project the plastic foams with a prescribed set of properties are of particular importance.

In the result of literature analysis **the following situation can be found to exist** in the mathematical modelling of deformative and structural properties of plastic foams with a strut-like structure.

1. The deformative properties of isotropic plastic foams have been investigated rather well by choosing some geometrically regular strut system as a model cell. The Young's modulus and the Poisson's coefficient were calculated, as well as their dependence on the space filling coefficient was investigated. Yet only separate elastic constants were determined for monotropic plastic foams. Stress - strain relationships for both the isotropic and the monotropic foams were characterized in uniaxial tension/compression. The models, however, did not reflect the essential polydispersity of the plastic foams structure and infinitely numerous spatial orientations of struts. The structure was artificially regularized. The shear deformations have not been considered at all. No complete set of elastic constants has been derived for the monotropic plastic foams.

2. Infinitely numerous spatial orientations of struts have been taken into account in mathematical models by using the methods of spatial averaging. However, all the struts were assumed to have the same length, and therefore no polydispersity of the foams was considered. One-type situations of the ensemble were formed by a single strut or a strut gas element. In result, the geometry of strut connection in the knot has been neglected. Stress - strain relationships have been determined for several types of deformation. The numerical values of elastic constants have been neither calculated, nor compared with experimental data.

3. Stochastic simulation models have taken into account the polydispersity of foams structure and the infinitely numerous spatial orientations of struts. The numerical calculations became too complicated due to a great execution time of standard PC programme. Consequently, model cells with completely stochastic characteristics were replaced by partially regular ones. According to these models some separate elastic constants have been derived. No complete set of elastic constants of monotropic plastic foams has been calculated.

4. In experimental investigations elastic properties of foam samples have practically never been determined together with all essential structural

characteristics, which made it difficult to use these experimental data for elaborating theoretical investigations.

In view of all this, objective of the investigation presented is to elaborate a mathematical model as well as the corresponding numerical calculation methods for describing and predicting the deformative properties of monotropic/isotropic plastic foams with a pronounced strut-like structure in dependence of the plastic foams structure and polymeric phase properties.

In order to realize this objective **the following problems should be treated:**

1. Elaboration of a local structure model cell of monotropic/isotropic plastic foams and an ensemble of structural elements considering the essential polydispersity of plastic foams structure.

2. Modelling the uniaxial compression/tension deformation parallel and perpendicular to rise direction, as well as the shear deformation. Testing the minimum of deformation energy as the criterion for finding the post-deformation form of the model cell.

3. Elaboration of mathematical models for calculating five independent and seven dependent , altogether twelve, effective elastic constants. Application of the orientational averaging method for calculating the plastic foams effective deformative properties.

4. Working out the numerical calculation procedures for evaluating and predicting the dependence of deformative properties on the plastic foams structure and properties of the polymeric phase.

The investigation proposed **has been presented in the following chapters:**

Chapter 1. Urgency of the investigation is motivated. A plastic foams group with a strut-like structure is outlined in order to subject it to a

further theoretical treatment. The present situation in theoretical and experimental studies is characterized according to the literature analysis. The objective and problems of the investigation are generally formulated.

Chapter 2 describes the proposed mathematical model of deformation and structure of monotropic plastic foams. The choice of independent effective elastic constants to be calculated is specified in the axis of elastic symmetry. The replacement of averaging physical quantities throughout the volume with an averaging throughout the ensemble is justified in calculations of integral characteristics of plastic foams.

Calculation of the corresponding elastic constants for the compression/tension deformation parallel to rise direction, and assumption of the semiaxes hypothesis are discussed in **Chapter 3.** The possibility to use a minimum of potential deformation energy as the criterion to calculate a post - deformation form of the model cell is demonstrated.

Two types of deformation of struts, as well as the finding of average stresses in the model cell are described. Methods of numerical calculations and inaccuracies of results are characterized.

Deformation of the model cell under compression/tension parallel to rise direction and the assumption of the volume deformation hypothesis are presented in **Chapter 4.** Analysis of numerical results permits to conclude that both mathematical models (Chapters 3 and 4) are fully compatible.

Chapter 5 deals with deformative properties in compression/tension applied perpendicular to rise direction. Necessity to use the hypothesis of volume deformation as well as the hypothesis of a linear relationship between the volume deformation and the degree of anisotropy is motivated. Analysis of Poisson's coefficients numerical values shows a mutual compatibility of all the three mathematical models of uniaxial compression/tension (Chapters 3, 4 and 5).

Shear in the plane perpendicular to the plane of isotropy is considered in **Chapter 6.** Unlike cases of uniaxial compression/tension, the

post - deformation form of the model cell is defined by spatial transformation uniquely because of the lack of an appropriate deformation energy minimization criterion.

Comparison of numerical results permits to check a mutual compatibility of mathematical models of shear and compression/tension deformations. Consequently, the calculation of independent constants has been completed.

In **Chapter 7** dependent elastic constants are derived using results of the previous calculations. Comparing the theoretical results with experimental data permits to evaluate both types of struts deformation.

Chapter 8 gives main conclusions.

2 Mathematical Model of the Structure and Deformation of Monotropic Plastic Foams

2.1 Elastic Constants

As regards deformative properties the free-rise plastic foams are monotropic (isotropic in the boundary case) materials with the isotropy plane perpendicular to the rise direction (Fig.2.1).

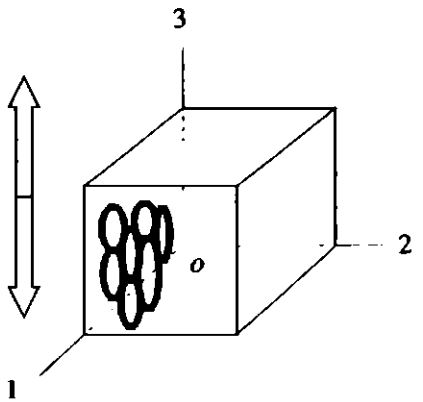

Fig.2.1
Monotropic plastic foams.

$o12$ is the plane of isotropy;
$o3$ is the rise direction.

An elastic potential of the monotropic plastic foams w can be expressed as follows [6,43]:

$$w = w(\sigma_{33}, \sigma_{11} + \sigma_{22}, \sigma_{31}^2 + \sigma_{23}^2, \sigma_{11}\sigma_{22} - \sigma_{12}^2, I_{3\sigma})$$

Within limits of the linear elasticity theory and by neglecting the cubic invariant $I_{3\sigma}$ the elastic potential can be expressed as a quadratic form of stresses:

$$w = C_1\sigma_{33}^2 + C_2(\sigma_{11} + \sigma_{22})^2 + C_3\sigma_{33}(\sigma_{11} + \sigma_{22}) +$$

$$+ C_4(\sigma_{31}\sigma_{13} + \sigma_{23}\sigma_{32}) + C_5(\sigma_{11}\sigma_{22} - \sigma_{12}\sigma_{21}) , \qquad (2.1)$$

where $C_{1,2,\ldots,5}$ are constants.

Strains in the elastic material are connected with the elastic potential in the following manner:

$$\varepsilon_{ij} \quad \frac{1}{2} \left[\frac{\partial w}{\partial \sigma_{ij}} + \frac{\partial w}{\partial \sigma_{ji}} \right] \tag{2.2}$$

Therefore: $\varepsilon_{ij} = \varepsilon_{ij} (\sigma_{kl}, C_m)$, where $i,j,k,l = 1,2,3$
$m = 1,2,\ldots,5$

Expressions (2.1) and (2.2) result in

$$\begin{aligned}
\varepsilon_{11} &= 2C_2\sigma_{11} + (2C_2 + C_5)\sigma_{22} + C_3\sigma_{33} \\
\varepsilon_{22} &= (2C_2 + C_5)\sigma_{11} + 2C_2\sigma_{22} + C_3\sigma_{33} \\
\varepsilon_{33} &= C_3\sigma_{11} + C_3\sigma_{22} + 2C_1\sigma_{33} \\
\varepsilon_{23} &= C_4\,\sigma_{23}\,; \\
\varepsilon_{13} &= C_4\,\sigma_{13} \\
\varepsilon_{12} &= -C_5\,\sigma_{12} \\
\varepsilon_{32} &= \varepsilon_{23} \qquad \varepsilon_{31} = \varepsilon_{13} \qquad \varepsilon_{21} = \varepsilon_{12}
\end{aligned} \tag{2.3}$$

The monotropic materials can be characterized by 12 elastic constants; five of them independent [45,49]. Evaluating the possibilities to elaborate mathematical models for calculation of constants, the following technical constants are chosen as independent:

$$\nu_{21} \quad \nu_{23} \quad \nu_{31} \quad E_3 \quad G_{13}$$

Here and further in Poisson's coefficients the first (stress) index corresponds to the loading direction, while the second (deformation) one denotes the direction, in which the transversal deformation is measured.

For a better outline of relationships between the elastic constants, the Hooke's law for orthotropic materials is used. These materials are also characterized by 12 constants (nine of them independent), but the level of symmetry is lower than that of monotropic materials [49]:

$$\varepsilon_{11} \quad \frac{1}{E_1}\sigma_{11} \quad \frac{\nu_{21}}{E_2}\sigma_{22} \quad \frac{\nu_{31}}{E_3}\sigma_{33};$$

$$\varepsilon_{22} \quad \frac{\nu_{12}}{E_1}\sigma_{11} + \frac{1}{E_2}\sigma_{22} - \frac{\nu_{32}}{E_3}\sigma_{33};$$

$$\varepsilon_{33} \quad \frac{\nu_{13}}{E_1}\sigma_{11} \quad \frac{\nu_{23}}{E_2}\sigma_{22} + \frac{1}{E_3}\sigma_{33};$$

$$\varepsilon_{23} = \frac{1}{2}\frac{1}{G_{23}}\sigma_{23} \qquad (2.4)$$

$$\varepsilon_{13} \quad \frac{1}{2}\frac{1}{G_{13}}\sigma_{13}$$

$$\varepsilon_{12} \quad \frac{1}{2}\frac{1}{G_{12}}\sigma_{12}$$

$$\varepsilon_{32} \quad \varepsilon_{23} \quad \varepsilon_{31} \quad \varepsilon_{13} \quad \varepsilon_{21} \quad \varepsilon_{12}$$

By comparing the coefficients at equal stresses in systems (2.3) and (2.4), mutual relationships between technical constants are found, expressing them with five independent ones:

$$\nu_{12} = \nu_{21} \quad \nu_{13} = \nu_{23} \quad \nu_{32} = \nu_{31}$$

$$E_1 = E_2 \quad \frac{\nu_{23}}{\nu_{31}} E_3 \qquad (2.5)$$

$$G_{23} = G_{13} \quad G_{12} = \frac{\nu_{23}}{2\nu_{31}(1 + \nu_{21})} E_3$$

In the boundary case, when isotropic plastic foams are considered, ν and E are chosen as two independent constants. The third one can be expressed as follows: $G = E / [\,2\,(1 + \nu)]$

Microscopical observations and photographs show that the plastic foams are microscopically nonhomogeneous composite materials [20,26,52].

Since the aim of the present research is to characterize the plastic foams as integral materials, an introduction of effective elastic constants is necessary. The tensor of effective elastic constants $\mathbf{C}^*$ characterizes deformative properties of a nonhomogeneous material as an integral one. It connects stresses and strains averaged throughout the material [54]:

$$< \sigma > = \mathbf{C}^* < \varepsilon >$$

The ergodic hypothesis is assumed to be valid in further calculations. This permits to replace an averaging of physical quantities throughout the volume of material with an averaging throughout a cluster of one-type situations (an ensemble). The ensemble is presented by a local model of the plastic foams which undergoes all the possible structural microsituations according to relationships (2.6) defined further. We shall neglect however, the interconnection of separate model cells of ensemble.

Consequently, it is necessary to determine the following effective technical constants of the monotropic plastic foams:

$$\nu_{21}^* \qquad \nu_{23}^* \qquad \nu_{31}^* \qquad E_3^* \qquad G_{13}^*$$

2.2 Local Model

In order to obtain an ensemble of microsituations of plastic foams structure, a local model is proposed. Model cell is chosen to be in the form of a rotational ellipsoid [23,24], Fig.2.2. An extension degree $A = c_0 / a_0$ of the model cell is equal to the average extension degree of ellipsoidal gaseous incorporations in the plastic foams:

$$A \approx \bar{d}_3 / \bar{d}_1 = \bar{d}_3 / \bar{d}_2$$

where $\bar{d}_1$ $\bar{d}_2$, $\bar{d}_3$ are average values of projections D_1 D_2, D_3 of ellipsoidal incorporation axes d_1 d_2 d_3 on the measuring plane [52]. Monotropy of plastic foams is directly related to A.

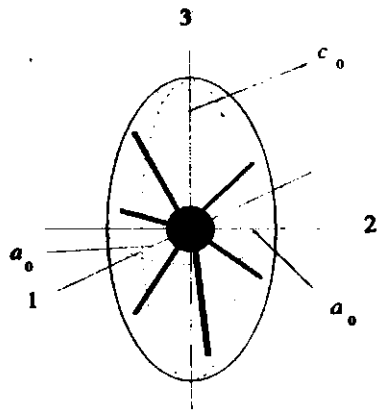

Fig.2.2
A local structure model of monotropic plastic foams.

a_0 , c_0 are semiaxes of an ellipsoidal model cell with a strut system and a knot situated inside.

The mass of base polymer comprised in the model cell is denoted by m_{pol}. The model cell is treated both as a model of continuous media and as that of local structure.

In order to define stresses in the corresponding point of plastic foams, the foams in the model cell are regarded as a continuous monotropic medium. The monotropy axis of this medium is parallel to the longer semiaxis c_0 of the model cell. Density of the plastic foams to be modelled is ascribed to the continuous medium:

$$\varrho_f = m_{pol} / V_{mc} \qquad V_{mc} = 4/3\pi\, a_0^2 c_0$$

where V_{mc} is volume of the model cell.

A local structure model cell is obtained by cutting out a rotational ellipsoid (or a sphere when isotropic plastic foams are considered) around a polymeric knot so that a half of each strut entering the knot would belong to the model cell. *For the sake of simplicity here and further the half-struts are referred to as struts , except for calculations of the strut stability (3.24), where the whole length of the strut is essential.* Space filling coefficient $P1$ of the plastic foams

$$P1 = \varrho_f / \varrho_{pol} = m_{pol} / (V_{mc}\, \varrho_{pol})$$

is ascribed to the model cell.

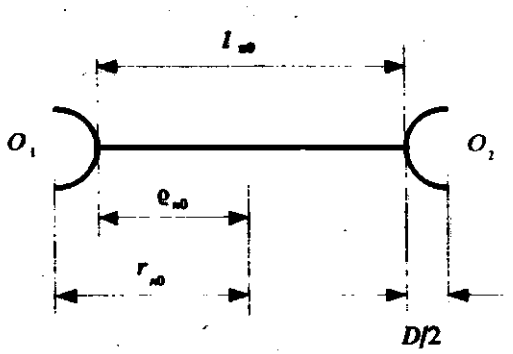

Fig.2.3
Dimensions of structural elements of the model cell before and after deformation.

l_{n0} , l_n are lengths of the n-th strut;
ϱ_{n0} , ϱ_n are lengths of the n-th half- strut;
r_{n0} , r_n are lengths of the n-th radiusvector directed along the n-th half-strut;
D is diameter of the knot.

The following relationships exist between the dimensions of structural elements

$$l_{n0} = 2\,\varrho_{n0}\,; \quad l_n = 2\,\varrho_n;$$

$$r_{n0} = \varrho_{n0} + D/2\,; \quad r_n = \varrho_n + D/2.$$

Since the spatial distribution of struts in isotropic plastic foams is uniform, a uniform distribution of N struts entering a knot in the local structure model cell has to be known. It is found by minimizing the aim function Φ constructed in the following way [23]:

$$\Phi = \sum_{i=1}^{N} \sum_{j=i+1}^{N} L_{ij}^{-2}$$

where L_{ij} is a distance between crossing points of i-th and j-th struts with the surface of unity sphere. The function Φ reaches its minimum when the

spatial distribution of N struts is uniform. Orientation of the n-th strut is defined by spherical coordinates φ_{n0}, θ_{n0} in the $o\xi\eta\tau$ frame of reference, connected with N struts system. Then the function Φ can be expressed as follows:

$$\Phi = \sum_{i=1}^{N} \sum_{j=i+1}^{N} [\, 2(1 - \sin\theta_{i0}\sin\theta_{j0}\cos\varphi_{i0}\cos\varphi_{j0} + \\ + \sin\theta_{i0}\sin\theta_{j0}\sin\varphi_{i0}\sin\varphi_{j0} + \cos\theta_{i0}\cos\theta_{j0}) \,]^{-2}$$

where $\varphi_{n0}, \theta_{n0}$ are the sought angles.

The aim function is minimized by using the steepest descent method for the following numbers of struts: $N = 2,3,\ldots,14$. It is clear that $N = 2,3$ struts uniformly distributed in space do not form a spatial configuration and therefore cannot represent adequately the deformation of plastic foams. In the plastic foams, knots with $N = 2,3$ entering struts are found only as separate defects, not as common structural elements. Knots with the smallest and most frequently met N are those with $N \quad 4$, and after minimization the respective strut configuration will be spatial. Accordingly, $N = 4$ is assumed to be the lower boundary of strut number N investigated in further calculations. The upper boundary of N - range is determined from stabilizing the dependence "effective moduli - strut number N" when N increases and the law of "great numbers" starts operating.

The stabilization begins at $N > 9$, therefore $N = 10$ is the greatest number of struts used in calculations. The results of $\varphi_{n0}, \theta_{n0}$ calculations are summarized in Table 2.1.

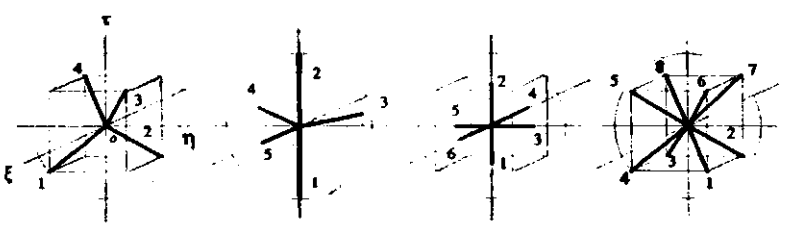

Fig.2.4 Spatial configurations of $N = 4,5,6,8$ struts in the body frame of reference $o\xi\eta\tau$.

Table 2.1 Spherical coordinates of N struts uniformly distributed in space.

Number of struts N	Spher. coord. $\theta_{n0};\varphi_{n0}$, rad	Order number n of a strut, $n = 1,2,\ldots,N$									
		$n = 1$	$n = 2$	$n = 3$	$n = 4$	$n = 5$	$n = 6$	$n = 7$	$n = 8$	$n = 9$	$n = 10$
4	θ_{n0};	2.186	2.186	0.955	0.955						
	φ_{n0}	5.498	2.356	0.785	3.927						
5	θ_{n0};	3.142	0.000	1.571	1.571	1.571					
	φ_{n0}	1.000	1.000	2.094	4.189	0.000					
6	θ_{n0};	3.142	0.000	1.571	1.571	1.571	1.571				
	φ_{n0}	1.000	1.000	1.571	3.142	4.712	0.000				
7	θ_{n0};	2.503	1.018	2.104	0.970	2.136	0.710	1.571			
	φ_{n0}	1.043	1.525	2.823	3.404	4.679	5.202	6.283			
8	θ_{n0};	2.186	2.186	2.186	2.186	0.955	0.955	0.955	0.955		
	φ_{n0}	0.785	2.356	3.927	5.498	5.498	0.785	2.356	3.927		
9	θ_{n0};	0.499	1.647	2.143	0.961	1.886	0.779	1.859	2.859	1.571	
	φ_{n0}	0.702	1.293	2.472	2.724	3.800	4.537	5.102	6.435	6.283	
10	θ_{n0};	0.905	2.040	0.417	1.473	2.452	1.430	1.899	0.833	2.685	1.571
	φ_{n0}	1.032	1.337	3.061	2.397	3.138	3.774	4.840	5.294	6.058	6.283

Spatial configurations for those N which make it possible to form an obvious drawing: $N = 4,5,6$ and 8, are depicted in Fig.2.4. When $N = 4,6$ and 8, the configurations found in the result of minimization are equal to those found with geometric considerations and using the symmetry properties of a cube.

It must be taken into account that the struts may occupy any spatial orientation in the isotropic plastic foams. Therefore, the system of N struts uniformly distributed in the model cell as one whole is turned around the initial point o of the laboratory frame of reference $o123$. In the process of turning, the strut system goes throughout all possible spatial orientations defined by the Euler's angles θ_E, φ_E, ψ_E. Thus, a cluster or an ensemble of one-type situations is obtained. With the following transformation matrix g_{lm} [39]:

$$g_{lm} = \begin{vmatrix} \cos\psi_E\cos\varphi_E - \sin\psi_E\sin\varphi_E\cos\theta_E & -\cos\psi_E\sin\varphi_E - \sin\psi_E\cos\varphi_E\cos\theta_E & \sin\psi_E\sin\theta_E \\ \sin\psi_E\cos\varphi_E + \cos\varphi_E\sin\varphi_E\cos\theta_E & -\sin\psi_E\sin\varphi_E + \cos\psi_E\cos\varphi_E\cos\theta_E & \cos\psi_E\sin\theta_E \\ \sin\varphi_E\sin\theta_E & \cos\varphi_E\sin\theta_E & \cos\theta_E \end{vmatrix}$$

where $l,m = 1,2,3$, new spherical coordinates θ_E, φ_E of the n - th strut in $o123$ frame of reference in every microsituation θ_E, φ_E, ψ_E can be found [25]:

$$\theta_n = \arccos [\, \sin\theta_{n0}\sin\theta_E\sin(\varphi_{n0} + \varphi_E) + \cos\theta_{n0}\cos\theta_E \,]$$

$$\sin\varphi_n = (\, \sin\theta_{n0}\cos\varphi_{n0}\, g_{21} + \sin\theta_{n0}\sin\varphi_{n0}\, g_{22} + \cos\theta_{n0}\, g_{23} \,) / \sin\theta_n \qquad (2.6)$$

$$\cos\varphi_n = (\, \sin\theta_{n0}\cos\varphi_{n0}\, g_{11} + \sin\theta_{n0}\sin\varphi_{n0}\, g_{12} + \cos\theta_{n0}\, g_{13} \,) / \sin\theta_n ,$$

where $n = 1,2,\ldots,N$.

In order to model a nonuniform distribution of the struts observed in the monotropic plastic foams it is assumed that the distribution in question develops gradually out of the uniform distribution observed in isotropic plastic foams. When a chemical compound is foamed in a high and narrow vessel, an additional orientation in the rise direction appears in the uniform distribution of struts (defined by a random distribution of gas bubbles). A model cell of the monotropic plastic foams is obtained from the model cell of isotropic plastic foams by the following space transformation (transversal dimensions of the model cell are assumed to remain constant):

$$x_1' = x_1 \qquad x_2' = x_2 \; ; \quad x_3' = Ax_3 \; ; \quad A = c_0/a_0 \tag{2.7}$$

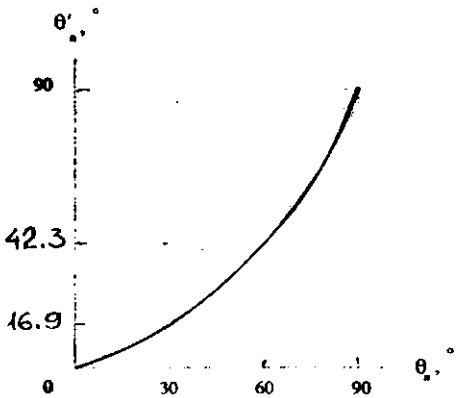

Fig.2.5 Change (2.8) of the spherical coordinate $0 \le \theta_n < \pi/2$ of uniformly distributed struts when monotropy is introduced by the transformation (2.7) (the calculations are carried out for θ_n values after every ten degrees). $A = 1.9$.

After an introduction of monotropy by Eq.(2.7), spherical coordinates of the n-th strut become as follows (Fig.2.5):

$$\begin{aligned} &\theta_n && arctg\,(A^{-1}\,tg\theta_n) && 0 \le \theta_n < \pi/2 \\ &\theta_n' && \theta_n && \theta_n = \pi/2 \\ &\theta_n' = \pi - && arctg\,[A^{-1}\,tg(\pi - \theta_n)] && \pi/2 < \theta_n \le \pi \; ; \end{aligned} \tag{2.8}$$

$$\varphi_n' = \varphi_n = \text{const.}\,, \qquad n = 1,2,\ldots,N\,.$$

From (2.6), (2.8) it can be concluded that

$$\theta_n' = \theta_n'(\varphi_E, \theta_E) ;$$

$$\varphi_n' \equiv \varphi_n = \varphi_n(\theta_E, \varphi_E, \psi_E)$$

Transformation (2.7) changes the spherical model cell of the isotropic plastic foams with radius a_0 into a model cell of anisotropic plastic foams in the form of a rotational ellipsoid with semiaxes a_0 , c_0

In order to characterize every microsituation of the ensemble, expressions (2.6) comprising all the three Euler's angles are used. Therefore, an averaging of physical quantities is made in the following manner [44,54]:

$$< \sigma > = \frac{1}{8\pi^2} \int_0^{2\pi} \int_0^{2\pi} \int_0^{\pi} \sigma(\theta_E, \varphi_E, \psi_E)\, f(\theta_E, \varphi_E, \psi_E) \times$$

$$\times \sin\theta_E \, d\theta_E d\varphi_E d\psi_E . \qquad (2.9)$$

Integral plastic foams (having foamed inner core which changes gradually into solid base polymer in the outer layer of a foams sample) are left unconsidered, so the texture function becomes the following:

$$f(\theta_E, \varphi_E, \psi_E) = 1 .$$

2.3 Dimensions of Structural Elements in Model Cell of Local Structure

Volume of the model cell of local structure V_{mc} and volume of the polymer in this model cell V_{pol} are the following:

$$V_{mc} = 4/3\ \pi a_0^2 c_0 \qquad V_{pol} = P1\ V_{mc}.$$

Effective constants are calculated for two cases of the mathematical model: a model cell of local structure has no knot ($D = 0$) and it has a knot. In the first case the polymer volume V_{pol} is distributed between N struts with a total volume V_{st}

$$V_{st} = F \sum_{n=1}^{N} \varrho_{n0}$$

$$\varrho_{n0} = r_{n0} = a_0 c_0 / (c_0^2 \sin\theta_n' + a_0^2 \cos\theta_n')^{1/2}$$

Then a cross-sectional area F of the struts can be calculated as follows

$$F \quad \frac{4}{3} \quad \frac{\pi\ P1\ a_0}{\sum_{n=1}^{N} (c_0^2 \sin^2\theta_n' + a_0^2 \cos^2\theta_n')^{-1/2}}$$

If the cross-section shape is assumed to be an equilateral triangle, its side t is

$$t = \sqrt{F / 0.433}$$

In the second case an attempt to introduce a knot with a constant volume V_k when $P1$ is given ($V_k \sim t^3(P1)$), does not allow us to model a whole variety of the plastic foams observed in experiments with $P1$ =const. Therefore, the knot is introduced as an undeformable sphere with

surface area S_k completely or partially covered by cross-sectional area S_N of N struts entering the knot:

$$S_k = \pi D^2 \qquad S_N = NF \qquad k = S_N / S_k ;$$

where D is a diameter of the knot. Quantity k is further denoted as parameter of the knot. Variation of the parameter k in the following range:

$$0.1 \leq k \leq 1.0 ; \quad \text{when } Pl = \text{const.}$$

permits us to model various distributions of the polymer between the struts and the knot when k is given.

As mentioned in [15] the parameter k remains constant for each compound of the plastic foams (irrespectively of the space filling coefficient Pl obtained in the result of the foaming process) provided the frothing technique and surface properties of the uncured compound are kept unchanged. Thus, once the parameter k has been determined for a few samples with Pl = const., the same value can be used for all the subsequent samples prepared by the same process, even when Pl changes. The above statements, however, have been supported by no experimental proofs.

Dimensions t, F, and D of structural elements in the model cell having a knot can be found from the following equations [6]:

$$Pl = Pl_k + Pl_{\mu} ;$$

$$Pl \quad \frac{D^3}{8 c_0 a_0^2} \quad \frac{3FN}{4\pi c_0 a_0^2} \sum_{n=1}^{N} \varrho_{n0}(\theta_n') \tag{2.10}$$

where Pl_k and Pl_{μ} are space filling coefficients of the plastic with knots or struts.

In view of

$$\varrho_{n0}(\theta_n') = r_{n0}(\theta_n') - D/2 ;$$

$$D = \sqrt{NF/(\pi k)} \quad \text{and} \quad F = 0.433\, t^2$$

expression (2.10) results in the following cubic equation with respect to t

$$Gt^3 + Ht^2 + J = 0\,, \tag{2.11}$$

where

$$G = -\frac{\pi}{6}\left[\frac{bN}{\pi k}\right]^{3/2} \qquad \frac{bN}{2}\left[\frac{bN}{\pi k}\right]^{1/2}$$

$$H = b\sum_{n=1}^{N} r_{n0}(\theta_n')$$

$$r_{n0}(\theta_n') = a_0 c_0 / (c_0^2 \sin^2\theta_n' + a_0^2 \cos^2\theta_n')^{1/2}$$

$$J = -4/3\pi\, P1 c_0 a_0^2 \qquad b = 0.433$$

With substitution $t = y - H/3$ Eq.(2.11) is reduced to its canonical form:

$$y^3 + py + q = 0 \quad \text{where } p = -H^2/3 \quad q = 2(H/3)^3 + J.$$

Further treatment of the problem depends on the value of quantity Q [40]:

$$Q = (p/3)^3 + (q/2)^2$$

which may be positive, negative or zero. Control calculations showed that all the three cases were realizable. The Cardano formula and the trigonometric solution method were used to find roots. One root of the three was chosen according to the following conditions:
1)the side length t of the struts cross-section lies in the range of

$$0 < t \le 2a_0\,,$$

2)t can assume only one numerical value. When t, F and D are calculated in every microsituation, their average values $<t>$ $<F>$ and $<D>$ are found according to Eq.(2.9).

The discussed kind of a knot introduction into the model cell has the following disadvantage : a mathematical model with a knot cannot be reduced to a knotless model in a direct way. The model cell always comprises a knot, whatever the combinations of k and $P1$ may be.

2.4 Conclusions

For consideration of monotropic plastic foams in the main axes of elastic symmetry five independent elastic constants have been chosen from twelve constants to be calculated according to the possibilities to elaborate mathematical models. The remaining seven constants are expressed by independent ones. In order to characterize deformative properties of the plastic foams as integral materials the elastic constants are defined as effective ones.

A local model consisting of a model of continuous medium and a model of local structure has been proposed. The model of a local structure comprises an ellipsoidal model cell with N struts orientated spatially uniformly By turning the system of struts as one whole around the knot centre, a cluster of one-type situations is obtained permitting to define average quantities. The way of introducing monotropy has been proposed, as well as dimensions of structural elements in model cell have been calculated. In order to model various distributions of polymer between struts and the knot when $P1$ is constant, an empiric coefficient, a knot parameter k, is introduced.

3 Deformative Properties in Compression/Tension Applied Parallel to Rise Direction. (Semiaxes Hypothesis)

3.1 Mathematical Model

3.1.1 Effective Moduli

If the strain ε_{33} parallel to the rise direction is applied to a model cell of monotropic plastic foams:

$$\varepsilon_{33} = (c - c_0)/c_0 = \text{const.} \tag{3.1}$$

effective Poisson's coefficients ν_{31}^*, ν_{32}^* and effective Young's modulus E_3^* can be expressed as follows:

$$\nu_{31}^* \quad <\varepsilon_{11}>/\varepsilon_{33} \;\; ; \; \nu_{32}^* = \nu_{31}^* \tag{3.2}$$

$$E_3^* \quad <\sigma_{33}>/\varepsilon_{33} \qquad \text{where}$$

$$<\varepsilon_{11}> \quad \frac{1}{8\pi^2} \int_0^{2\pi}\int_0^{2\pi}\int_0^{\pi} \varepsilon_{11}(\theta_E,\varphi_E,\psi_E)\sin\theta_E d\theta_E d\varphi_E d\psi_E$$

The value of $< \sigma_{33} >$ can be calculated in the same way as $<\varepsilon_{11}>$
From the viewpoint of deformations, the model cell can be considered as a rotational ellipsoid cut out in an infinite plastic foam medium. It is assumed that model cell retains its ellipsoidal (not obligatory rotational) form, when a compression/tension deformation is applied in the direction of one of the coordinate axes. Then deformation of the surface of model cell is defined by nondegenerated, linear transformation T_{ij} [38]:

$$T_{ij} = \begin{vmatrix} \lambda_1 & 0 & \lambda_3\sin\gamma \\ 0 & \lambda_2 & 0 \\ 0 & 0 & \lambda_3\cos\gamma \end{vmatrix} \tag{3.3}$$

$$\lambda_1 = a_1 / a_0 ; \quad \lambda_2 = a_2 / a_0 ; \quad \lambda_3 = c / c_0 .$$

The angle of pure shear is $\gamma = 0$ when compression/tension deformation is considered. To calculate $\varepsilon_{11}(\theta_E, \varphi_E, \psi_E)$ in every microsituation, the semiaxis a_1 of the model cell after deformation has to be known:

$$\varepsilon_{11}(\theta_E, \varphi_E, \psi_E) = \frac{a_1(\theta_E, \varphi_E, \psi_E) - a_0}{a_0}$$

Although $<\varepsilon_{22}> \quad <\varepsilon_{11}>$, when the monotropic plastic foams are considered, semiaxis $a_2(\theta_E, \varphi_E, \psi_E)$ is not obligatory equal to $a_1(\theta_E, \varphi_E, \psi_E)$. So parameters of the ellipsoidal model cell are the following:

Coordinate axes	Semiaxes of the model cell before deformation	Semiaxes of the model cell after deformation
$o1$	a_0	$a_1(\theta_E, \varphi_E, \psi_E)$
$o2$	a_0	$a_2(\theta_E, \varphi_E, \psi_E)$
$o3$	c_0	c = const.

At first we consider the most general case, when the axes to be calculated are completely independent. The values of a_1 and a_2 are found from the local structure model, using a variational analysis of after-deformation form a_1 , a_2 , c of the model cell. The variational analysis is based on the theorem of the potential energy minimum of deformation. According to this theorem, due to deformation the model cell assumes such a form a_1 , a_2 , c , which corresponds to deformation energy minimum W_{min} of the N strut system:

$$W_{min}(a_1, a_2, c, \theta_E, \varphi_E, \psi_E) = \min \sum_{n=1}^{N} W_n(a_1, a_2, c, \theta_E, \varphi_E, \psi_E), \qquad (3.4)$$

where energy to be minimized is calculated according to Eqs.(3.8), (3.9) or (3.14), (3.17). Here and in further Chapters the following assumptions are made:

1) The clamping of struts ends in the knot is hinge-like. The struts carry axial loads only.

2) The deformation of a single strut and therefore of the whole model cell is restricted (Paragraph 3.2.1) so no buckling occurs.

An unconditional minimization of the corresponding two-argument energy function has shown the incapability of a model with independent varying semiaxes to describe adequately the experiments. In some microsituations, in directions of axes $o1$ and $o2$ reaction strains by several orders exceeding the deformation ε_{33} applied may appear. Then few or no struts have directions $o1$ and $o2$, which means that large deformations in these directions are energetically favourable to the model cell. Practically an interaction of neighbouring cells in the plastic foams does not permit large reaction deformations of one cell. To take into account the interaction of neighbouring cells , the axes to be calculated have to be connected by some tie condition.

A tie condition is formulated using two experimentally measurable macroproperties of the plastic foams: a monotropy and an effective relative volume deformation ε^* The macroscopically monotropic plastic foams are known to deform equally in all directions of the isotropy plane, if the deformation applied is parallel to the monotropy axis. Assigning this macroproperty as a hypothesis to the model cell in the form of a rotational ellipsoid, after deformation the model cell retains the same form in the case of the mentioned above deformation. So the axes a_1 and a_2 to be calculated are mutually equal in every microsituation $\theta_E,\varphi_E,\psi_E$ (the semiaxes hypothesis, Fig.3.1):

$$a_1(\theta_E,\varphi_E,\psi_E) = a_2(\theta_E,\varphi_E,\psi_E) = a(\theta_E,\varphi_E,\psi_E). \qquad (3.5)$$

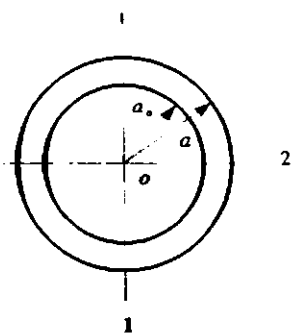

Fig.3.1 Deformation of the model cell in isotropy plane $o12$, when the compression deformation applied is parallel to monotropy axis $o3$ and the semiaxes hypothesis (3.5) is assumed.

In case of the semiaxes hypothesis a volume deformation $\varepsilon(\theta_E,\varphi_E,\psi_E)$ of the model cell changes from one microsituation to another. Then the effective volume deformation ε^- can be calculated as follows:

$$\varepsilon^- \quad \frac{1}{8\pi^2} \int_0^{2\pi}\int_0^{2\pi}\int_0^{\pi} \varepsilon(\theta_E,\varphi_E,\psi_E)\sin\theta_E d\theta_E d\varphi_E d\psi_E, \qquad (3.6)$$

where $\varepsilon = \varepsilon_{11} + \varepsilon_{22} + \varepsilon_{33}$

Deformation of the model cell, when $\varepsilon(\theta_E,\varphi_E,\psi_E) = \text{const.}$ in all microsituations (the volume deformation hypothesis), is considered in Chapters 4 and 5.

3.1.2 Deformation Energy ($\Delta\varrho_n$ - Calculation Scheme)

It is assumed that in the local structure model the struts do not change their spatial orientation due to deformation. Initially, we consider a no-knot model cell $D = 0$. Then (Fig.2.3)

$$r_{n0} = \varrho_{n0} \qquad r_n = \varrho_n\,, \quad \text{where } n = 1,2,\ldots,N$$

Now deformation energy of the n-th strut in every microsituation $\theta_E,\varphi_E,\psi_E$ can be expressed as follows:

$$W_n = 1/2\ P_n\Delta\varrho_n \quad \text{where } \Delta\varrho_n = \varrho_n - \varrho_{n0}$$

Here P_n is an axial load carried by the n-th strut.

As $$P_n = E_0F\Delta\varrho_n/\varrho_{n0}\,,$$

then: $$W_n = 1/2\ E_0F(\Delta\varrho_n)^2/\varrho_{n0} \qquad (3.7)$$

where E_0 is the Young's modulus of the base polymer.

In order to express $\Delta\varrho_n$ for the model cell of local structure in the form of a rotational ellipsoid the length ϱ_{n0} and ϱ_n of the n-th strut (that is, half-strut) is calculated:

$$\varrho_{n0} = \frac{a_0 c_0}{(c_0^2 \sin^2\theta_n' + a_0^2 \cos^2\theta_n')^{1/2}}$$

$$\varrho_n = \frac{ac}{(c^2 \sin^2\theta_n' + a^2 \cos^2\theta_n')^{1/2}} \qquad (3.8)$$

where θ_n' is a spherical coordinate of the n-th strut in the laboratory reference frame after modelling of the monotropy (2.7) ($\theta_n' = \theta_n$, when isotropic plastic foams are considered). Now deformation potential energy of the knotless model cell can be expressed (3.4, 3.7) as:

$$W(a, \theta_E, \varphi_E) = \frac{E_0 F}{2 a_0 c_0} \sum_{n=1}^{N} \sqrt{f_{n0}} \left[\frac{a(\theta_E, \varphi_E)\, c}{\sqrt{f_n}} - \frac{a_0 c_0}{\sqrt{f_{n0}}} \right]^2 \qquad (3.9)$$

where $f_{n0} = c_0^2 \sin^2\theta_n' + a_0^2 \cos^2\theta_n'$

$$f_n = c^2 \sin^2\theta_n' + a^2(\theta_E, \varphi_E) \cos^2\theta_n'$$

In the case of a model cell of local structure having a knot, the deformation potential energy is:

$$W(a, \theta_E, \varphi_E) = \frac{E_0 F}{2} \sum_{n=1}^{N} \frac{(r_n - r_{n0})^2}{r_{n0} - D/2} \qquad (3.10)$$

$$r_{n0} = a_0 c_0 / (f_{n0})^{1/2} \qquad r_n = ac / (f_n)^{1/2} \qquad (3.11)$$

Half-axis a is obtained by minimizing Eq.(3.9) or (3.10). According to Eqs.(3.9) and (3.10), the deformation energy depends only on θ_n' - coordinate of the struts. However, as it has been proved in Section 2.2, θ_n' does not depend on ψ_E. Consequently, min W, a and ε_{11} are independent of angle ψ_E, too: $\varepsilon_{11} = \varepsilon_{11}(\theta_E, \varphi_E)$.

The numerical value of ε_{11} found from the model cell of local structure is related to the point of a continuous medium. Then the deformation $\varepsilon_{11}(\theta_E,\varphi_E)$ of the plastic foams viewed as a continuous medium is calculated in every microsituation of the ensemble, and calculation of $<\varepsilon_{11}>$ simplifies:

$$<\varepsilon_{11}> \quad \frac{1}{4\pi}\int_0^{2\pi}\int_0^{\pi} \varepsilon_{11}(\theta_E,\varphi_E)\sin\theta_E d\theta_E d\varphi_E \qquad (3.12)$$

Further in the text a notation "$\Delta\varrho_n$ - calculation scheme" is used to denote equations describing such a deformation of the struts, when their length is changed on $\Delta\varrho_n$, but their spatial orientation remains unchanged.

3.1.3 Deformation Energy (λ_n - Calculation Scheme)

The numerical calculations show that the results given by the $\Delta\varrho_n$ calculation scheme do not always agree with experimental data (Paragraph 3.3.3). Therefore, it is assumed that struts in the local structure model may change their spatial orientation due to deformation of the model cell.

Initially, the model cell without a knot is considered. If projections of a unity vector $\overline{\mathbf{n}}$ directed along the n-th strut in an undeformed model cell are:

$$\begin{cases} x_n & \cos\varphi_n \sin\theta_n' \\ y_n & \sin\varphi_n \sin\theta_n' \\ z_n & \cos\theta_n' \end{cases}$$

a relative change λ_{nT} in the n-th strut length after deformation T_{ij} (3.3) is:

$$\lambda_{nT} = \varrho_n/\varrho_{n0} = (T_{mi}T_{mj}\,x_i x_j)^{1/2}$$

$$\lambda_{nT} = (\lambda_x^2\cos^2\varphi_n\sin^2\theta_n' + \lambda_y^2\sin^2\varphi_n\sin^2\theta_n' + \lambda_z^2\cos^2\theta_n')^{1/2}, \qquad (3.13)$$

where $n = 1,2,\ldots,N$ (For the sake of obviousness the $oxyz$ frame of reference is considered in Paragraph 3.1.3)

According to the semiaxes hypothesis:

$$\lambda_x = \lambda_y = \lambda = a / a_0 \quad \text{and}$$

$$\lambda_{nT} = (\lambda^2 \sin^2\theta_n' + \lambda_z^2 \cos^2\theta_n')^{1/2}$$

Deriving ϱ_{n0} from Eq.(3.8) and taking into consideration that θ_n' does not depend on ψ_E the deformation energy of N-strut system in each microsituation θ_E, φ_E can be presented as:

$$W(\lambda,\theta_E,\varphi_E) = \frac{E_0 F}{2} \sum_{n=1}^{N} [\, \lambda_{nT}(\lambda,\theta_E,\varphi_E) - 1 \,]^2 \, \varrho_{n0}(\theta_E,\varphi_E) \,. \quad (3.14)$$

Semiaxis $a_x = a$ is calculated by using variational analysis of the after-deformation form of the model cell and minimizing energy W, Eq.(3.14). Likewise as in Paragraph 3.1.2, it can be proved that $<\varepsilon_{xx}>$ is calculated from Eq.(3.12).

When a model cell of local structure with a knot is considered, the relative change in the n-th strut length λ_{nc} is derived by using the coordinates of struts ends (Fig.3.2):

$$\lambda_{nc} = \varrho_n / \varrho_{n0} = \left[\frac{(x_{n2} - x_{n0})^2 + (y_{n2} - y_{n0})^2 + (z_{n2} - z_{n0})^2}{(x_{n1} - x_{n0})^2 + (y_{n1} - y_{n0})^2 + (z_{n1} - z_{n0})^2} \right]^{1/2} . \quad (3.15)$$

In conformity with $x_i = T_{ij} x_j$ we have

$$x_{n2} = \lambda_x x_{n1} \quad y_{n2} = \lambda_y y_{n1} \quad z_{n2} = \lambda_z z_{n1}$$

In view of

$$\begin{cases} x_{n1} = x_{n0} + \varrho_{n0} \cos\alpha_n \cos\varphi_n ; \\ y_{n1} \quad y_{n0} + \varrho_{n0} \cos\alpha_n \sin\varphi_n ; \\ z_{n1} = z_{n0} + \varrho_{n0} \sin\alpha_n , \end{cases}$$

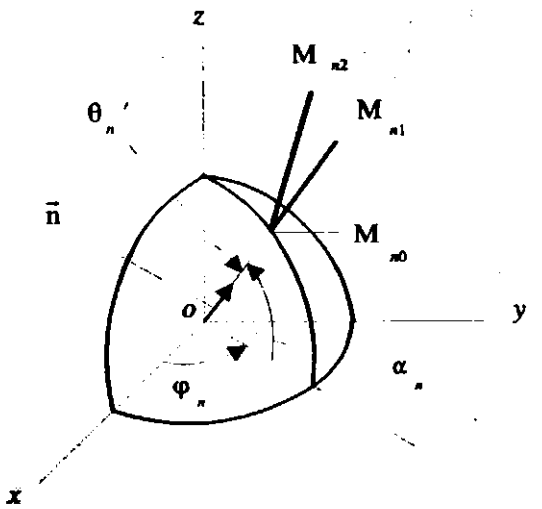

Fig.3.2 Change in the n-th strut spatial orientation due to space transformation T_{ij}.

x_{n0}, y_{n0}, z_{n0} is a point of the n-th strut entering the knot;

x_{n1}, y_{n1}, z_{n1} and x_{n2}, y_{n2}, z_{n2} are points of the n-th strut crossing the model cells surface before and after deformation, respectively.

and $\sin \alpha_n = \dfrac{z_{n0}}{D/2}$ $\cos \alpha_n = \dfrac{x_{n0}}{D/2 \cos\varphi_n}$ we obtain:

$$\begin{cases} x_{n1} = x_{n0} (1 \quad 1/\beta_n) \\ y_{n1} \quad y_{n0} (1 \quad 1/\beta_n) \\ z_{n1} \quad z_{n0} (1 \quad 1/\beta_n) \end{cases} \qquad \beta_n \quad D / (2\varrho_{n0})$$

As $x_{n0}^2 + y_{n0}^2 + z_{n0}^2 = (D/2)^2$ then:

$$\begin{aligned} \lambda_{nc} = \{ & [\lambda_x(\beta_n + 1) - \beta_n]^2 \cos^2\varphi_n \sin^2\theta_n' + \\ & + [\lambda_y(\beta_n + 1) - \beta_n]^2 \sin^2\varphi_n \sin^2\theta_n' + \\ & + [\lambda_z(\beta_n + 1) - \beta_n]^2 \cos^2\theta_n' \}^{1/2} \end{aligned} \tag{3.16}$$

(If there is no knot, $\beta_n = 0$ for each $n = 1, 2, \ldots, N$ and λ_{nc} reduces to λ_{nT} $\lambda_{nc} \equiv \lambda_{nT}$.) According to the hypothesis of semiaxes, $\lambda_x = \lambda_y = \lambda$, and

$$\begin{aligned} \lambda_{nc} = \{ & [\lambda(\beta_n + 1) - \beta_n]^2 \sin^2\theta_n' + \\ & + [\lambda_z(\beta_n + 1) - \beta_n]^2 \cos^2\theta_n' \}^{1/2} . \end{aligned}$$

Deriving r_{n0} from Eq.(3.11) and taking into consideration that θ_n' does not depend on ψ_E, the deformation energy of N strut system in each microsituation θ_E, φ_E can be presented:

$$W(\lambda,\theta_E,\varphi_E) = \frac{E_0 F}{2} \sum_{n=1}^{N} [\lambda_{mc}(\lambda, \theta_E, \varphi_E) - 1]^2 (r_{n0} - D/2) \quad (3.17)$$

Likewise to Paragraph 3.1.2, it can be proved that $<\varepsilon_{xx}>$ can be calculated from Eq.(3.12).

Further in the text the notation " λ_n - calculation scheme" will be used for equations describing such a deformation of the struts when they change not only their spatial orientation but also their length.

3.1.4 Average Stress

In order to calculate average stress $<\sigma_{33}>$ from Eq.(3.2), stress $\sigma_{33}(\theta_E,\varphi_E,\psi_E)$ in every microsituation $\theta_E,\varphi_E,\psi_E$ of the plastic foams structure has to be known. The stress in question is considered for the local model cell of continuous medium (Section 2.2), with force P applied parallel to rise direction $o3$ (Fig.3.3). The force P deforms the model cell by $\varepsilon_{33} = (c - c_0)/c_0$ Eq.(3.1). According to the semiaxes hypothesis, after deformation the shape of model cell is still a rotational ellipsoid. The stress $\sigma_{33}(\theta_E,\varphi_E,\psi_E)$ is defined as the volume-averaged stress considering the post-deformation volume V_{mc} of the model cell. Then:

$$\sigma_{33}(\theta_E,\varphi_E,\psi_E) = \bar{\sigma}_{33}^{mc},$$

where $$\bar{\sigma}_{33}^{mc} \quad \frac{1}{V_{mc}} \int_{V_{mc}} \bar{\sigma}_{33}^{mc}(M_{mc})\, dV_{mc} \quad (3.18)$$

To perform averaging using Eq.(3.18), a three-dimensional stress state of the rotational ellipsoid under uniaxial compression/tension deformation ε_{33} has

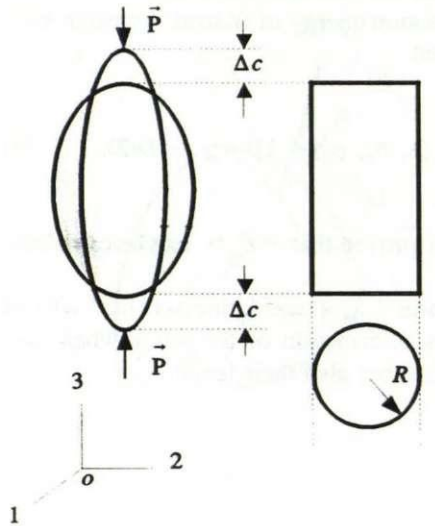

Fig.3.3
A local model of the plastic foams considered as a continuous medium (see Section 2.2) and used for the calculation of stress $\sigma_{33}(\theta_E,\varphi_E,\psi_E)$.

$R(\theta_E,\varphi_E)$ is the radius of the cylinder.

to be known. Since solution of such a problem is unknown to the author, the post-deformation rotational ellipsoid is replaced by a circular cylinder [5,39] whose height h and volume V_{cyl} are equal to those of the rotational ellipsoid:

$$h = 2c; \quad V_{cyl} = V_{mc}$$

As

$$V_{mc} = 4/3\pi c\, a_1^2(\theta_E,\varphi_E) \quad \text{and} \quad V_{cyl} = 2\pi c R^2$$

the radius of the cylinder can be calculated as follows:

$$R = \sqrt{2/3}\; a_1(\theta_E,\varphi_E) = R(\theta_E,\varphi_E), \tag{3.19}$$

where $a_1(\theta_E,\varphi_E)$ is derived from Eq.(3.4).
Therefore:

$$\sigma_{33}(\theta_E,\varphi_E,\psi_E) = \bar{\sigma}_{33}^{cyl},$$

where $$\bar{\sigma}_{33}^{cyl} = \frac{1}{V_{cyl}} \int_{\omega} \sigma_{33}^{cyl}(M_{cyl})\, dV_{cyl}$$

Since in cylindrical model cell the stress $\sigma_{33}^{cyl}(M_{cyl})$ is known to remain constant throughout the whole volume

$$\sigma_{33}^{cyl}(M_{cyl}) = P/(\pi R^2) = \text{const.} \quad \text{for every } M_{cyl} \in V_{cyl} ,$$

then $$\sigma_{33}(\theta_E,\varphi_E,\psi_E) = \bar{\sigma}_{33}^{cyl} = P/(\pi R^2) \tag{3.20}$$

The force P in every microsituation is calculated from the model cell of local structure. When $\varepsilon_{33} = \Delta c/c_0$, deformation energy of the model cell is the following:

$$W(\theta_E,\varphi_E,\psi_E) = 1/2 P(\theta_E,\varphi_E,\psi_E)\, \Delta h ;$$

$$\Delta h = 2\Delta c = 2(c - c_0)$$

$$P(\theta_E,\varphi_E,\psi_E) = W(\theta_E,\varphi_E,\psi_E)/ (c - c_0)$$

The deformation energy of the model cell is also equal to the energy (3.9), (3.10), (3.14) or (3.17) accumulated in N struts.

Then the force P is

$$P = P(\theta_E,\varphi_E) = \frac{1}{c - c_0} \min \sum_{n=1}^{N} W_n(a_1, \theta_E, \varphi_E) \tag{3.21}$$

According to Eqs.(3.19), (3.20) and (3.21), the stress σ_{33} can be calculated in every microsituation θ_E , φ_E:

$$\sigma_{33} = \sigma_{33}(\theta_E,\varphi_E) = \frac{3}{2\pi(c - c_0)} \frac{\min \sum_{n=1}^{N} W_n(a_1,\theta_E,\varphi_E)}{a_1^2(\theta_E,\varphi_E)} .$$

$$\sigma_{33} \neq \sigma_{33}(\psi_E)$$

Since the stress σ_{33} is independent of angle ψ_E, the calculation of average stress $<\sigma_{33}>$ using Eq.(2.9) simplifies:

$$<\sigma_{33}> \quad \frac{1}{4\pi} \int_0^{2\pi} \int_0^{\pi} \sigma_{33}(\theta_E, \varphi_E) \sin\theta_E d\theta_E d\varphi_E$$

3.1.5 Compatibility of Mathematical Models

Mathematical models of uniaxial compression/tension of the foams (Chapters 3, 4 and 5) should be mutually compatible. It means that in the case of isotropic foams when deformative characteristics are independent of the loading direction, constants ν^* and E^* calculated according to these different models should be equal in the limits of calculation errors.

To calculate the post-deformation shape of the model cell in mathematical models of uniaxial compression/tension, a variational analysis of post-deformation form was used. In calculating shear modulus G_{13}^* (Chapter 6), the post-deformation form of the model cell is uniquely defined by transformation matrix T_{ij}, Eq.(6.3). Therefore, a mutual compatibility of these different theoretical approaches has also to be checked. It can be done in case of the isotropic plastic foams, when:

$$G^* = E^* / [2(1 + \nu^*)] \tag{3.22}$$

Derivation of G^* from Eq.(3.22), therefore, employs the data obtained by variational analysis of post-deformation form of the model cell. The values of G^* calculated in this way are compared with the values calculated in Chapter 6, and the data should be equal in the limits of calculation errors.

3.2 Numerical Calculations

3.2.1 Small Deformations of Model Cell

The proportional limit, as experimentally determined for plastic foams, in tension ε_{lt} is greater than that in compression ε_{lc} [9,20,52]. For rigid, isotropic polyurethane foams:

$$\varepsilon_{lc} \approx -1.0\ \% \ ; \ \varepsilon_{lt} \approx 1.5\ \%$$

When elastic, isotropic polyurethane foams are considered these characteristics are almost by one order greater:

$$\varepsilon_{lc} \approx -6.5\ \% \ ; \ \varepsilon_{lt} \approx 12.0\ \%$$

Therefore, for a greater versatility of the mathematical model, the numerical value of deformation ε_{33} applied to the model cell has been restricted:

$$|\varepsilon_{33}| \leq |\varepsilon_{lc}| = 1.0\ \% \qquad (3.23)$$

Since we are lacking information about the proportionality region for monotropic plastic foams and its dependence on the degree of anisotropy and the loading direction, Eq.(3.23) of isotropic plastic foams has been used initially as deformation for the model cell of monotropic plastic foams. Simultaneously, a subsequent testing of the strut stability was carried out.

Although the strain ε_{33}, Eq.(3.1), applied to the whole model cell is smaller than the limit strain, the critical deformation $\varepsilon_{cr.n}$ may be exceeded in compression for some separate strut when $P1$ becomes very small [30]:

$$\varepsilon_{cr.n} = -\frac{\pi^2 I_{01}}{4 F C^2 (r_{n0} - D/2)^2} \qquad (3.24)$$

where I_{01} is a minimum inertia moment of struts cross-section, $C = 1$ for a hinge-like clamping of struts end in the knot. If $\varepsilon_{cr.n}$ is exceeded for some

strut of the model cell, the limit strain of the whole plastic foam is considered to be exceeded. In this case deformation of the model cell is reduced by a half and the calculations are repeated (Fig.3.4) (control of the strut stability is realized during calculation of all the five independent constants).

As concluded later from numerical calculations, the elastic constants are independent of length of the semiaxes a_0, c_0. But we are also interested in dimensions t, F, D of structural elements (these characteristics depend on absolute values of a_0, c_0). Therefore, values of a_0, c_0 are chosen equal to those determined experimentally. The distance $2a_0$ between the centres of cells is independent of $P1$ for rigid PUR open-cell plastic foams when $P1 \leq 0.1$ [52]:

$$2a_0 = 2 \times 10^{-4}\ \mathrm{m} = \mathrm{const.} \qquad P1 \leq 0.1$$

3.2.2 Numerical Averaging and Variational Series

For numerical calculations of the effective constants, the programme "CONSTANTS" with flowcharts depicted in Figs.3.4 and 3.5 has been used. Average values $<\sigma_{33}>$, $<\varepsilon_{11}>$ etc. are calculated by numerical integration with the Simpson's formula [48]. To provide the desired accuracy of data averaging, the effect of numerical integration steps $\Delta\theta_E$, $\Delta\varphi_E$ should be evaluated.

Since the parameters to be averaged are complicated functions of θ_E and φ_E, it is practically impossible to determine how they affect the calculation data by just using the remainder term of the Simpson's formula. That is why the effect was judged from changes in the data caused by reduction of $\Delta\theta_E$, $\Delta\varphi_E$ values. The calculation data presented in Table 3.1 allow us to draw the following conclusions

1) Changes in the effective constants caused by reducing $\Delta\theta_E$, $\Delta\varphi_E$ from 10° to 5° are close to the errors $\Delta\nu_{31}^*$, ΔE_3^*, ΔG^* brought in by the minimization process The errors, in their turn, are basically independent of $\Delta\theta_E$, $\Delta\varphi_E$.
2) A reduction of $\Delta\theta_E$, $\Delta\varphi_E$ increases considerably the time for

executing a PC job of standard problem, whereas data changes are insignificant as compared with absolute values of the data to be calculated. It can be summarized that steps $\Delta\theta_E = \Delta\varphi_E = 10°$ give data sufficiently accurate for solving standard problems. The values in Table 3.1 have been calculated for a model cell with a knot according to the λ_n scheme, although all the conclusions drawn may also be applied to knotless model cell and $\Delta\varrho_n$ - scheme.

If steps in numerical integration of Eq.(2.9) are $\Delta\theta_E$, $\Delta\varphi_E$, $\Delta\psi_E$ the theoretically infinite number of ensembles microsituations $\theta_E, \varphi_E, \psi_E$ will be substituted by a set of microsituations of finite number θ_{Ei}, φ_{Ej}, ψ_{Ek}

$$\theta_{Ei} = (i - 1)\Delta\theta_E \; ; \; \varphi_{Ej} = (j - 1)\Delta\varphi_E ; \; \psi_{Ek} = (k - 1)\Delta\psi_{Ek} \; ,$$

$$\text{where } i = 1,2,\ldots,I \; ; \; j = 1,2,\ldots,J \; ; \; k = 1,2,\ldots,K \; ;$$

$$I = \pi/\Delta\theta_E + 1 \; ; \; J = 2\pi/\Delta\varphi_E + 1 \; ; \; K = 2\pi/\Delta\psi_E + 1$$

Altogether there are $NN = I \times J \times K$ microsituations. An averaging of the physical values throughout NN microsituations requires that a mutual difference of these values in various microsituations is evaluated. For this purpose local values of the data to be averaged are stored in arrays. Each array is a selection x_n , $n = 1,2,\ldots,NN$ from the general set of the infinite number of microsituations. Elements of the selection x_n are grouped into $MM = 10$ classes. Minimum and maximum elements of the selection x_{min} , x_{max} as well as the class interval $c1$, $c1 \approx (x_{max} - x_{min})/MM$ are calculated. A starting number of the first class is chosen to be equal to x_{min} and a variational series is formed so that central numbers $\bar{x}_m$ are given instead of classes:

$$\bar{x}_m = \sum_{m}^{M_m} \frac{x_m}{M_m} \qquad m = 1,2,\ldots,MM.$$

After calculating the frequency M_m of each class, a histogram of the variational series of selection x_n is drawn (Paragraph 3.3.3). Asymmetry AS and excess EX are calculated for the series obtained. Characteristics of AS and EX calculated are compared with those of normal distribution: AS=0, EX = 0 [1].

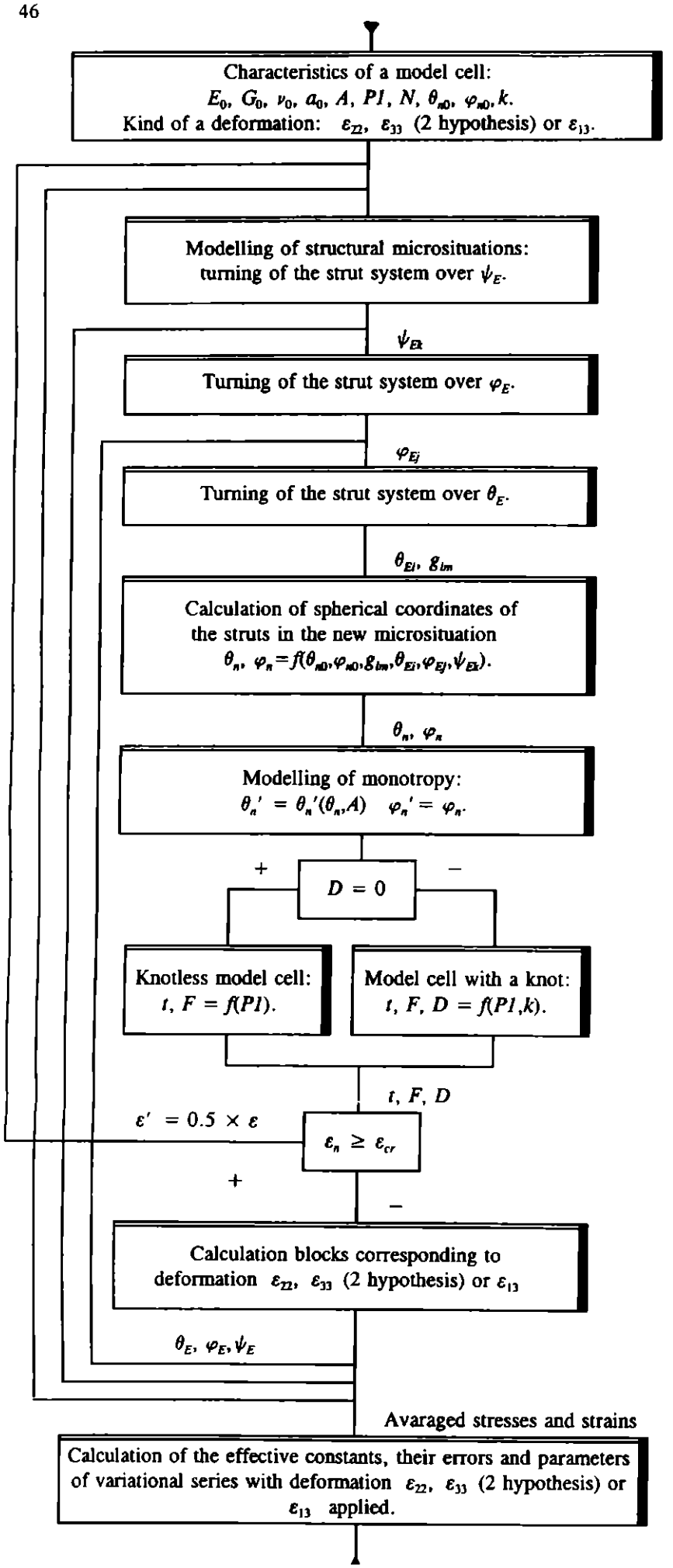

Fig.3.4 Flowchart of the programme "CONSTANTS" for calculating effective elastic constants of the monotropic plastic foams.

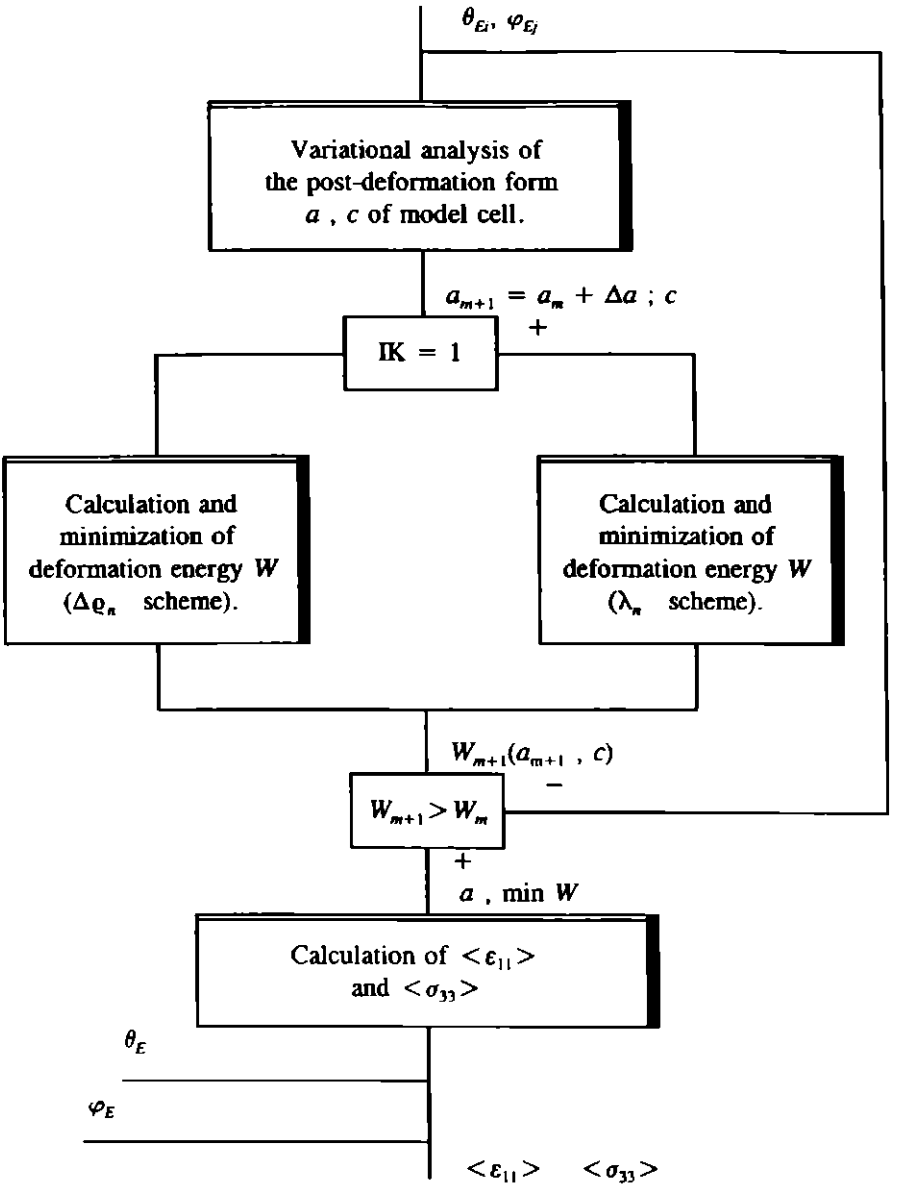

Fig.3.5 Calculation blocks corresponding to deformation ε_{33} in the programme "CONSTANTS" (Fig.3.4) when the semiaxes hypothesis is assumed.

Table 3.1 Effect of numerical integration steps $\Delta\theta_E$, $\Delta\varphi_E$ on the calculation data.

N°	$\Delta\theta_E$; $\Delta\varphi_E$, °	A	Range of semiaxis a		$\nu^* \pm \Delta\nu^*$; $\nu_{31}{}^* \pm \Delta\nu_{31}{}^*$	$E^* \pm \Delta E^*$; $E_3{}^* \pm \Delta E_3{}^*$, MPa	$G^* \pm \Delta G^*$, MPa	$\varepsilon^* \pm \Delta\varepsilon^*$, %	t_{ex},
			$(a_{min} \pm \Delta a) \times 10^{-3}$, m	$(a_{max} \pm \Delta a) \times 10^{-3}$, m					
1	10	1.0	0.100130 ±0.000001 (±0.001%)	0.100494 ±0.000001 (±0.01%)	0.256 ±0.001 (±0.4%)	23.547 ± 0.001 (±0.004%)	9.37 ±0.01 (±0.1%)	−0.487 ±0.002 (±0.4%)	0'30"
2	5	1.0	0.100124	0.100494	0.256	23.552	9.37	−0.487	1'50"
3	10	1.5	0.100181	0.101107	0.399	37.171	–	−0.200	0'50"
4	5	1.5	0.100163	0.101107	0.399	37.189	–	−0.201	2'40"

Initial calculation data: PUR plastic foams, $E_0 = 2300$MPa, $P1 = 0.075$, $N = 4$, $k = 0.1$, λ_n scheme, $c = 0.99c_0$ (1% compression), $\Delta a = 10^{-5} \times a_0$, $a_0 = 10^{-4}$ m

3.2.3 Deformation Energy Minimization. Errors Caused by Minimization Process

A minimum of deformation energy W is sought for by varying the post-deformation form of the model cell. For this purpose the semiaxis to be calculated is varied in the range (3.25) with a step Δa (Fig.3.5):

$$a_{start} \le a \le a_{finish} ; \qquad (3.25)$$

$$a_m = a_{start} + \Delta a_m , \text{ where } m = 0,1, \ldots, (a_{finish} - a_{start}) / \Delta a$$

A graph of the energy function $W(a)$ calculated in several points was found to be a concave parabola with its top corresponding to the minimum value of energy $\min W$ and the sought value $a_{\min}$ of semiaxis a (the function $W(a)$ has an absolute, unconditional minimum). The function $W(a)$ remains nonnegative for all values of argument a and parameters a_0 c_0 , c. Moving from a_{start} with a given step Δa, the function $W(a)$ is calculated in every step. The minimum of deformation energy $\min W = W(a_{\min})$ when the semiaxis a equals $a = a_{\min}$ is considered to be found whenever:

$$W(a + \Delta a) > W(a) ,$$

Accuracy of the values calculated in the minimization process depends on step Δa:

$$a_{\min} = a \pm \Delta a \qquad \min W = W(a) \pm \Delta W$$

$$\text{where} \qquad \Delta W = W(a \pm \Delta a) - W(a)$$

Therefore, we need to evaluate effect of Δa on the calculation results. (Spherical coordinates $\varphi_{n0}, \theta_{n0}$ found by minimization of function Φ have been also determined not quite precisely. However, their effect is insignificant, therefore it is neglected). Since the error Δf of multivariate function f is [1]:

$$\Delta f \approx \sum_{i=1}^{n} f_{X_i}' \ (X_1, X_2, \ldots, X_n) \ \Delta X_i ,$$

and $\Delta < f > \quad < \Delta f >$, we obtain the following:

$$\Delta \nu_{31}^{*} = -1/\varepsilon_{33} \; <\Delta \varepsilon_{11}>$$

$$\Delta E_3^{*} = 1/\varepsilon_{33} \; <\Delta \sigma_{33}>$$

$$\Delta G^{*} \quad \Delta E^{*} / [2(1 + \nu^{*})] - E^{*}\Delta \nu^{*} / [2(1 + \nu^{*})^2]$$

$$\Delta \varepsilon^{*} = 2 <\Delta \varepsilon_{11}>$$

where ΔE^{*}, $\Delta \nu^{*}$ are errors of effective constants of the isotropic plastic foams. It can be proved that

$$\Delta \varepsilon_{11} = \Delta a / a_0 ;$$

$$\Delta \sigma_{33} \quad \frac{3}{2\pi(c - c_0)} \left[\frac{\Delta W}{a^2} - 2W\frac{\Delta a}{a^3} \right]$$

Considering that the maximum error $| \Delta f |$ depends on relationship:

$$| \Delta f | \leq \sum_{i=1}^{n} \left| f_{x_i}'(x_1, x_2, \ldots, x_n) \, \Delta x_i \right| \tag{3.26}$$

we obtain the evaluation of maximum errors of the values to be calculated as a function of step Δa:

$$| \Delta \nu_{31}^{*} | \leq \left| \frac{c_0}{a_0(c - c_0)} \Delta a \right|$$

$$| \Delta E_3^{*} | \leq \frac{3c_0}{8\pi^2(c - c_0)} \int_0^{2\pi} \int_0^{\pi} \left\{ \left| \frac{\Delta W}{a^2} \right| + \left| \frac{2W\Delta a}{a^3} \right| \right\} \times$$

$$\times \sin \theta_E \, d\theta_E \, d\varphi_E ;$$

$$| \Delta G^{*} | \leq \frac{| \Delta E^{*} |}{2(1 + \nu^{*})} + \frac{E^{*}}{2(1 + \nu^{*})^{2}} | \Delta \nu^{*} |$$

$$| \Delta \varepsilon^{*} | \leq 2\Delta a / a_0 \qquad (3.27)$$

Investigations performed by the Monte-Carlo method have revealed that practically the error is usually smaller than the maximum one determined by equality sign in Eq.(3.26). Therefore, the evaluation (3.27) is considered to be sufficient.

According to the calculation results given in Tables 3.2 and 3.3 the following conclusions can be made:

1) When $\Delta a = 10^{-4} \times a_0$ or $\Delta a = 10^{-5} \times a_0$ relative errors of the values to be calculated are less than 5%. It can be considered to be of sufficient accuracy as compared with the variation range of these values in the investigated relationships ν_{31}^{*}, E_3^{*}, $\varepsilon^{*} = f(P1, k, A)$.

2) Step Δa has the most significant effect on Poisson's coefficients ν^{*}, ν_{31}^{*} It may be concluded that step $\Delta a = 10^{-4} \times a_0$ insures a sufficient accuracy of results.

3) Reduction of step Δa (an improvement of the accuracy)increases considerably the time t_{ex} of executing standard problems PC job.

All the previous conclusions are true also for knotless model cells and $\Delta\varrho_n$ scheme.

Table 3.2 Effect of minimization step Δa on calculation data.
Isotropic plastic foams, $A = 1.0$.

N°	A	Step Δa, m	ν^*	$\pm\Delta\nu^*$	E^*, MPa	$\pm\Delta E^*$, MPa	G^*, MPa	$\pm\Delta G^*$, MPa	ε^*, %	$\pm\Delta\varepsilon^*$, %	t_{ex} ' "
1	1.0	$10^{-3}\times a_0$	0.2	0.1 (50%)	23.6	0.8 (3%)	9	1 (10%)	−0.4	0.2 (50%)	0'50"
2		$10^{-4}\times a_0$	0.25	0.01 (4%)	23.55	0.01 (0.04%)	9.37	0.08 (1%)	−0.48	0.02 (4%)	1'00"
3		$10^{-5}\times a_0$	0.256	0.001 (0.4%)	23.553	0.001 (0.004%)	9.374	0.008 (0.1%)	−0.487	0.002 (0.4%)	1'50"

Initial calculation data: PUR plastic foams, $E_0 = 2300$MPa, $P1 = 0.075$, $N = 4$, $k = 0.1$, λ_n - scheme, $c = 0.99c_0$ (1% compression), $\Delta\theta_E = \Delta\varphi_E = 5°$ $a_0 = 10^{-4}$ m

Table 3.3 Effect of minimization step Δa on calculation data. Monotropic plastic foams, $A = 1.5$.

N°	A	Step Δa, m	ν_{31}^*	$\pm\Delta\nu_{31}^*$	E_3^*, MPa	$\pm\Delta E_3^*$, MPa	ε^*, %	$\pm\Delta\varepsilon^*$, %	t_{ex}, ′ ″
1	1.5	$10^{-3}\times a_0$	0.4	0.1 (25%)	37.2	0.7 (2%)	−0.1	0.2 (200%)	0′40″
2		$10^{-4}\times a_0$	0.39	0.01 (3%)	37.18	0.01 (0.02%)	−0.20	0.02 (10%)	0′50″
3		$10^{-5}\times a_0$	0.399	0.001 (0.3%)	37.189	0.001 (0.002%)	−0.201	0.002 (1%)	2′40″

Initial calculation data: PUR plastic foams, $E_0 = 2300$MPa, $P1 = 0.075$, $N = 4$, $k = 0.1$, λ_n - scheme, $c = 0.99c_0$ (1% compression), $\Delta\theta_E = \Delta\varphi_E = 5°$, $a_0 = 10^{-4}$ m

3.3 Analysis of Calculation Results

3.3.1 Dimensions of Structural Elements in Model Cell of Local Structure (Isotropic Plastic Foams)

For a better understanding of the mathematical model presented, it is necessary to determine dimensions of structural elements in the local structure model cell of isotropic plastic foams (the radius of the model cell is: $a_0 = 1.0 \times 10^{-4}$ m). In Fig.3.6 the dependence of $<t>$ and $<D>$ (Section 2.3) on $P1$ is depicted for those values of parameter k, which permit the modelling of PUR ($k = 0.1$) and PVC ($k = 0.5$) plastic foams. It is obvious that for all the values of $P1 \leq 0.175$

$$<D> > <t> \quad \text{when } k = 0.1 \text{ and}$$

$$<D> \quad <t> \text{ when } k = 0.5$$

The numerical values of $<t>$ and $<D>$ are in good agreement with other theoretical [52] and experimental data [11,20].

In Fig.3.7 the distribution of base polymer between structural elements is depicted in dependence of knot parameter k when $P1 = 0.075$.

$$V_{rst} = V_{st} / V_{pol}, \quad V_{rk} = V_k / V_{pol},$$

$$V_{pol} = P1 V_{mc};$$

where V_{rst} and V_k are relative volumes of struts and knot,

V_{pol} is volume of base polymer in the model cell.

It is seen that with growth of the parameter k the polymer volume in struts increases while in the knot decreases. The same theoretical result was obtained in [15]. However, no experimental data for this relationship are available to the author.

Figure 3.8 shows the dependence of strut's characteristic $\beta = <t>/l_0$ on the parameter k for $P1 = 0.075$. The struts are the thickest when $k = 0.5$ and β reaches its maximum. Besides this graph determines

the character of relationships $E^*/E_0 = f(k)$ and $G_{13}^*/G_0 = f(k)$ (Figs.3.15 and 6.6). A similar result based on another method has been obtained in [15].

The calculated dimensions of structural elements for $N = 4$ and $k = 0.1$; $k = 0.5$ are depicted in schematic planar scheme, Fig.3.9. When $k = 0.1$, the struts are thin and the knot is well expressed while at $k = 0.5$ the struts become not so thin and the knot is less distinguished. The proportions in the figures presented are in good agreement with those in photographs of PUR and PVC plastic foams given in [20].

Since the model cell of the isotropic plastic foams is a sphere, dimensions of the structural elements are the same for all microsituations.

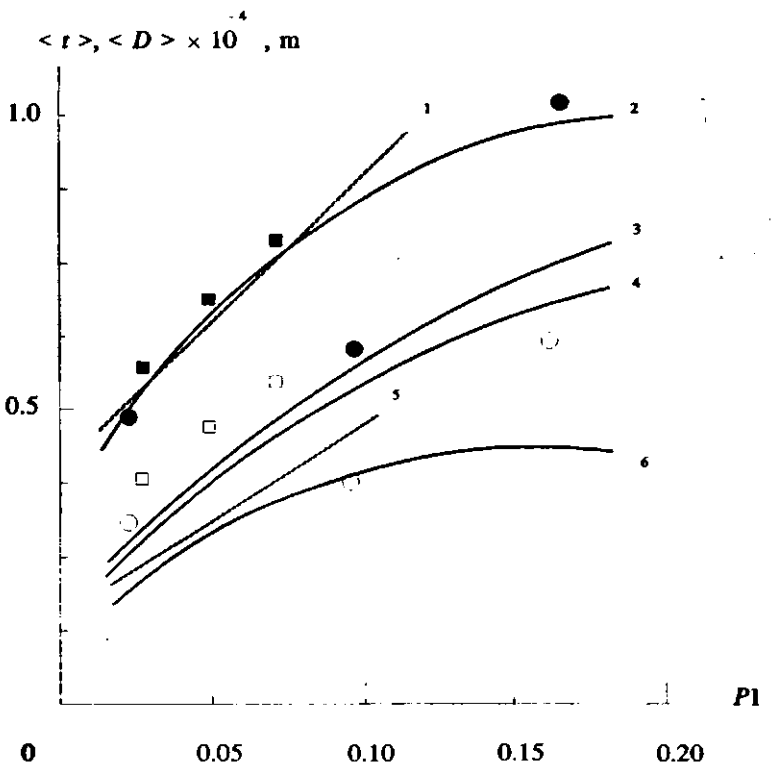

Fig.3.6 Dependence of average struts cross-section side $<t>$ and average knot diameter $<D>$ on space filling coefficient $P1$.

Theoretical results.

1,5 $<D>$, $<t>$, [52];
2,6 $<D>$, $<t>$, $k = 0.1$;
3,4 $<D>$, $<t>$, $k = 0.5$;

Experimental data.

■,□ $<D>$, $<t>$, [11];
●,○ $<D>$, $<t>$, [20].

Initial calculation data: $P1 = 0.075$, $N = 4$, $a_0 = 10^{-4}$m, λ_n scheme, $\Delta\theta_E = \Delta\varphi_E = 10°$, $\Delta a = 10^{-4} \times a_0$.

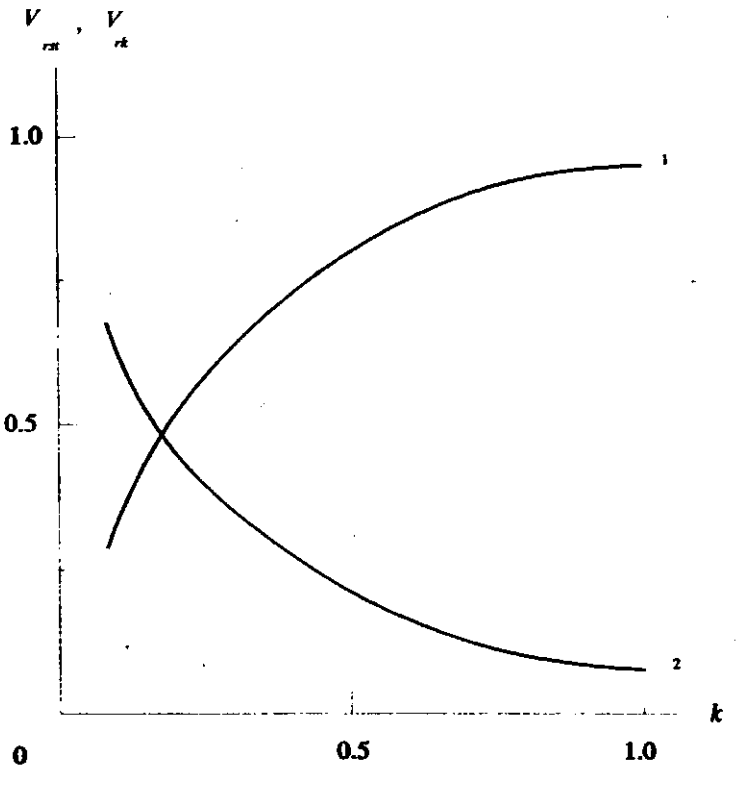

Fig.3.7 Distribution of base polymer volume V_{pol} between structural elements in dependence of the knot parameter k.

Theoretical results.

1 relative volume of struts V_{rst};
2 - relative volume of knot V_k.

Initial calculation data: $Pl = 0.075$, $N = 4$, $a_0 = 10^{-4}$m, λ_n - scheme, $\Delta\theta_E = \Delta\varphi_E = 10°$, $\Delta a = 10^{-4} \times a_0$.

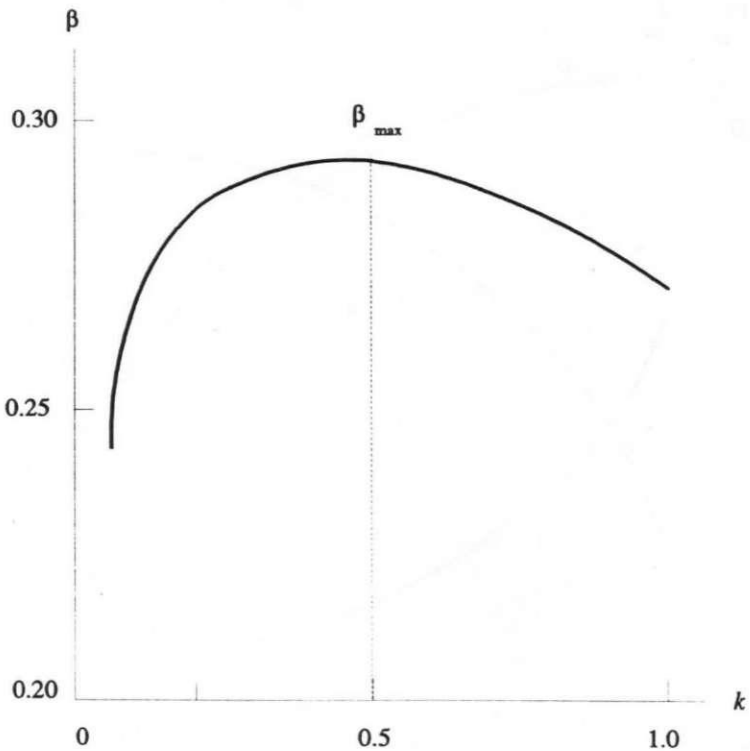

Fig.3.8 Dependence of the strut characteristic β $<t>/l_0$ on knot parameter k.

Theoretical results.

Initial calculation data: $P1 = 0.075$, $N = 4$, $a_0 = 10^{-4}$m, λ_n scheme, $\Delta\theta_E = \Delta\varphi_E = 10°$, $\Delta a = 10^{-4} \times a_0$.

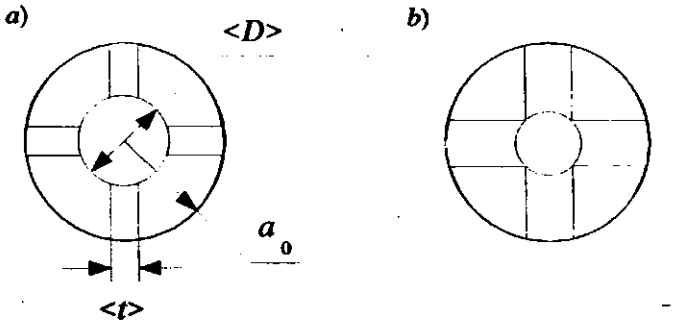

Fig.3.9 Dimensions of the structural elements (a planar scheme).

a) $k = 0.1$, $<t> = 0.31\times10^{-4}$m, $<D> = 0.73\times10^{-4}$m;
b) $k = 0.5$, $<t> = 0.44\times10^{-4}$m, $<D> = 0.46\times10^{-4}$m.

Initial calculation data: $P1 = 0.075$, $N = 4$, $a_0 = 10^{-4}$m, λ_n - scheme, $\Delta\theta_E = \Delta\varphi_E = 10°$, $\Delta a = 10^{-4}\times a_0$.

3.3.2 Dependence of Calculation Results on the State of Strut System

It is important that the effect of the state of strut system on calculation results is known. Strut systems state comprises: the number of struts N, the character of spatial system formed by these struts, dimensions, the spatial orientation and defects of strut system, etc. The calculation data have revealed that the semiaxes hypothesis (3.5) yields the following relationships for semiaxes a_1 and a_2 in various orientations of the strut system:

I. $\varepsilon_{33} < 0$, compression:

$$a_1 = a_2 = a \geq 0 ;$$

$$\text{II. } \varepsilon_{33} > 0 \quad \text{tension} \tag{3.28}$$

$$a_1 = a_2 = a \leq 0$$

It means that compression/tension deformation ε_{33}, applied parallel to rise direction $o3$, causes either a buckling/ shrinking of the strut system in the plane of isotropy in all orientations or there occurs no deformation at all.

In model cells with uniform spatial distribution of the struts based on the cube symmetry ($N = 4, 6, 8$; Fig.2.4), there exist orientations where transversal deformation in plane $o12$ takes place, yet at the same time no energy is consumed:

$$a(\theta_E, \varphi_E) \neq a_0 \; ; \qquad W(\theta_E, \varphi_E) = 0$$

The struts distributed according to the cube symmetry in several orientations make it possible to trace the surface of the deformed model cell through crossing-points of the struts with the surface of an undeformed model cell (Fig.3.10). Then the struts do not change their length and no energy is consumed. This conclusion can also be referred to model cells of the monotropic plastic foams, where a uniform distribution of the struts in space is based on the symmetry of a parallelepiped.

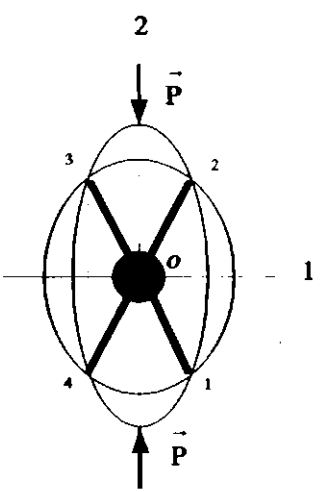

Fig.3.10 Model cell of the isotropic plastic foams, $N = 4$ (a planar scheme).

An orientation where surface of a deformed model cell can be traced through crossing-points of the struts and the surface of an undeformed model cell.

When the number of struts in a model cell of isotropic, as well as monotropic plastic foams is $N = 5, 6$ a uniform distribution of the struts

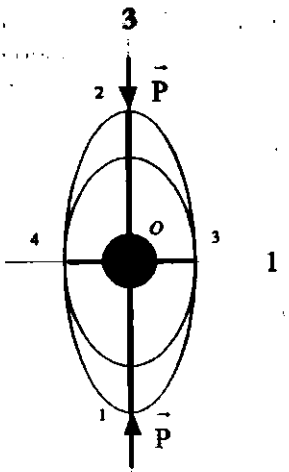

Fig.3.11 Model cell of the isotropic plastic foams, $N = 5$ or 6.

(In the planar scheme the $o2$ axis is perpendicular to the scheme plane and the fifth and sixth struts are not shown).

An orientation where load carrying struts 1 and 2 are perpendicular to the location plane of other struts $o12$.

in space in the body frame of reference is the following (Fig.3.11): two struts are placed on one straight line perpendicular to the plane where the other N 2 struts are situated. In these orientations where the two struts mentioned are situated along $o3$ axis in the laboratory frame of reference, while the others are found in $o12$ plane, the deformation energy is consumed, but no transversal deformation occurs:

$$a(\theta_E, \varphi_E) = a_0 \; ; \qquad W(\theta_E, \varphi_E) \neq 0$$

This situation can be explained in the following manner: the load-carrying struts are situated perpendicular to the location plane of other struts, but mutually perpendicular forces are known to have no interaction. These two kinds of orientations of the strut system will be further called singular orientations.

To evaluate the effect of a slight deviation of some struts from their uniform distribution in space, the spherical coordinate θ_{n0} of the two struts is assigned with an initial deviation $\Delta\theta_0 = 10°$. The calculation results remain unchanged.

In averaging the values to be calculated, the results are independent of the initial orientation of the strut system as a whole in the laboratory frame of reference.

The elastic constants under consideration are independent of the absolute values of the semiaxes a_0 , c_0 of the model cell. For the isotropic plastic foams the dependence of results on the number N of struts entering the knot is quite insignificant. Therefore, the deformation energy minimization and the numerical integration were carried out with increased accuracy:

$$\Delta a = 10^{-5} \times a_0 ; \quad \Delta\theta_E = \Delta\varphi_E = 5^\circ$$

For the monotropic plastic foams, however, the dependence of results on N is greater, and consequently, the calculations were carried out with usual accuracy:

$$\Delta a = 10^{-4} \times a_0 ; \quad \Delta\theta_E = \Delta\varphi_E = 10^\circ$$

The following conclusions may be made basing on the data of Tables 3.4 and 3.5 (Initial calculation data: PUR plastic foams, E_0 = 2300MPa, $P1$ = 0.075, A = 1.0 or A = 3.0, k = 0.1, λ_n scheme, $c = 0.99c_0$ (1% compression), $\Delta\theta_E = \Delta\varphi_E = 5^\circ$, $a_0 = 10^{-4}$ m):

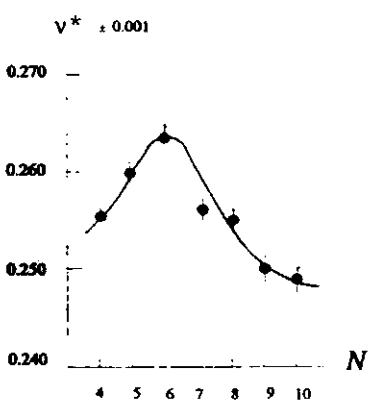

1)Relative dependence of results on N is insignificant for the isotropic plastic foams (Fig.3.12). The effect of N on ν_{31}^* and E_3^* is considerable for the monotropic plastic foams.

Fig.3.12
Dependence of Poisson's ratio of isotropic plastic foams ν^* on the number of struts N in the model cell (Table 3.4).

Table 3.4 Dependence of calculation data on the number N of struts entering the knot (a model cell of the isotropic plastic foams).

N°	N	Range of semiaxis a		$\nu^* \pm \Delta\nu^*$	$E^* \pm \Delta E^*$, MPa	$G^* \pm \Delta G^*$, MPa	$\varepsilon^* \pm \Delta\varepsilon^*$, %	t_{ex}
		$(a_{min} \pm \Delta a) \times 10^{-3}$ m	$(a_{max} \pm \Delta a) \times 10^{-3}$ m					
1	4	0.100124 ±0.000001 (±0.001%)	0.100494 ±0.000001 (±0.001%)	0.256 ±0.001 (±0.4%)	23.552 ±0.001 (±0.004%)	9.374 ±0.008 (±0.1%)	−0.487 ±0.002 (±0.4%)	1'50"
2	5	0.100000	0.100424	0.260	23.214	9.206	−0.487	2'05"
3	6	0.100000	0.100494	0.263	22.858	9.047	−0.473	2'20"
4	7	0.100005	0.100408	0.256	23.511	9.352	−0.486	3'00"
5	8	0.100124	0.100494	0.256	23.552	9.374	−0.487	3'30"
6	9	0.100211	0.100329	0.250	24.154	9.660	−0.499	3'45"
7	10	0.100217	0.100276	0.249	24.192	9.678	−0.500	4'00"

Table 3.5 Dependence of calculation data on the number N of struts entering the knot (a model cell of the monotropic plastic foams).

N°	N	Range of semiaxis a		$\nu_{31}^{*} \pm \Delta\nu_{31}^{*}$	$E_3^{*} \pm \Delta E_3^{*}$, MPa	$\varepsilon^{*} \pm \Delta\varepsilon^{*}$, %	t_{ex}
		$(a_{min} \pm \Delta a) \times 10^{-3}$ m	$(a_{max} \pm \Delta a) \times 10^{-3}$ m				
1	4	0.10013 ±0.00001 (±0.001%)	0.10434 ±0.00001 (±0.001%)	0.96 ±0.01 (±1%)	64.58 ± 0.01 (±0.02%)	0.0092 ±0.0002 (±0.23%)	0'20"
2	6	0.10000	0.10386	1.09	61.31	0.0118	0'25"
3	10	0.10019	0.10176	0.65	72.27	0.0030	0'34"

2) With N increasing, ν_{31}^{*} decreases and E_3^{*} grows: the plastic foams become more rigid. When the value of N is relatively great, the results become stable: the law of great numbers starts operating. With a small number of struts, the results depend on the geometry of strut system ($N = 6$).

3) Since the strut system with $N = 4$ struts is sufficiently representative and the most commonly found in plastic foams it is used in further calculations.

All the previous conclusions can be referred both to model cells without and with knot, as well as to both calculation schemes ($\Delta\varrho_n$ and λ_n).

3.3.3 Analysis of Results and Conclusions

a) Variational Analysis

Deformation $\varepsilon_{11\max}$ corresponding to maximum element $a_{\max}$ of the selection a_n of semiaxis a is about four times greater than deformation $\varepsilon_{11\min}$ corresponding to minimum element $a_{\min}$ (a model cell of the isotropic plastic foams, $N = 4$, Fig.3.13, 1). For monotropic plastic foams, $\varepsilon_{11\max}$ exceeds $\varepsilon_{11\min}$ by one order (Fig.3.13, 2)). Consequently, the structural microsituations θ_{Ei}, φ_{Ej}, ψ_{Ek} are quite different from one another and the averaging of deformation ε_{11} Eq.(3.12) has a physical sense. When the number of struts N becomes greater ($N = 10$), the range of a - values $a_{\min} \leq a \leq a_{\max}$ narrows: the microsituations become equivalent. Theoretically, when N is sufficiently great, the semiaxes are almost equal in all microsituations and no averaging of ε_{11} is necessary:

$$<\varepsilon_{11}> = \varepsilon_{11}(\theta_{Ei}, \varphi_{Ej}, \psi_{Ek})$$

For model cell of the isotropic plastic foams, the averaging can be avoided already when $N \geq 10$ (Fig.3.13, 3)). Usually in practice for plastic foams $N < 10$, and the averaging of ε_{11} can be maintained.

Elements of the selection a_n are not subjected to the normal distribution AS $\neq$ 0, EX $\neq$ 0.

b) Elastic Constants, Isotropic Plastic Foams

When the number of struts is N = 4, 5, ..., 8, the Poisson's coefficient $\nu^* = 0.26$ (Table 3.4). It has been found that the value of ν^* does not depend either on such characteristics of the plastic foams as E_0, $P1$, k, a_0, whether the model cell has or has not a knot. Yet it does depend on N, i.e. the geometry of strut system. The calculated and experimental results have been found to agree well (Fig.3.14) in the limits of $P1$ considered in the present investigation.

When the space filling coefficient of model cell $P1$ increases, the Young's modulus E^* increases, too (Figs.3.15, 3.17 and 3.18). The range of E^*/E_0 values defined by values of knot parameter k ($0.1 \leq k \leq 1.0$) and that calculated for a knotless model cell is situated within the experimental data set E^*/E_0 of various plastic foams [3,9,15,16,17,20,52]. It is impossible to vary values of E^* in the knotless model cell in the limits of $P1$ = const., (Fig.3.16). This leads to E^* = const. and it does not match with the experimental data.The modulus E^* reaches its greatest values when a half of the knot surface is covered by struts: $k = 0.5$ This result agrees well with the theoretical results obtained in [15].

The comparison of the calculated relationships $E^* = E^*(P1)$ (Figs.3.17 and 3.18) with experimental data when PUR and PVC foams are concerned gives a sufficient agreement. For PUR plastic foams, this agreement realizes in a wide range of parameter k values: $0.1 \leq k \leq 1.0$. For PVC plastic foams , the experimental data available are insufficient, and the best agreement has been found for the theoretical curve corresponding to $k = 0.5$.

All the presented statements are correct for both deformation modes of the model cell: according to $\Delta\varrho_n$ and λ_n - scheme.

c) Elastic Constants, Monotropic Plastic Foams

The Poisson's coefficient $\nu_{31}^* = \nu_{31}^*(A)$ depicted in Fig.3.19 is presented together with coefficients ν_{21}^* and ν_{23}^* calculated in Chapter 5. When extension degree A of the model cell increases, ν_{31}^* increases, too,

and this agrees well with the experimental data. If the deformation energy is determined according to the $\Delta\varrho_n$ - scheme, ν_{31}^* increases very slightly, and it contradicts with the experimental data. Effect of a knot of the model cell, as well as the parameter k is so small that it can be neglected. The calculations have revealed, however, a slight dependence of ν_{31}^* on the number of struts N. As a result it can be generalized that the Poisson's coefficients are governed by the following relationships:

$$\nu_{31}^* \geq \nu_{21}^* \geq \nu_{23}^*$$

which has been confirmed experimentally in Table 3.6, [32].

The Young's modulus $E_3^* = E_3^*(P1)$ depicted in Figs.3.21 and 3.22 is presented together with moduli E_1^*, E_2^* calculated in Chapter 7. In calculations it has been assumed that $A = 1.05$, $k = 0.1$ for the PUR plastic foams and $A = 1.5$, $k = 0.5$ for the PVC plastic foams. It can be generalized that:

$$E_3^* > E_1^* , E_2^* \qquad \text{when } A > 1.$$

The agreement with the experimental data is sufficient. All the calculations were performed according to the λ_n - scheme, because data given by the $\Delta\varrho_n$ scheme contradicted with the experimental data.

There are no direct experimental data available to the author for the relationship $E_3^* = E_3^*(A)$, Fig.3.23. Yet judging from photographs [8,11,20] the icrease of A is associated with an additional orientation of load - carrying elements - struts in the direction of $o3$ axis. Accordingly, it can be expected that E_1^* and E_2^* will, at least, remain constant or decrease, while E_3^* will increase. This consideration has been also confirmed by experimental data of relationship $E_3^*/E_1^* = f(A)$, Fig.3.20, [52] where relation E_3^*/E_1^* ($E_3^*/E_1^* = E_3^*/E_2^*$) increases rapidly with the growth of A. Modulus E_3^* calculated according to the $\Delta\varrho_n$ - scheme increases too slowly compared with the experimental data presented in Fig.3.20.

The theoretical results concerning modulus are equal both for tension and compression (in the limits of calculation process errors). Experimental data show (Figs.3.17 and 3.18) that Young's modulus for light-weight foams is usually greater in tension than in compression tests. This happens because of reorientation of the load-carrying elements struts in the direction of tension load [52]. As it can be seen from Figs.3.17 and 3.18 the theoretical results are situated between experimental data of tension/compression tests.

Conclusions

1. A knotless model cell does not allow to describe all the variety of plastic foams structural and deformative properties possible for $P1 = \text{const}$.

2. The elastic constants calculated according to the $\Delta\varrho_n$ - scheme do not always agree well with the experimental data.

3. The elastic constants ν^*, E^*, ν_{31}^*, E_3^* calculated for a model cell with a knot and according to the λ_n - scheme exhibit good agreement with the experimental data.

4. The theoretical results of Young's modulus and Poisson's coefficients concerned are equal for tension and compression .

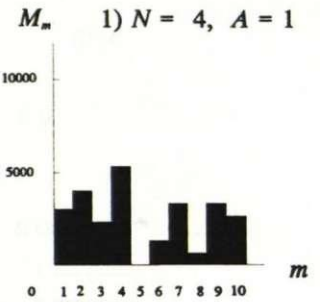

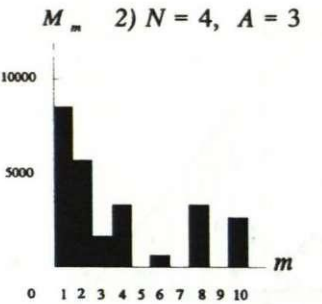

$a_{min} = 0.100130 \times 10^{-3}$ m;
$a_{max} = 0.100494 \times 10^{-3}$ m;
$\bar{a}_4 = 0.100257 \times 10^{-3}$ m.

$a_{min} = 0.100129 \times 10^{-3}$ m;
$a_{max} = 0.104343 \times 10^{-3}$ m;
$\bar{a}_1 = 0.100340 \times 10^{-3}$ m.

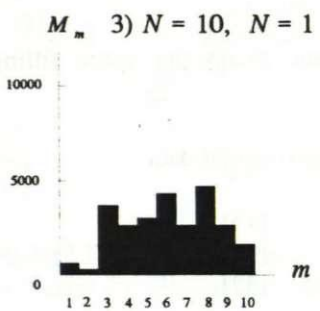

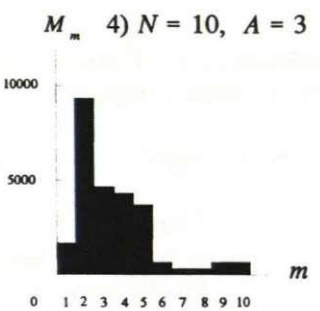

$a_{min} = 0.10022 \times 10^{-3}$ m;
$a_{max} = 0.10028 \times 10^{-3}$ m;
$\bar{a}_8 = 0.10026 \times 10^{-3}$ m.

$a_{min} = 0.10019 \times 10^{-3}$ m;
$a_{max} = 0.10176 \times 10^{-3}$ m;
$\bar{a}_2 = 0.10042 \times 10^{-3}$ m.

Fig.3.13 Histograms of variational series of selection a_n.

Initial calculation data: $k = 0.1$, $c = 0.99c_0$ (1% compression), λ_n - scheme, $\Delta\theta_E = \Delta\varphi_E = \Delta\psi_E = 10°$, $\Delta a = 10^{-5} \times a_0$.

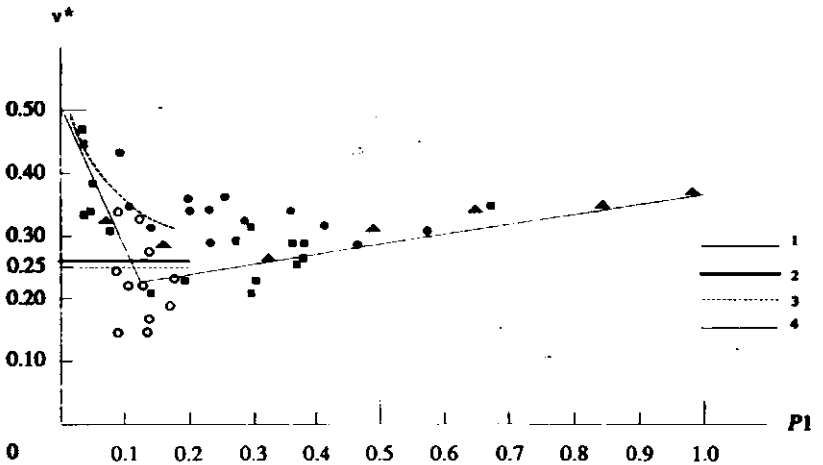

Fig.3.14 Dependence of Poisson's coefficient ν^* on the space filling coefficient Pl. Isotropic plastic foams.

Theoretical results:		Experimental data:	
1	[20];	○	[15];
2	present investigat.	●	- [9];
3	[9,15];	■, ▲	[32].
4	[32].		

Initial calculation data: $N = 4$, $k = 0.1$, $A = 1$, $c = 0.99c_0$ (1% compression), $\Delta\varrho_n$ and λ_n - schemes, $\Delta\theta_E = \Delta\varphi_E = 10°$, $\Delta a = 10^{-4} \times a_0$.

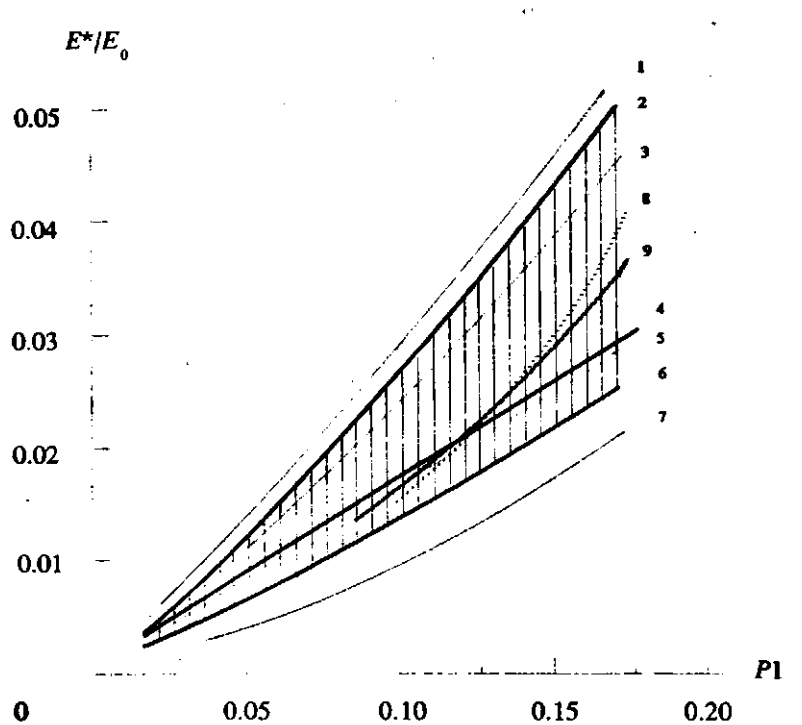

Fig.3.15 Dependence of relative Young's modulus E^*/E_0 on the space filling coefficient $P1$. Elastic and rigid isotropic plastic foams.

Theoretical results:
- Shaded area - $0.1 \leq k \leq 1.0$;
- 2 - $k = 0.5$;
- 3 - $k = 1.0$;
- 5 - no knot model cell;
- 6 - $k = 0.1$.

Experimental data:
- 1,7 [52,3];
- 4 empiric relationship $E^*/E_0 = 1/6\ P1$, [19];
- 1÷7 [16,17,52,20,9,15];
- 8,9 - elastic latex foams [9,15].

Initial calculation data: $P1 = 0.075$, $N = 4$, $0.1 \leq k \leq 1.0$, $A = 1$, $c = 0.99c_0$ (1% compression), $\Delta\varrho_n$ and λ_n schemes, $\Delta\theta_E = \Delta\varphi_E = 10°$, $\Delta a = 10^{-4} \times a_0$.

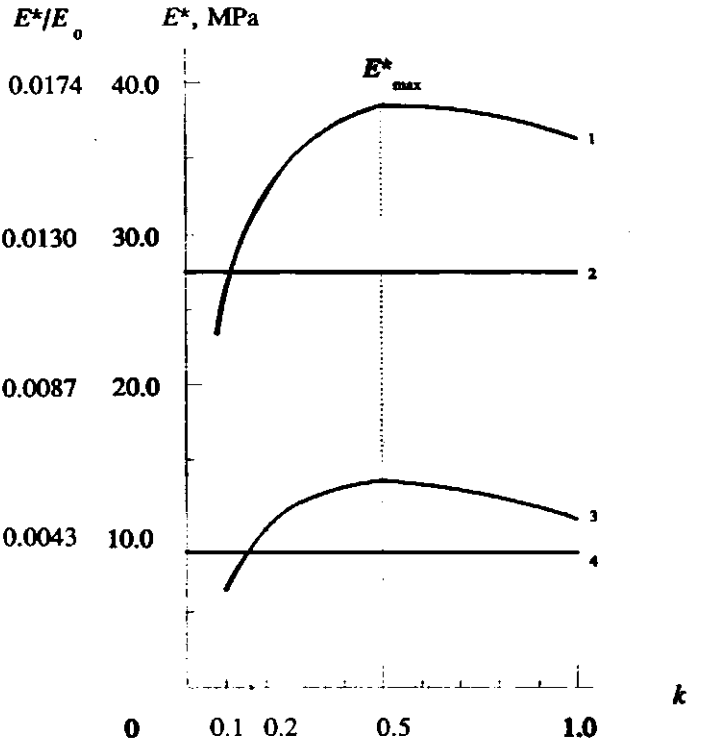

Fig.3.16 Dependence of relative Young's modulus E^*/E_0 on the knot parameter k. Isotropic plastic foams.

Theoretical results.

1 $P1 = 0.075$;
2 $P1 = 0.075$, no knot model cell;
3 $P1 = 0.025$;
4 $P1 = 0.025$, no knot model cell.

Initial calculation data: $E_0 = 2300$MPa, $A = 1$, $N = 4$, $c = 0.99c_0$ (1% compression), $\Delta\varrho_n$ - scheme, λ_n - scheme, $\Delta\theta_E = \Delta\varphi_E = 10°$, $\Delta a = 10^{-4} \times a_0$.

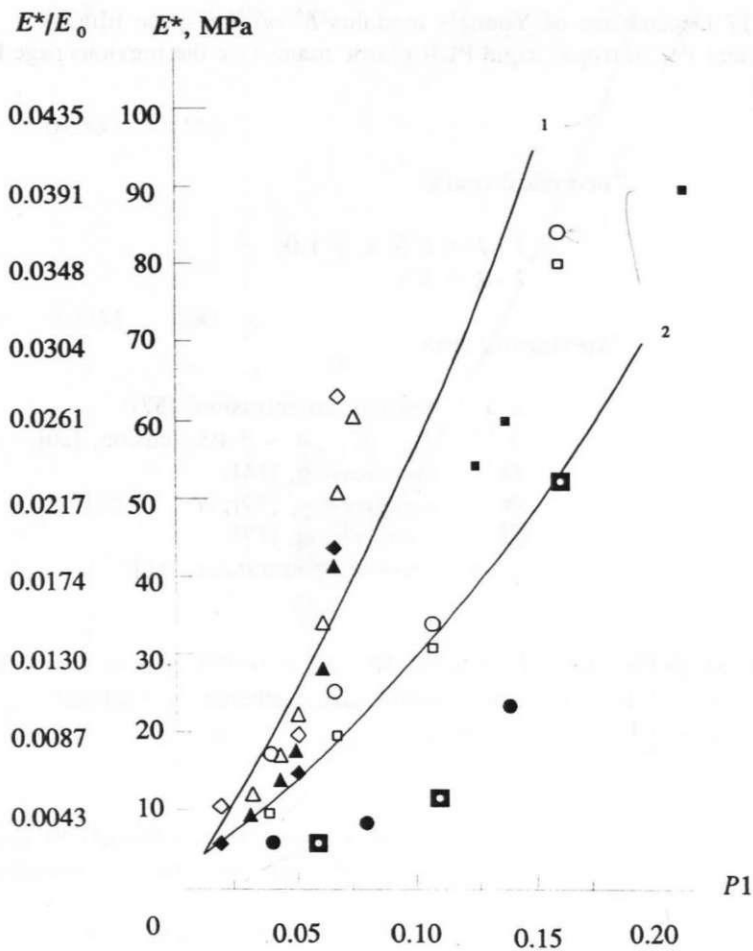

Fig.3.17 Dependence of Young's modulus E^{-} on the space filling coefficient $P1$. Isotropic, rigid PUR plastic foams (see the next page for initial calculation data).

Fig.3.17 Dependence of Young's modulus E^* on the space filling coefficient $P1$. Isotropic, rigid PUR plastic foams (see the previous page for graph).

Theoretical results:

1 - $k = 0.5$, $k = 1.0$;
2 - $k = 0.1$.

Experimental data:

▵, ▲ - tension, compression, [52];
○, □ - E^*_3, E^*_1, $A \approx 1.05$, tension, [20];
■ - compression, [14];
● - compression, [19];
◘ - compression, [17];
◇, ◆ tension, compression, [16].

Initial calculation data: $E_0 = 2300$MPa, $P1 = 0.075$, $N = 4$, $k = 0.1$, $A = 1$, $c = 0.99c_0$ (1% compression), $\Delta\varrho_n$ - scheme, λ_n - scheme, $\Delta\theta_E = \Delta\varphi_E = 10°$, $\Delta a = 10^{-4} \times a_0$.

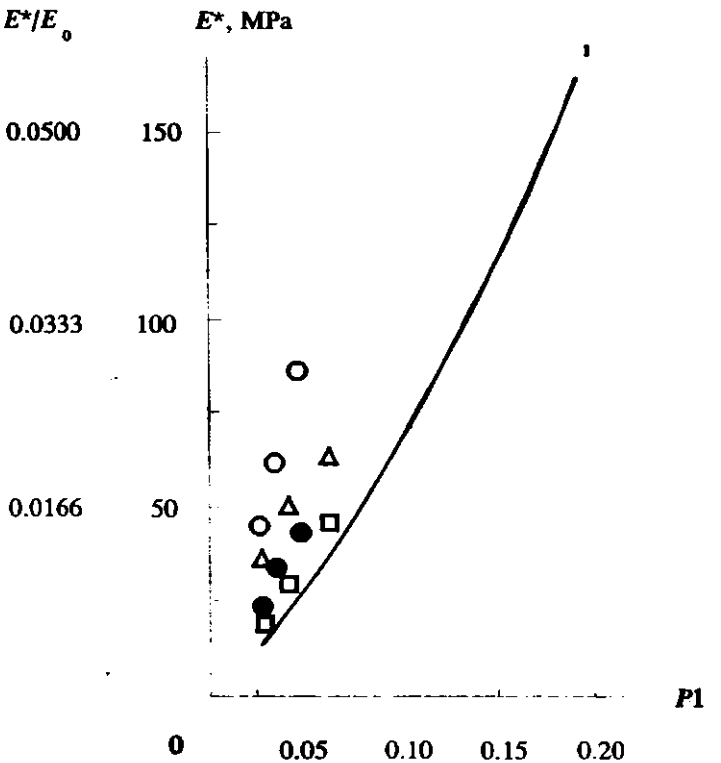

Fig.3.18 Dependence of Young's modulus E^* on the space filling coefficient $P1$. Isotropic, rigid PVC plastic foams.

Theoretical results.
1 present investigation.

Experimental data:
○, ● tension, compression, [52];
△, □ - E_3^*, E_1^*, $A \approx 1.50$, tension, [20].

Initial calculation data: $E_0 = 3000$MPa, $N = 4$, $k = 0.5$, $A = 1$ $c = 0.99c_0$ (1% compression), λ_n and $\Delta\varrho_n$ schemes, $\Delta\theta_E = \Delta\varphi_E = 10°$, $\Delta a = 10^{-4} \times a_0$.

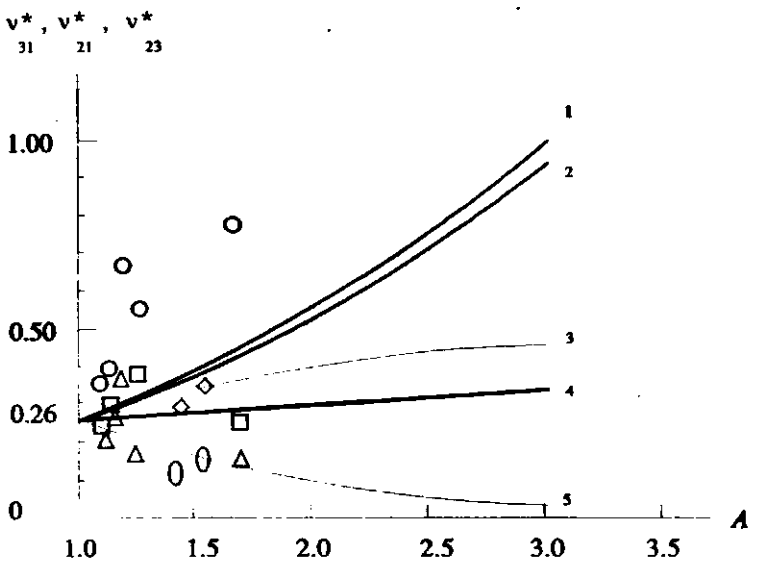

Fig.3.19 Dependence of Poisson's coefficients ν_{31}^*, ν_{21}^*, ν_{23}^* on the extension degree A of model cell. Monotropic, rigid plastic foams.

Theoretical results:			Experimental data:	
1	ν_{31}	$k = 0.5$, $k = 1.0$;	◇,0	ν_{31}^*, ν_{23}^*, [18],
2	ν_{31}^*	$k = 0.1$;		loading mode
3	ν_{21}^*	$k = 0.1$, $k = 0.5$;		unknown;
4	ν_{31}^*	$k = 0.1$, $\Delta\varrho_n$ scheme;	○,□,△	ν_{31}^* ν_{21}^* ν_{23}^*,
5	ν_{23}^*	$k = 0.1$, $k = 0.5$.		tension in Table 3.6, [32].

Initial calculation data: $P1 = 0.075$, $N = 4$, $c = 1.01c_0$ (1% tension), λ_n scheme, $\Delta\theta_E = \Delta\varphi_E = 10°$, $\Delta a = 10^{-4} \times a_0$.

Table 3.6 Experimental data for Poisson's coefficients ν_{31}^{*} ν_{21}^{*} ν_{23}^{*} of various monotropic, rigid plastic foams in tension (T) and compression (C), [18,32,34].

N°	Foams	ν_{31}^{*}		ν_{21}^{*}		ν_{23}^{*}		$\nu_{31}^{*}/\nu_{23}^{*}$		A , **)	
		T	C	T	C	T	C	T	C	T	C
1	PI-1, plastic, [32].	0.33	0.33	0.23		0.22		1.50		1.12	
2	PUR-305, plastic, [32].	0.40	0.39	0.30	0.32	0.26	0.25	1.54	1.56	1.16	1.32
3	PUR-3, plastic, [34].	0.69			–	0.38	–	1.82	–	1.24	
										1.20 (exp.)	
4	PUR-305, plastic, [32].	0.57	0.56	0.39	0.38	0.30	0.30	1.90	1.87	1.25	1.43
										1.30 (exp.)	
5	Carbon, [18].	0.25				0.12		2.08		1.48	
6	Carbon, [18].	0.33				0.15		2.20		1.50	
7	PUR-3, plastic, [32].	0.77	0.75	0.24	0.25	0.18	0.19	4.28	3.95	1.70	1.86

**) The degree of monotropy A is determined after relation $\nu_{31}^{*}/\nu_{23}^{*}$ using experimental data from [52], Fig.3.19.

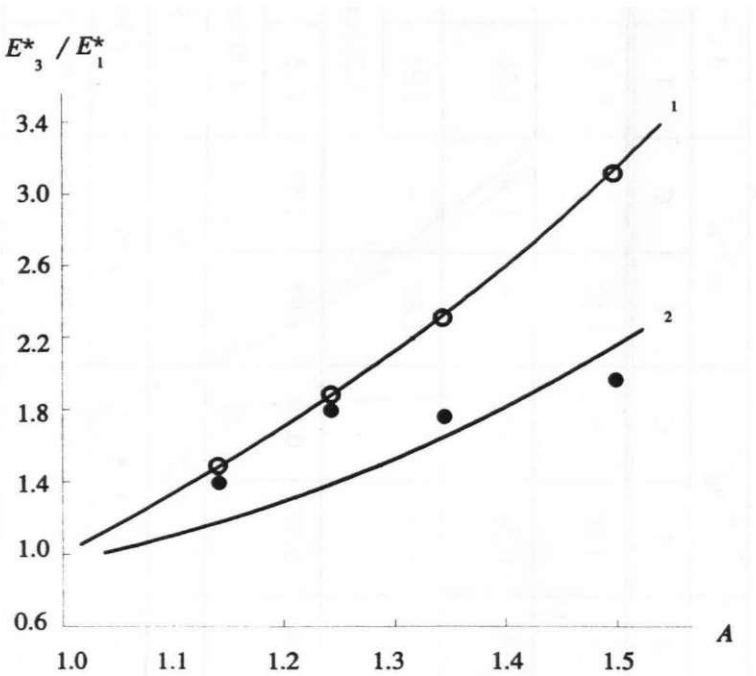

Fig.3.20 Experimental data for relationship E_3^*/E_1^* in dependence of degree of anisotropy A of elastic PUR plastic foams, [52].

○ tension;
● - compression.

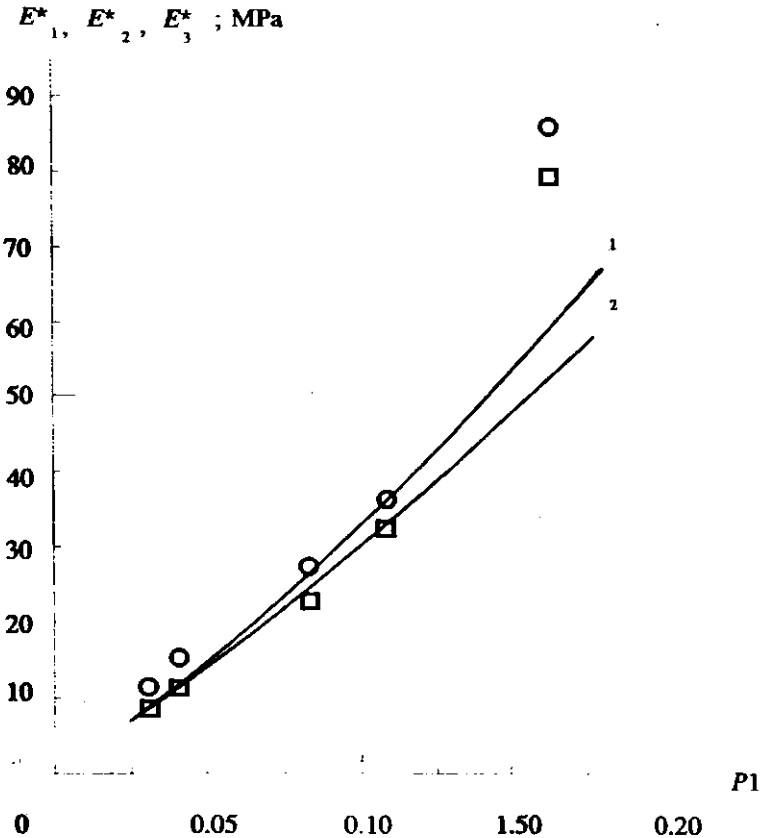

Fig.3.21 Dependence of Young's moduli E_1^*, E_2^*, E_3^* on the space filling coefficient $P1$. Monotropic, rigid PUR plastic foams.

Theoretical results:

1 Young's modulus E_3^*;
2 Young's moduli E_1^* E_2^*

Experimental data:

○,□ E_3^*, E_1^* tension, [20].

Initial calculation data: E_0 = 2300MPa, k = 0.1, A = 1.05, N = 4, c = 1.01c_0 (1% tension), λ_n scheme, $\Delta\theta_E = \Delta\varphi_E = 10°$, $\Delta a = 10^{-4} \times a_0$.

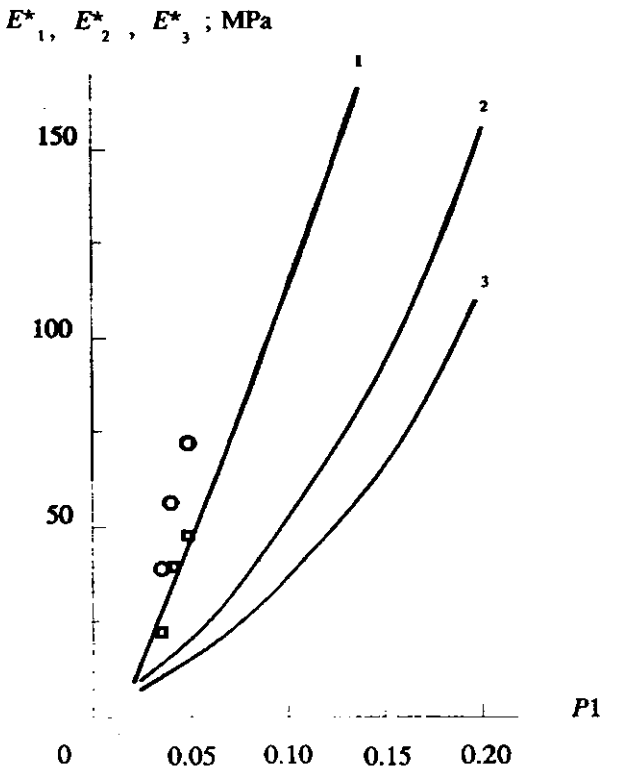

Fig.3.22 Dependence of Young's moduli E_1^*, E_2^*, E_3^* on the space filling coefficient $P1$. Monotropic, rigid PVC plastic foams.

Theoretical results:

1 E_3^*;
2 E^*, isotropic foams;
3 E_1^* E_2^*

Experimental data:

○,□ - E_3^*, E_1^* tension, [20].

Initial calculation data: E_0 = 3000MPa, k = 0.5, A = 1.5, N = 4, c = 1.01c_0 (1% tension), λ_n scheme, $\Delta\theta_E = \Delta\varphi_E = 10°$, $\Delta a = 10^{-4} \times a_0$.

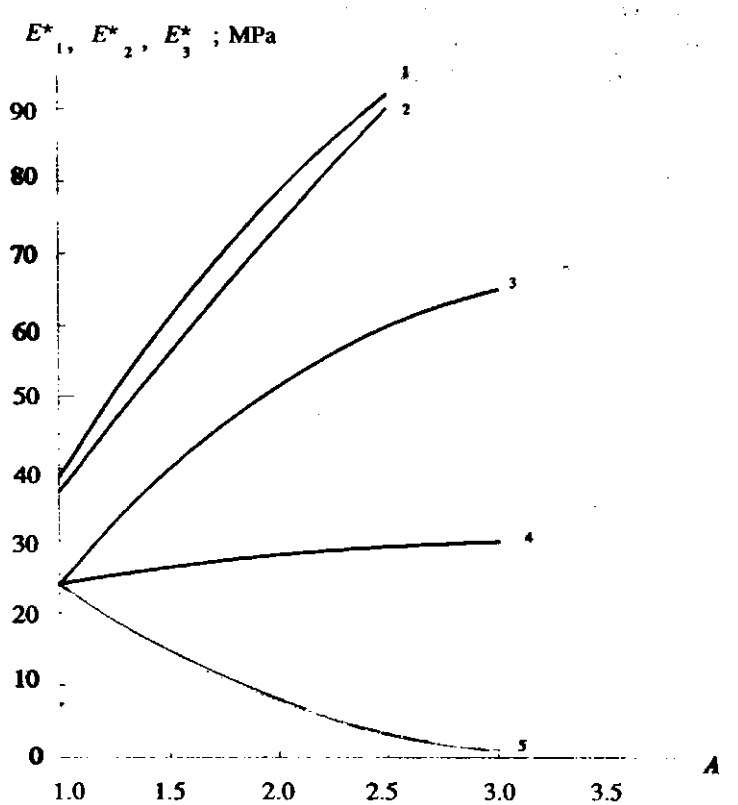

Fig.3.23 Dependence of Young's moduli E_1^* E_2^*, E_3^* on the extension degree A. Monotropic, rigid PUR plastic foams.

Theoretical results:

1 E_3^* $k = 0.5$;
2 E_3^* $k = 1.0$;
3 E_3^* $k = 0.1$;
4 E_3^*, $k = 0.1$, $\Delta\varrho_n$ scheme;
5 E_1^* E_2^*, $k = 0.1$.

Initial calculation data: $E_0 = 2300$MPa, $P1 = 0.075$, $N = 4$, $c = 0.99c_0$ (1% compression), λ_n - scheme, $\Delta\theta_E = \Delta\varphi_E = 10°$, $\Delta a = 10^{-4} \times a_0$.

4 Deformative Properties in Compression/Tension Applied Parallel to Rise Direction (Volume Deformation Hypothesis)

4.1 Mathematical Model

4.1.1 Effective Moduli

In Chapter 3 the calculation of moduli ν_{31}^*, ν_{32}^* and E_3^* has been based on the hypothesis (3.5) that a model cell shaped as a rotational ellipsoid retains the same form after deformation applied parallel to the rise direction. However, deformation of the model cell subjected to the loading parallel to the rise direction can be defined otherwise, yet in an equivalent manner. Macroproperty of plastic foams concerning their experimentally measurable effective relative volume deformation ε^* is also related to the model cell. The relative volume deformation of the model cell ε is assumed to be numerically equal to ε^* and to remain constant in all microsituations (the volume deformation hypothesis):

$$\varepsilon(\theta_E,\varphi_E,\psi_E) = \varepsilon^* = \text{const.} \tag{4.1}$$

According to numerical calculations when hypothesis (4.1) is assumed (Section 4.3), semiaxes a_1 and a_2 are mutually linked, but not obligatory equal (Fig. 4.1):

$$a_2(\theta_E,\varphi_E,\psi_E) = \frac{a_0^2\, c_0\, (1 + \varepsilon^*)}{c\; a_1(\theta_E,\varphi_E,\psi_E)} \tag{4.2}$$

It can be generalized that assuming the tie condition (4.2) the post-deformation form of model cell in various microsituations can be a rotational, as well as a three-axial ellipsoid.

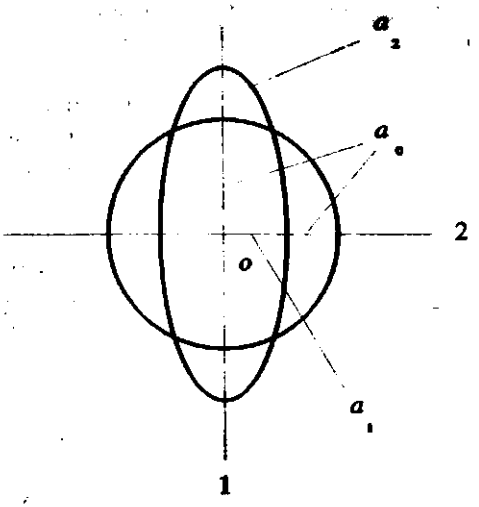

Fig.4.1
Deformation of model cell in the isotropy plane $o12$ by the strain applied parallel to the axis of monotropy $o3$ and the volume deformation hypothesis 4.1 assumed.

Then effective Poisson's coefficients ν_{31}^*, ν_{32}^* and effective Young's modulus E_3^* can be expressed as follows:

$$\nu_{31}^* \quad <\varepsilon_{11}>/\ \varepsilon_{33} \qquad \nu_{32}^* \quad <\varepsilon_{22}>/\ \varepsilon_{33}$$

$$E_3^* = <\sigma_{33}>/\ \varepsilon_{33} \tag{4.3}$$

where $<\varepsilon_{11}>$, $<\varepsilon_{22}>$ and $<\sigma_{33}>$ are calculated according to Eq.(2.9). Then the semiaxes a_1 a_2 of model cell after deformation have to be determined from

$$\varepsilon_{11}(\theta_E,\varphi_E,\psi_E) \quad \frac{a_1(\theta_E,\varphi_E,\psi_E) \quad a_0}{a_0}$$

$$\varepsilon_{22}(\theta_E,\varphi_E,\psi_E) \quad \frac{a_2(\theta_E,\varphi_E,\psi_E) - a_0}{a_0} \tag{4.4}$$

With other considerations similar to those in Paragraph 3.1.1, a_1 and a_2 are calculated from the local structure model cell using variational analysis of the post-deformation form a_1, a_2, c of model cell and the deformation

energy (4.5), (4.6) or (4.7), (4.8) minimization (3.4). The tie condition (4.2) allows to reduce the two-argument minimization of energy function to one-argument minimization.

To calculate ν_{31}^* ν_{32}^*, E_3^* from Eq.(4.3) in a wide range of extension degree $A = c_0/a_0$ of the model cell, the experimental data for relationship $\varepsilon^* = \varepsilon^*(A)$ should be known. However, such data are not available to the author. Moduli ν_{31}^*, ν_{32}^*, E_3^* calculated in Chapter 3 agree well with the experimental data (Paragraph 3.3.2). Then the effective volume deformation ε^* calculated from Eq.(3.6) can also be considered to be in good agreement with the experimental data. Therefore, in further calculations will be used those numerical values of ε^*, which have been obtained in Chapter 3 using the semiaxes hypothesis.

4.1.2 Deformation Energy (ΔQ_n - Calculation Scheme)

Since the post-deformation form of model cell is a three-axial ellipsoid with determined semiaxis c, $a_1(\theta_E,\varphi_E,\psi_E)$, $a_2(\theta_E,\varphi_E,\psi_E)$ are the semiaxes to be calculated. Considerations are similar to those in Paragraph 3.1.2. Then deformation energy of a knotless model cell can be expressed as follows:

$$W(a_1,a_2,\theta_E,\varphi_E,\psi_E) \qquad \frac{E_0 F}{2a_0c_0} \sum_{n=1}^{N} \sqrt{f_{n0}} \times$$

$$\times \left[\frac{a_1(\theta_E,\varphi_E\psi_E)\; a_2(\theta_E,\varphi_E\psi_E)\; c}{\sqrt{f_{n1}}} \qquad \frac{a_0c_0}{\sqrt{f_{n0}}} \right]^2 \tag{4.5}$$

where $f_{n0} = c_0^2\sin^2\theta_n' + a_0^2\cos^2\theta_n'$

$$f_{n1} \quad [\, a_2(\theta_E,\varphi_E,\psi_E)c \sin\theta_E'\cos\varphi_n \,]^2 +$$

$$+ [\, a_1(\theta_E,\varphi_E,\psi_E)c \sin\theta_E'\sin\varphi_n \,]^2 +$$

$$+ [\, a_1(\theta_E,\varphi_E,\psi_E)\, a_2(\theta_E,\varphi_E,\psi_E)\, \cos\theta_n' \,]^2 \qquad n = 1,2,\ldots,N$$

If the model cell of local structure has a knot, then:

$$W(a_1,a_2,\theta_E,\varphi_E,\psi_E) \qquad \frac{E_0 F}{2} \sum_{n=1}^{N} \frac{(r_n - r_{n0})^2}{r_{n0} - D/2} \tag{4.6}$$

where $r_{n0} = a_0\, c_0 / \sqrt{f_{n0}}$ $\quad r_n = a_1\, a_2\, c / \sqrt{f_{n1}}$

Expressions of the deformation energy (4.5) and (4.6) comprise a spherical coordinate φ_n of the n-th strut. In Section 2.2 it has been proved that $\varphi_n = \varphi_n(\theta_E,\varphi_E,\psi_E)$. Then semiaxes a_1, a_2, strains ε_{11}, ε_{22} and stress σ_{33} in every microsituation depend on all the three Euler's angles θ_E, φ_E, ψ_E.

The values of $\varepsilon_{11}(\theta_E,\varphi_E,\psi_E)$, $\varepsilon_{22}(\theta_E,\varphi_E,\psi_E)$ calculated from the model cell of local structure are related to the point of plastic foams when foams are considered as a continuous medium. Therefore, average strains $<\varepsilon_{11}>$ and $<\varepsilon_{22}>$ in the plane of isotropy can be derived from Eq.(4.4) and (2.9).

4.1.3 Deformation Energy (λ_n - Calculation Scheme)

With considerations similar to those in Paragraph 3.1.3, the deformation energy of a knotless model cell can be expressed as follows:

$$W(\lambda_1,\lambda_2,\theta_E,\varphi_E,\psi_E) \qquad \frac{E_0 F}{2} \sum_{n=1}^{N} [\, \lambda_{n1}(\lambda_1,\lambda_2,\theta_E,\varphi_E,\psi_E) - 1 \,]^2\, \varrho_{n0}(\theta_E,\varphi_E),$$

where $\lambda_1(\theta_E,\varphi_E,\psi_E) \qquad a_1(\theta_E,\varphi_E,\psi_E) / a_0$;

$$\lambda_2(\theta_E,\varphi_E,\psi_E) = a_2(\theta_E,\varphi_E,\psi_E) / a_0 . \tag{4.7}$$

λ_{nT} is calculated from Eq.(3.13) and ϱ_{n0} from Eq.(3.8).
If the model cell of local structure has a knot then:

$$W(\lambda_1,\lambda_2,\theta_E,\varphi_E,\psi_E) \qquad \frac{E_0 F}{2} \sum_{n=1}^{N} [\, \lambda_{nc}(\lambda_1,\lambda_2,\theta_E,\varphi_E,\psi_E) - 1 \,]^2 \times$$

$$\times [\, r_{n0}(\theta_E,\varphi_E) - D/2 \,], \qquad (4.8)$$

where λ_{nc} is calculated from Eq.(3.16) and r_{n0} from Eq.(3.11).

Average strains $<\varepsilon_{11}>$ $<\varepsilon_{22}>$ in the plane of isotropy can be derived from Eq.(4.4) and (2.9).

4.1.4 Average Stress

The average stress is defined for the local model cell of a continuous medium. Post-deformation form of the model cell can be either a rotational, or a three-axial ellipsoid, Eq.(4.2). Theoretical considerations are equal to those described in Paragraph 3.1.4, except the post-deformation form of model cell which is approximated now with an ellipsoidal and not a circular cylinder. Then, the stress in every microsituation is the following:

$$\sigma_{33}(\theta_E,\varphi_E,\psi_E) \qquad \frac{P(\,\theta_E,\varphi_E\psi_E\,)}{\pi\, R_1(\,\theta_E,\varphi_E\psi_E\,)\, R_2(\,\theta_E,\varphi_E\psi_E\,)}$$

where $P(\theta_E,\varphi_E,\psi_E)$ is a force applied to the model cell, and $R_1(\theta_E,\varphi_E,\psi_E)$, $R_2(\theta_E,\varphi_E,\psi_E)$ are semiaxes of cylinders base ellipse.

To calculate product R_1R_2, heights and volumes of the ellipsoid and the cylinder are assumed to be equal: $V_{mc} = V_e = V_{cyl}$. Since:

$$V_e = 4/3\pi\, c\, a_1(\theta_E,\varphi_E,\psi_E) a_2(\theta_E,\varphi_E,\psi_E);$$

$$V_{cyl} = 2\pi\, c\, R_1(\theta_E,\varphi_E,\psi_E) R_2(\theta_E,\varphi_E,\psi_E), \quad \text{then}$$

$$R_1(\theta_E,\varphi_E,\psi_E) R_2(\theta_E,\varphi_E,\psi_E) = 2/3\; a_1(\theta_E,\varphi_E,\psi_E) a_2(\theta_E,\varphi_E,\psi_E).$$

Force P in every microsituation can be calculated from the model cell of local structure:

$$P(\theta_E,\varphi_E,\psi_E) = W(\theta_E,\varphi_E,\psi_E)/\Delta c.$$

On the other hand, according to Paragraph 3.1.4:

$$P(\theta_E,\varphi_E,\psi_E) = \frac{1}{c - c_0} \min \sum_{n=1}^{N} W_n(\, a_1, a_2, \theta_E, \varphi_E \psi_E \,)$$

Hence, stress σ_{33} can be calculated in every microsituation θ_E, φ_E, ψ_E:

$$\sigma_{33}(\theta_E,\varphi_E,\psi_E) = \frac{3}{2\pi(c - c_0)} \frac{\min \sum_{n=1}^{N} W_n(\, a_1, a_2, \theta_E, \varphi_E \psi_E \,)}{a_1(\, \theta_E, \varphi_E \psi_E \,)\; a_2(\, \theta_E, \varphi_E \psi_E \,)}, \quad (4.9)$$

where W_n is derived from Eqs.(4.5), (4.6) or (4.7), (4.8). Then the average stress $<\sigma_{33}>$ is calculated using Eqs.(4.9) and (2.9).

4.2 Numerical Calculations

Parameters used for the numerical calculations are similar to those described in Paragraph 3.2.1. The numerical value of strain ε_{33} applied to model cell has been restricted, for a greater versatility of the mathematical model, to $|\, \varepsilon_{33} \,| \leq 1\%$ The calculations have been carried out according to programmes depicted in Figs.3.4 and 4.2. In conformity with control calculations, numerical integration steps $\Delta\theta_E = \Delta\varphi_E = \Delta\psi_E = 10°$ provided sufficient accuracy of the data obtained. Analysis of variational series was carried out for a selections of semiaxes a_{1n} and a_{2n}, $n = 1,2,\ldots, NN$.

Variational analysis of the post-deformation form of model cell was carried out with a step $\Delta a_1 = 10^{-4} \times a_0$ Effect of Δa_1 on the calculation data was evaluated

$$|\Delta \nu_{31}^*| \leq \left| \frac{\Delta a_1}{a_0 \varepsilon_{33}} \right|$$

$$|\Delta \nu_{32}^*| \leq \left| \frac{a_0 c_0}{8\pi^2 \varepsilon_{33} c} \right| \int_0^{2\pi} \int_0^{2\pi} \int_0^{\pi} \left[\frac{\Delta \varepsilon^*}{a_1} + \left| \frac{(1 + \varepsilon^*)\Delta a_1}{a_1^2} \right| \right] \times$$

$$\times \sin \theta_E d\theta_E d\varphi_E d\psi_E;$$

$$|\Delta E_3^*| \leq \left| \frac{3}{16\pi^3 (c - c_0)\varepsilon_{33}} \right| \int_0^{2\pi} \int_0^{2\pi} \int_0^{\pi} \left[\left| \frac{\Delta W}{a_1 a_2} \right| + \right.$$

$$\left. \left| \frac{W \Delta a_1}{a_1^2 a_2} \right| \left| \frac{W \Delta a_1}{a_1 a_2^2} \right| \right] \sin \theta_E d\theta_E d\varphi_E d\psi_E;$$

$$|\Delta G^*| \leq \frac{|\Delta E^*|}{2(1 + \nu^*)} + \frac{E^*}{2(1 + \nu^*)} |\Delta \nu^*|$$

where $\Delta W = W(a_1 \pm \Delta a_1) - W(a_1)$;

ν^* E^*, G^* are effective constants of isotropic plastic foams;

ε^*, $\Delta \varepsilon^*$ are calculated according to the mathematical model described in Chapter 3.

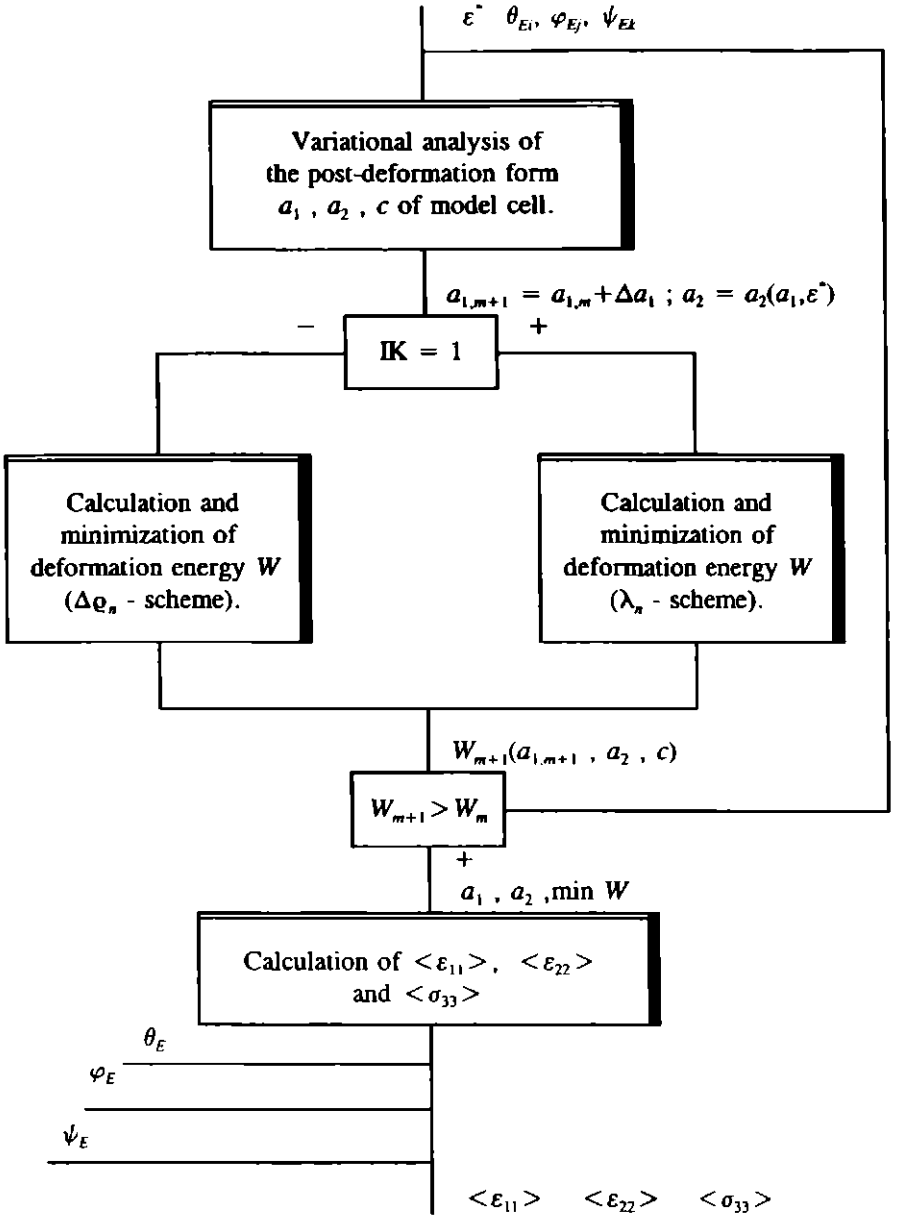

Fig.4.2 Calculation blocks corresponding to deformation ε_{33} in the programme "CONSTANTS" (Fig.3.4) when the hypothesis of volume deformation is assumed.

4.3 Analysis of Results and Conclusions

The calculation results when the hypothesis of volume deformation (4.1) is applied, have revealed the following relationships between the semiaxes a_1 and a_2 in various orientations of the strut system:

I. $\varepsilon_{33} < 0$, compression

1) $a_1 \leq a_0$, $a_2 \leq a_0$;

2) $a_1 > a_0$, $a_2 < a_0$;

3) $a_1 < a_0$, $a_2 > a_0$

II. $\varepsilon_{33} > 0$, tension

1) $a_1 \geq a_0$, $a_2 \geq a_0$;

2) $a_1 > a_0$, $a_2 < a_0$;

3) $a_1 < a_0$, $a_2 > a_0$

It means that in several orientations compression/tension ε_{33} causes buckling/shrinking of the strut system in the plane of isotropy along both semiaxes a_1 , a_2 ; or no deformation occurs at all. Unlike to the model cell deformation (3.28) according to semiaxes hypothesis, there are now also such orientations where shrinking may occur along one semiaxis and buckling along the other: I.2) I.3) and II.2) ; II.3) The other conclusions about effect of the state of strut system on the calculation results are the same as those described in Paragraph 3.3.2.

Semiaxes with corresponding great deformations, for example:

$$a_1 = a_{1\min} = 0.9319 \times 10^{-4} \text{ m} ; \quad \varepsilon_{11} = -7\%$$

have appeared (Fig.4.3) in value sets of a_1 and a_2 in distinction to those calculated in Chapter 3. Since the strains ε_{11} , ε_{22} corresponding to various values of semiaxes a_1 , a_2 are mutually very different, the averaging of ε_{11} and ε_{22} when $N < 10$ has a physical sense. The elements of selections a_{1n} , a_{2n} are not subjected to normal distribution.

Conclusions

The calculation results depicted in Figs.4.4 to 4.9 allow us to draw the following conclusions (as calculation of constants ν_{31}^{-}, E_3^{-} when $A > 2$ on personal computer was extremely time-consuming it was omitted):

1. The calculations based on the semiaxes (Chapter 3) and volume deformation (Chapter 4) hypothesis provide results, which practically coincide both for the isotropic and monotropic foams. Both mathematical models are mutually compatible.

2. The two mathematical models suggested for deformation of plastic foams parallel to rise direction $o3$ are equivalent.

3. The theoretical results of Young's modulus and Poisson's coefficients concerned are equal for tension and compression.

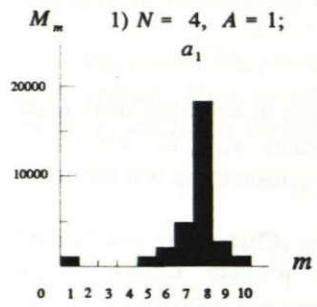

$a_{1\min} = 0.9609\times10^{-4}$ m;
$a_{1\max} = 0.1018\times10^{-3}$ m;
$\bar{a}_{1,8} = 0.1004\times10^{-3}$ m.

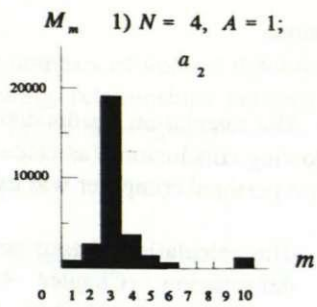

$a_{2\min} = 0.9870\times10^{-4}$ m;
$a_{2\max} = 0.1046\times10^{-3}$ m;
$\bar{a}_{2,3} = 0.1002\times10^{-3}$ m.

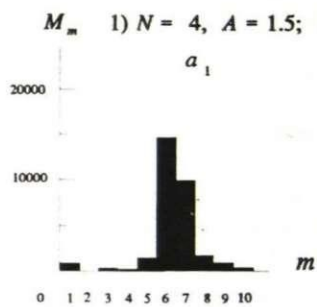

$a_{1\min} = 0.9319\times10^{-4}$ m;
$a_{1\max} = 0.1052\times10^{-3}$ m;
$\bar{a}_{1,6} = 0.9982\times10^{-4}$ m.

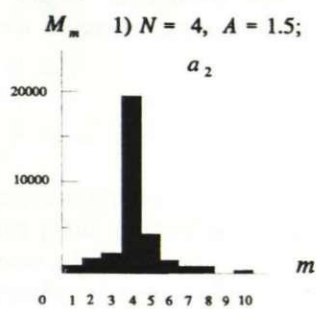

$a_{2\min} = 0.9577\times10^{-4}$ m;
$a_{2\max} = 0.1081\times10^{-3}$ m;
$\bar{a}_{2,4} = 0.1001\times10^{-3}$ m.

Fig.4.3 Histograms of variational series of selections a_{1n} , a_{2n}.

Initial calculation data: $N = 4$, $k = 0.1$, $c = 0.99c_0$ (1% compression), λ_n scheme, $\Delta\theta_E = \Delta\varphi_E = \Delta\psi_E = 10°$, $\Delta a_1 = 10^{-4}\times a_0$.

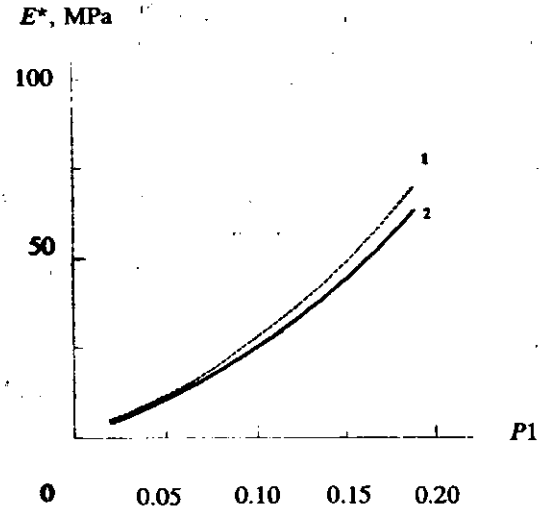

Fig.4.4 Dependence of Young's modulus E^* on the space filling coefficient $P1$, $\Delta\varrho_n$ scheme. Isotropic, rigid PUR plastic foams.

Theoretical results.

1 semiaxes hypothesis assumed, Chapter 3;
2 volume deformation hypothesis assumed.

Initial calculation data: E_0 = 2300MPa, $P1$ = 0.075, N = 4, k = 0.1, A = 1, c = 0.99c_0 (1% compression), $\Delta\varrho_n$ scheme, $\Delta\theta_E = \Delta\varphi_E = \Delta\psi_E$ = 10°, $\Delta a_1 = 10^{-4} \times a_0$.

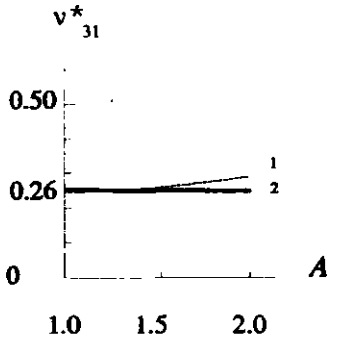

Fig.4.5 Dependence of Poisson's coefficient ν_{31}^* on the extension degree A of model cell, $\Delta\varrho_n$ - scheme.

Theoretical results.

1 - semiaxes hypothesis assumed, Chapter 3;
2 - volume deformation hypothesis assumed.

Initial calculation data: $N = 4$, $k = 0.1$, $c = 0.99c_0$ (1% compression), $\Delta\varrho_n$ - scheme, $\Delta\theta_E = \Delta\varphi_E = \Delta\psi_E = 10°$, $\Delta a_1 = 10^{-4} \times a_0$.

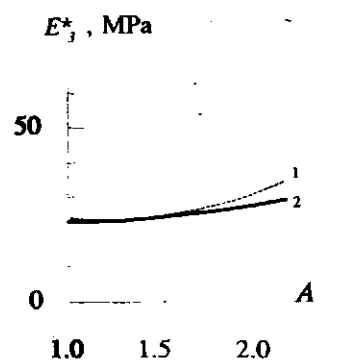

Fig.4.6 Dependence of Young's modulus E_3^* on the extension degree A, $\Delta\varrho_n$ - scheme. Rigid PUR plastic foams.

Theoretical results.

1 - semiaxes hypothesis assumed, Chapter 3;
2 volume deformation hypothesis assumed.

Initial calculation data: $E_0 = 2300$MPa, $P1 = 0.075$, $N = 4$, $k = 0.1$, $c = 0.99c_0$ (1% compression), $\Delta\varrho_n$ - scheme, $\Delta\theta_E = \Delta\varphi_E = \Delta\psi_E = 10°$, $\Delta a_1 = 10^{-4} \times a_0$.

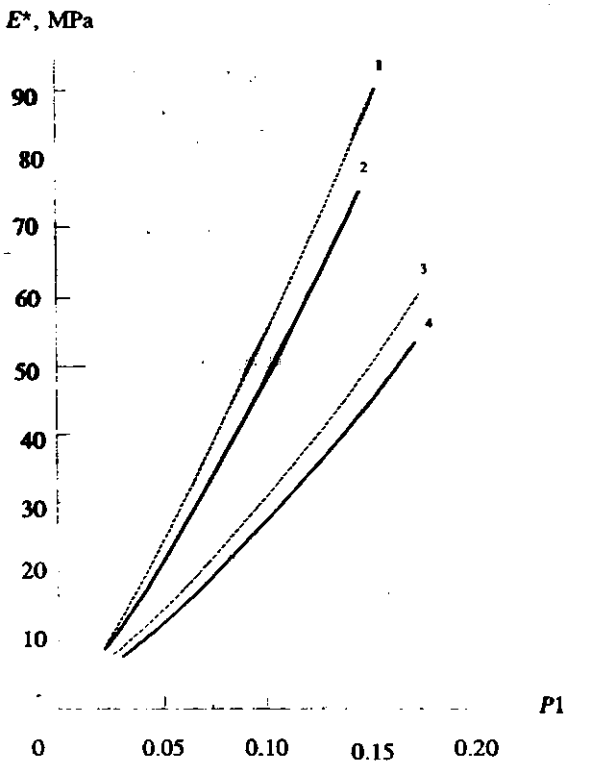

Fig.4.7 Dependence of Young's modulus E^* on the space filling coefficient $P1$, λ_n scheme. Isotropic, rigid PUR plastic foams.

Theoretical results.

1 - k = 0.5, semiaxes hypothesis assumed, Chapter 3;
2 - k = 0.5, volume deformation hypothesis assumed;
3 - k = 0.1, semiaxes hypothesis assumed, Chapter 3;
4 - k = 0.1, volume deformation hypothesis assumed.

Initial calculation data: E_0 = 2300MPa, N = 4, A = 1 , c = 0.99c_0 (1% compression), λ_n - scheme, $\Delta\theta_E = \Delta\varphi_E = \Delta\psi_E$ = 10°, $\Delta a_1 = 10^{-4} \times a_0$.

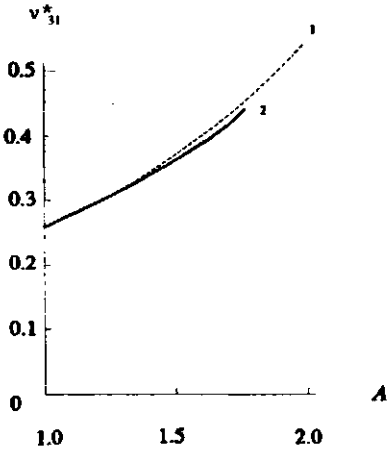

Fig.4.8 Dependence of Poisson's coefficient ν_{31}^* on the extension degree A of model cell, λ_n - scheme.

Theoretical results.

1 - semiaxes hypothesis assumed, Chapter 3;
2 - volume deformation hypothesis assumed.

Initial calculation data: $N = 4$, $k = 0.1$, $c = 0.99c_0$ (1% compression), λ_n scheme, $\Delta\theta_E = \Delta\varphi_E = \Delta\psi_E = 10°$, $\Delta a_1 = 10^{-4} \times a_0$.

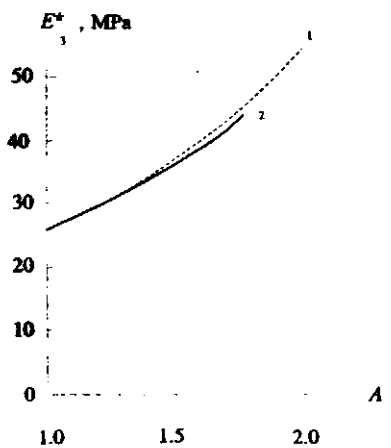

Fig.4.9 Dependence of Young's modulus E_3^* on the extension degree A λ_n scheme. Rigid PUR plastic foams.

Theoretical results.

1 semiaxes hypothesis assumed, Chapter 3;
2 - volume deformation hypothesis assumed.

Initial calculation data: $E_0 = 2300$MPa, $P1 = 0.075$, $N = 4$, $k = 0.1$, $c = 0.99c_0$ (1% compression), λ_n - scheme, $\Delta\theta_E = \Delta\varphi_E = \Delta\psi_E = 10°$,

5 Deformative Properties in Compression/Tension Applied Perpendicular to Rise Direction

5.1 Mathematical Model

5.1.1 Effective Moduli

If the strain ε_{22} is applied perpendicular to the rise direction of a local model cell of monotropic plastic foams [25]:

$$\varepsilon_{22} = \frac{a_2 - a_0}{a_0} = \text{const.}$$

effective Poisson's coefficients ν_{21}^* , ν_{23}^* can be expressed as follows

$$\nu_{21}^* = - <\varepsilon_{11}>/\varepsilon_{22} \qquad \nu_{23}^* = - <\varepsilon_{33}>/\varepsilon_{22}$$

where $<\varepsilon_{11}>$ and $<\varepsilon_{33}>$ are calculated from Eq.(2.9).

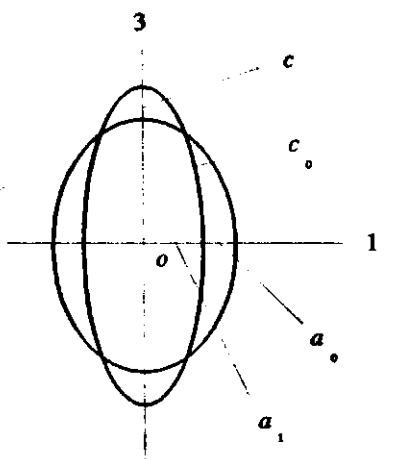

Fig.5.1
Deformation of the model cell in the plane $o13$ perpendicular to the loading direction $o2$.

To calculate the strains ε_{11}, ε_{33} in every microsituation θ_E, φ_E, ψ_E, semiaxes a_1 , c of the model cell after deformation have to be known

$$\varepsilon_{11}(\theta_E,\varphi_E,\psi_E) = \frac{a_1(\theta_E,\varphi_E\psi_E) - a}{a_0} ;$$

$$\varepsilon_{33}(\theta_E,\varphi_E,\psi_E) \qquad \frac{c(\theta_E,\varphi_E\psi_E) - c_0}{c_0} \tag{5.1}$$

Experimental data [32] show that monotropic plastic foams are governed by the following relationship:

$$\nu_{21}^{-} \geq \nu_{23}^{-}$$

Therefore, in various microsituations the semiaxes a_1, c should be allowed to vary not necessarily equally. In Paragraphs 3.1.1 and 4.1.1 it has already been proved that in such a case a tie condition between a_1 and c should be introduced. The condition expressed in the form of (4.2) provides a_1, c the required possibility to vary not necessarily equally, as well as it ensures a compatibility of the mathematical model presented with those described in Chapters 3 and 4.

For this reason the tie condition between a_1 and c has been expressed by the hypothesis of relative volume deformation:

$$\varepsilon(\theta_E,\varphi_E,\psi_E) = \varepsilon^{-} = \text{const.} \qquad \text{then}$$

$$c(\theta_E,\varphi_E,\psi_E) \qquad \frac{a_0^2\, c_0\, (1 + \varepsilon^{-})}{a_2\, a_1(\theta_E,\varphi_E\psi_E)} \tag{5.2}$$

To calculate ν_{21}^{-} ν_{23}^{-} for a wide range of extension degree A of the model cell, experimental data of relationships $\varepsilon^{-} = \varepsilon^{-}(A)$ should be known. Since there are no such data available, the plastic foams to be modelled are divided into several groups:

Group 1. Isotropic plastic foams,

$$A = 1$$

Group 2. Plastic foams with a medium degree of monotropy,

$$1 < A < 3;$$

Group 3. Plastic foams with a high degree of monotropy,

$$A \geq 3.$$

Mathematical models of these plastic foam groups differ with the tie condition between semiaxes a_1 , c and the mode of finding the numerical value of ε^*

Group 1.The numerical values of ε^* calculated in Chapter 3 Eq.(3.6) are used for tie condition (5.2) ;

Group 2.The semiaxes a_1 , c are connected with tie condition (5.2). To calculate the strain ε^* for every extension degree $1 < A < 3$, the data of foam groups 1 and 3 are used. As the values of strain ε^* in points $A = 1$ and $A = 3$ are known (Eqs.(3.6) and (5.5)), the relationship $\varepsilon^* = \varepsilon^*(A)$ is assumed to be linear (Fig.5.2). Then the strain ε^* can be calculated for each $1 < A < 3$

$$\frac{\varepsilon^* - \varepsilon_1^*}{\varepsilon_3^*} \quad \frac{A - 1}{(3 - 1)} \tag{5.3}$$

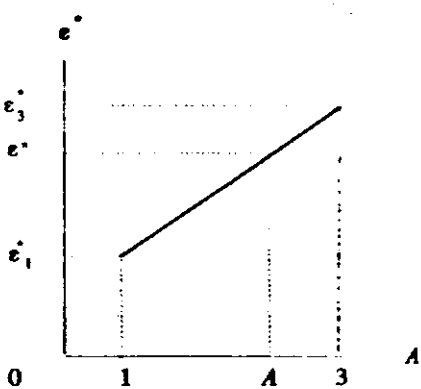

Fig.5.2
Calculation of effective volume strain ε^* in the mathematical model of plastic foams with a medium degree of monotropy.

Group 3. When the plastic foams with a high degree of monotropy are considered, the strut orientation in rise direction $o3$ is assumed to be so pronounced that practically no deformation occurs in this direction (the hypothesis of great monotropy)

$$\varepsilon_{33} = 0 \quad \text{then } c \equiv c_0 = \text{const.} \quad \text{and } \nu_{23}^* = 0 \tag{5.4}$$

Assuming (5.4), there is no need either for the tie condition (5.2) or the previous data of ε^* value, because only one semiaxis remains in the

expression of energy function, i.e., a_1. The effective volume strain ε^* corresponding to the condition (5.4) can be expressed as follows:

$$\varepsilon^* = <\varepsilon_{11}> + \varepsilon_{22} \qquad \varepsilon_{33} = 0 \tag{5.5}$$

It should be mentioned that boundaries of groups 2 and 3 of plastic foams are not strictly defined. The cell extension degree sufficient to realize condition (5.4) can be determined from photos of the plastic foams. When $A \geq 3$, the struts are oriented practically parallel to rise direction [20]. To define the lower boundary of group 3 correctly, it would be necessary to determine the relationship $\nu_{23}^* = \nu_{23}^*(A)$ experimentally.

The semiaxes a_1, c in every microsituation are found, using the variational analysis of the post-deformation form of model cell and the minimization of deformation energy (5.6), (5.7) or (5.8), (5.9). Tie conditions (5.2), (5.4) make it possible to reduce the two-argument minimization of deformation energy to that of one-argument.

5.1.2 Deformation Energy ($\Delta\varrho_a$ - Calculation Scheme)

According to tie conditions (5.2) and (5.4) the post-deformation form of model cell is a three-axial ellipsoid with determined semiaxis a_2. Then $a_1(\theta_E,\varphi_E,\psi_E)$, $c(\theta_E,\varphi_E,\psi_E)$ are the semiaxes to be calculated. Considerations are similar to those in Paragraph 3.1.2. Then deformation energy of a knotless model cell can be expressed as follows:

$$W(a_1,c,\theta_E,\varphi_E,\psi_E) \qquad \frac{E_0 F}{2 a_0 c_0} \sum_{n=1}^{N} \sqrt{f_{n0}} \times$$

$$\times \left[\frac{a_1(\theta_E,\varphi_B\psi_E)\; c(\theta_E,\varphi_B\psi_E) \quad a_2}{\sqrt{f_{n2}}} \qquad \frac{a_0\; c_0}{\sqrt{f_{n0}}} \right]^2 \tag{5.6}$$

where $f_{n0} = a_0^2\cos^2\theta_n' + c_0^2\sin^2\theta_n'$;

$$f_{n2} = [\, a_2\, c(\theta_E,\varphi_E,\psi_E)\sin\theta_n'\cos\varphi_n]^2 +$$

$$+[\, a_1(\theta_E,\varphi_E,\psi_E)\, c(\theta_E,\varphi_E,\psi_E)\sin\theta_n'\sin\varphi_n]^2 +$$

$$+[\, a_2\, a_1(\theta_E,\varphi_E,\psi_E)\cos\theta_n' \,]^2 \qquad n = 1,2,\ldots,N$$

If, however, the model cell of local structure has a knot, then:

$$W(a_1,c,\theta_E,\varphi_E,\psi_E) = \frac{E_0 F}{2} \sum_{n=1}^{N} \frac{(r_n - r_{n0})^2}{r_{n0} - D/2}\,, \qquad (5.7)$$

where $r_{n0} = a_0 c_0 / \sqrt{f_{n0}}$ $\qquad r_n = a_1 a_2 c / \sqrt{f_{2n}}$

Likewise to Paragraph 4.1.2, it can be proved that strains ε_{11} , ε_{33} depend on all the tree Euler's angles θ_E, φ_E,ψ_E. No simplification is possible in calculating average strains and therefore, $<\varepsilon_{11}>$ and $<\varepsilon_{33}>$ are calculated from Eqs.(5.1) and (2.9).

5.1.3 Deformation Energy (λ_n - Calculation Scheme)

Considering similar to Paragraph 3.1.3, the deformation energy of a knotless model cell can be expressed as follows:

$$W(\lambda_1,\lambda_3,\theta_E,\varphi_E,\psi_E) \qquad \frac{E_0 F}{2} \sum_{n=1}^{N} [\lambda_{nT}(\lambda_1,\lambda_3,\theta_E,\varphi_E\psi_E) \qquad 1]^2 \times$$

$$\times\ \varrho_{n0}(\theta_E,\varphi_E)\,; \qquad (5.8)$$

where $\lambda_1(\theta_E,\varphi_E,\psi_E) = a_1(\theta_E,\varphi_E,\psi_E) / a_0$

$\lambda_3(\theta_E,\varphi_E,\psi_E) = c(\theta_E,\varphi_E,\psi_E) / c_0$.

λ_{nT} is calculated from Eq.(3.13) and ϱ_{n0} from Eq.(3.8).

If, however, the model cell of local structure has a knot, then:

$$W(\lambda_1,\lambda_3,\theta_E,\varphi_E,\psi_E) \quad \frac{E_0F}{2}\sum_{n=1}^{N}[\lambda_{nc}(\lambda_1,\lambda_3,\theta_E,\varphi_E\psi_E) - 1]^2 \times$$

$$\times [\, r_{n0}(\theta_E,\varphi_E) - D/2\,], \qquad (5.9)$$

where λ_{nc} is calculated from Eq.(3.16) and r_{n0} from Eq.(3.11).

Average strains $<\varepsilon_{11}>$ and $<\varepsilon_{33}>$ are calculated from Eqs.(5.1) and (2.9).

5.2 Numerical Calculations

Parameters used in the numerical calculations are similar to those described in Paragraph 3.2.1. For a greater versatility of the mathematical model the numerical value of strain ε_{22} has been restricted to: $|\ \varepsilon_{22}\ | \leq 1\%$. The calculations were performed according to the programmes depicted in Figs.3.4 and 5.3. Control calculations showed that numerical integration steps $\Delta\theta_E = \Delta\varphi_E = \Delta\psi_E = 10°$ insured sufficient accuracy of data. Analysis of variational series was carried out for selections of semiaxes a_{1n} c_n $n = 1,2, \ldots, NN$. Variational analysis of the post-deformation form of model cell was carried out with a step $\Delta a_1 = 10^{-4}\times a_0$. Effect of Δa_1 on the calculation data was evaluated

Group 1 and 2 of the plastic foams.

$$|\ \Delta\ \nu_{21}^{*}\ | \quad \leq \quad \left| \frac{\Delta a_1}{\varepsilon_{22} a_0} \right|$$

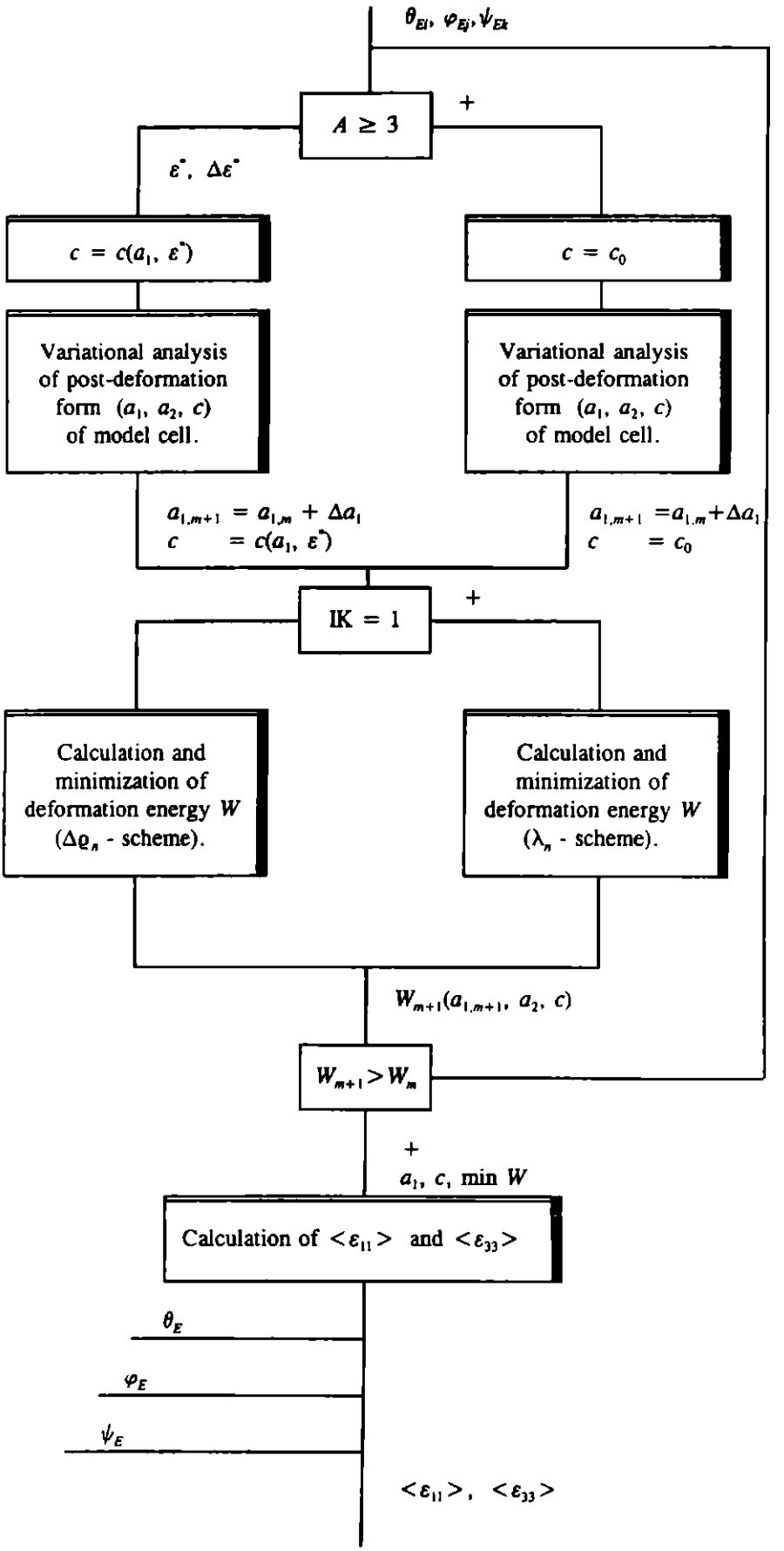

Fig.5.3 Calculation blocks corresponding to strain ε_{22} in the programme "CONSTANTS" (Fig.3.4).

$$|\Delta\nu_{23}^{*}| \leq \left| \frac{a_0^2}{8\pi^2 a_2 \varepsilon_{zz}} \right| \int_0^{2\pi}\int_0^{2\pi}\int_0^{\pi} \left[\left| \frac{\Delta\varepsilon^{*}}{a_1} \right| + \right.$$

$$\left. + \left| \frac{(1+\varepsilon^{*})\Delta a_1}{a_1^2} \right| \right] \sin\theta_E d\theta_E d\varphi_E d\psi_E,$$

where ε^{*}, $\Delta\varepsilon^{*}$ have been calculated in Chapter 3.

Group 3 of the plastic foams.

$$|\Delta\nu_{21}^{*}| \leq \left| \frac{\Delta a_1}{a_0 \varepsilon_{zz}} \right|; \quad |\Delta\nu_{23}^{*}| = 0$$

5.3 Analysis of Results and Conclusions

The calculation results have revealed that in various orientations of the strut system the following relationships exist between the semiaxes a_1 and c when plastic foams of groups 1 and 2 are considered

I. $\varepsilon_{zz} < 0$, compression

1) $a_1 \geq a_0$, $c \geq c_0$;

2) $a_1 > a_0$, $c < c_0$;

3) $a_1 < a_0$, $c > c_0$

II. $\varepsilon_{zz} > 0$, tension

1) $a_1 \leq a_0$, $c \leq c_0$;

2) $a_1 > a_0$, $c < a_0$;

3) $a_1 < a_0$, $c > c_0$.

It means that in several orientations of the strut system compression/tension deformation ε_{22} of model cell causes buckling/ shrinking of the strut system along both semiaxes a_1 , c ; or no deformation occurs at all: I.1) , II.1) Besides there are also such orientations where the shrinking occurs along one semiaxis and the buckling along the other: I.2) , I.3) , II.2) , II.3)

The mathematical model of group 3 of plastic foams provides the following relationships:

$$\text{I. } \varepsilon_{22} < 0 \text{ , compression}$$

$$a_1 > a_0 , \quad c \equiv c_0$$

$$\text{II. } \varepsilon_{22} > 0 , \quad \text{tension}$$

$$a_1 < a_0 , \quad c \equiv c_0$$

It means that in all orientations of the strut system compression/tension deformation ε_{22} of the model cell provides buckling/shrinking along semiaxis a_1 and no deformation along semiaxis c. All other conclusions about effect of the state of strut system on the calculation results are similar to those described in Paragraph 3.3.2.

Histograms of variational series of selections a_{1n} , c_n , $n = 1,2,\ldots, NN$ are depicted in Fig.5.4. As soon as the strains ε_{11} and ε_{33} corresponding to various values of a_1 and c mutually differ by several orders, the averaging of ε_{11} , ε_{33} when $N < 10$ is physically substantial. Elements of selections a_{1n} , c_n are not subjected to a normal distribution AS $\neq$ 0, EX $\neq$ 0.

Conclusions

The following conclusions can be made with regard to the Poisson's coefficients calculated (Fig.5.5):

1. In the case of isotropic plastic foams ($A = 1$) $\Delta\varrho_n$ and λ_n - schemes provide equal values of the Poisson's coefficient ν^*

$$\nu^* = 0.26 \pm 0.01$$

Since the ν^* - value is equal to that calculated for deformation ε_{33}

(Chapters 3 and 4), it can be concluded that the three mathematical models of uniaxial deformations ε_{zz} (one mode) and ε_{33} (two modes) are compatible.

2. In the case of monotropic plastic foams ($A > 1$) the ϱ_n - calculation scheme provides the following result:

$$\nu_{21}^{*} = \nu_{23}^{*}$$

In addition, values of Poisson's coefficients ν_{21}^{*} ν_{23}^{*} decrease when the extension degree A of model cell increases, which contradicts with experimental data. The results calculated according to the λ_n - scheme agree well with the experimental data:

$$\nu_{21}^{*} \geq \nu_{23}^{*} \qquad A \geq 1$$

When A increases, ν_{21}^{*} grows, too, while ν_{23}^{*} decreases.

The Poisson's coefficients ν_{21}^{*} ν_{23}^{*} are independent of such characteristics of plastic foams as E_0, $P1$ and k. ν_{21}^{*}, ν_{23}^{*} do not depend on whether the model cell has or has not a knot.

3. Experimental data [11,32,52] available to the author are depicted in Fig.5.6 for relationship

$$E_3^{*}/E_1^{*} = E_3^{*}/E_2^{*} = f(A)$$

But in conformity with Eq.(2.5) we have

$$E_3^{*}/E_1^{*} = E_3^{*}/E_2^{*} = \nu_{31}^{*}/\nu_{23}^{*}$$

Depicting the theoretical curve

$$\nu_{31}^{*}/\nu_{23}^{*} = f(A)$$

together with the experimental data a good agreement can be observed. Then the mathematical models described in Chapters 3, 4 and 5 characterize the transversal deformations (Poisson's coefficients ν_{31}^{*} ν_{23}^{*}) of monotropic plastic foams adequately

4. The theoretical results of Poisson's coefficients concerned are equal both for tension and compression .

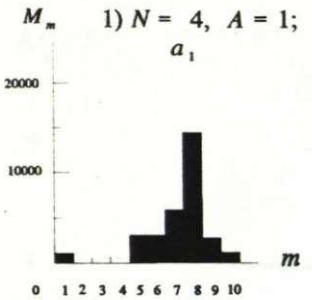

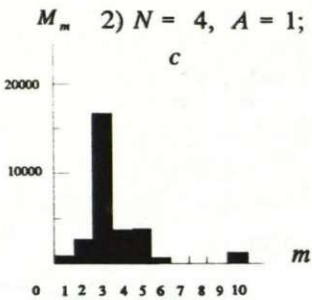

$a_{1min} = 0.9609 \times 10^{-4}$ m;
$a_{1max} = 0.1018 \times 10^{-3}$ m;
$\check{a}_{1,8} = 0.1004 \times 10^{-3}$ m.

$c_{min} = 0.9870 \times 10^{-4}$ m;
$c_{max} = 0.1046 \times 10^{-3}$ m;
$\check{c}_3 = 0.1002 \times 10^{-3}$ m.

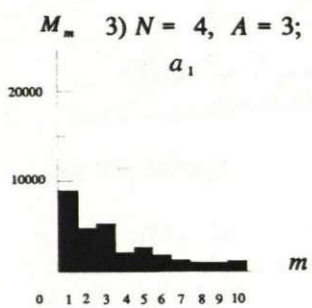

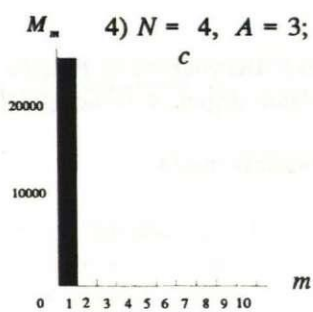

$a_{1min} = 0.1000 \times 10^{-3}$ m;
$a_{1max} = 0.1018 \times 10^{-3}$ m;
$\check{a}_{1,1} = 0.1001 \times 10^{-3}$ m.

$c \equiv c_0 = 3.0 \times 10^{-4}$ m;

Fig.5.4 Histograms of variational series of selection $a1_n$, c_n.

Initial calculation data: $N = 4$, $k = 0.1$, $a_2 = 0.99a_0$ (1% compression), λ_n scheme, $\Delta\theta_E = \Delta\varphi_E = \Delta\psi_E = 10°$, $\Delta a_1 = 10^{-5} \times a_0$.

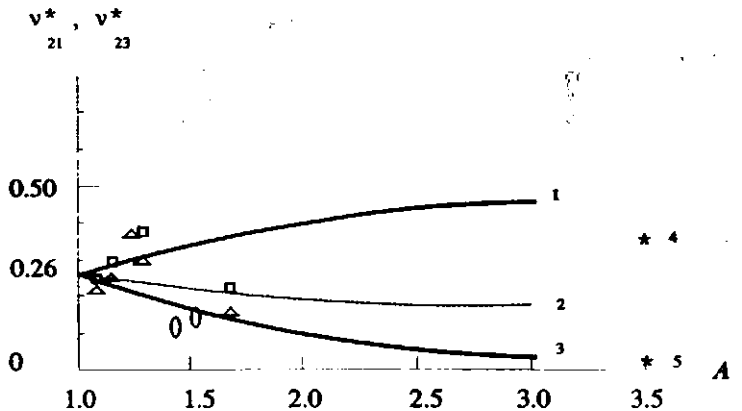

Fig.5.5 Dependence of Poisson's coefficients ν_{21}^*, ν_{23}^* on the extension degree A of model cell. Rigid plastic foams.

Theoretical results:

1 λ_n scheme, ν_{21}^*, $k = 0.1$, $k = 0.5$;
2 $\Delta\varrho_n$ - scheme, ν_{21}^* ν_{23}^*, $k = 0.1$;
3 λ_n - scheme, ν_{23}^* $k = 0.1$, $k = 0.5$.

Hypothesis of great monotropy assumed:
*4 $\Delta\varrho_n$ - scheme, ν_{21}^*, $k = 0.1$;
*5 $\Delta\varrho_n$ - scheme, ν_{23}^*, $k = 0.1$.

Eperimental data:

0 ν_{23}^*, [18];
□,△ ν_{21}^*, ν_{23}^*, tension, Table 3.6, [32,34].

Initial calculation data: $N = 4$, $a_2 = 1.01a_0$ (1% tension), $\Delta\theta_E = \Delta\varphi_E = 10°$, $\Delta a_1 = 10^{-4} \times a_0$.

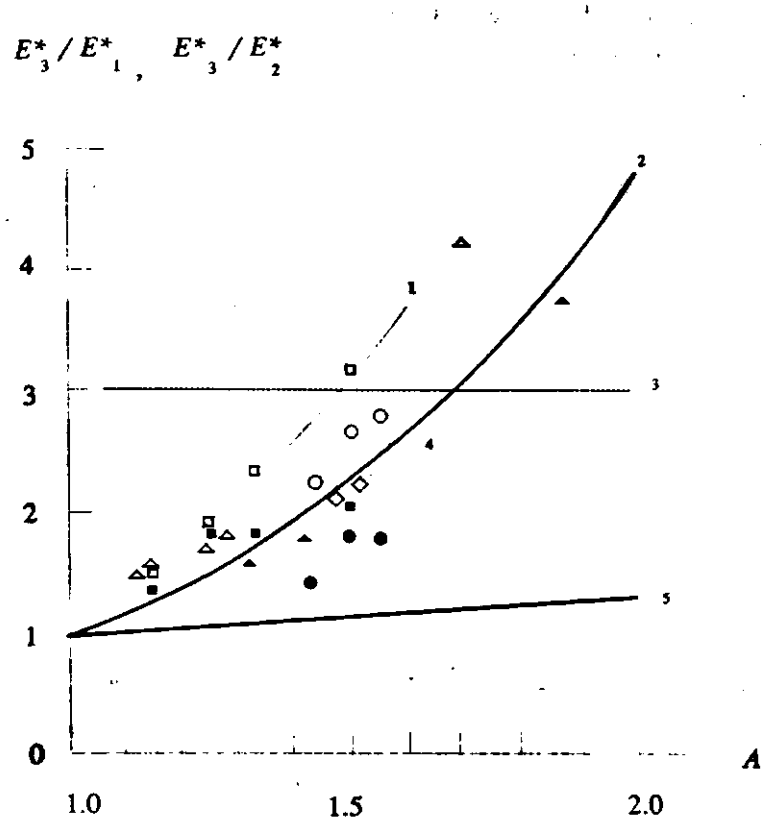

Fig.5.6 Dependence of relations $E_3^*/E_1^* = E_3^*/E_2^* = \nu_{31}^*/\nu_{23}$ on the extension degree A of model cell. Rigid and elastic plastic foams.

Theoretical results:

2 - λ_n scheme;

5 $\Delta\varrho_n$ scheme.

Experimental data:

□,■ tension 1, compression 4, [52];

3 - [8];

○,● - tension,compression, [11];

△,▲ - tension,compression, [32,34];

◇ [18].

Initial calculation data: $P1 = 0.075$, $N = 4$, $a_2 = 0.99a_0$ (1% compression), $k = 0.1$, $\Delta\theta_E = \Delta\varphi_E = 10°$, $\Delta a_1 = 10^{-4} \times a_0$.

6 Shear in the Plane Perpendicular to the Plane of Isotropy

6.1 Mathematical Model

6.1.1 Effective Shear Modulus

If the strain ε_{13} in the plane $o13$ is applied to the local model cell of monotropic plastic foams:

$$\varepsilon_{13} = 1/2\,\gamma\,,$$

effective shear modulus G_{13}^{*} can be expressed as

$$G_{13}^{*} = <\sigma_{13}> / (2\varepsilon_{13})\,,$$

where γ is a shear angle and $<\sigma_{13}>$ is the following

$$<\sigma_{13}> \quad \frac{1}{8\pi^2} \int_0^{2\pi}\int_0^{2\pi}\int_0^{\pi} \sigma_{13}(\theta_E,\varphi_E,\psi_E)\sin\theta_E d\theta_E d\varphi_E d\psi_E \qquad (6.1)$$

Stress $\sigma_{13}(\theta_E,\varphi_E,\psi_E)$ in every microsituation is defined for the local model cell of a continuous medium (Section 2.2). In pure shear ε_{13} the volume does not change, so the volume of model cell before and after deformation is the same:

$$V_{mc} = V'_{mc} = 4/3\pi\, c_0\, a_0^2 = \text{const.}$$

If the shear deformation energy accumulated in the unit volume of a continuous medium is the following [49,51]:

$$w_0 = 1/2\sigma_{ij}\varepsilon_{ij} = 1/2\,(\sigma_{13}\varepsilon_{13} + \sigma_{31}\varepsilon_{31}) = \sigma_{13}\varepsilon_{13}\,, \quad \text{then :}$$

$$\sigma_{13}(\theta_E,\varphi_E,\psi_E) \qquad \frac{W(\theta_E,\varphi_E,\psi_E)}{1/2\,V_{mc}\gamma} \tag{6.2}$$

where $W(\theta_E,\varphi_E,\psi_E)$ is the shear deformation energy accumulated in the whole model cell in every microsituation $\theta_E,\varphi_E,\psi_E$.

$$W(\theta_E,\varphi_E,\psi_E) = w_0 V_{mc} = 4/3\pi c_0 a_0^2 \sigma_{13}\varepsilon_{13}.$$

6.1.2 Deformation Energy (λ_n - Calculation Scheme)

Previously, in calculation of Young's moduli and Poisson's coefficients both deformation energy calculation schemes, $\Delta\varrho_n$ and λ_n, were used. When isotropic plastic foams are considered, the constants calculated are equal in both cases and are in good conformity with experimental data. When monotropic plastic foams are considered, the $\Delta\varrho_n$ - calculation scheme has been found to be inadequate (Table 6.1). The theoretical results obtained by using the $\Delta\varrho_n$ - scheme are in poor conformity with experimental data. Therefore, only λ_n calculation scheme is used for calculation of shear modulus G_{13} and dependent constants in Chapter 7.

A numerical value of the deformation energy in every microsituation may be determined from the local structure model. Then a post-deformation form of the model cell should be known. Deformation of the model cells surface is determined by transformation T_{ij}, Eq.(3.3). For pure shear [38]:

$$\lambda_1 = \lambda_2 = 1 \qquad \lambda_3 = 1/\cos\gamma$$

Then :

$$T_{ij} = \begin{vmatrix} 1 & 0 & tg\gamma \\ 0 & 1 & 0 \\ 0 & 0 & 1 \end{vmatrix}. \tag{6.3}$$

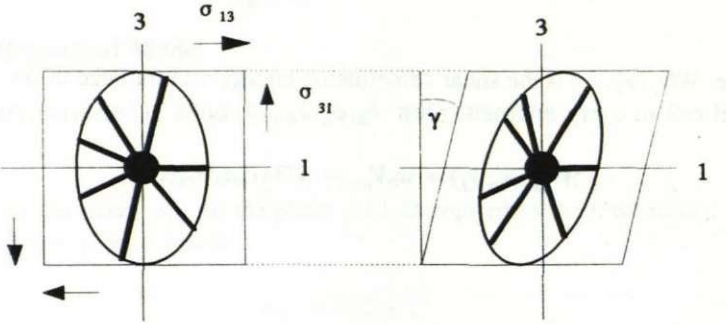

Fig.6.1 Deformation of model cell in the plane $o13$, when the post-deformation form of model cells surface is determined by transformation T_{ij} , Eq.(6.3).

At first, a knotless model cell is considered: $D = 0$. A relative length change λ_{nT} of the n-th strut can be calculated (with neglecting the bending of struts axial line due to deformation) as follows [38]:

$$\lambda_{nT} = \varrho_n/\varrho_{n0} = (T_{mi}\, T_{mj}\, \xi_i\, \xi_j)^{1/2} =$$

$$\left[\sin^2\theta_n' + \left(\frac{\cos\theta_n'}{\cos\gamma} \right)^2 + 2\, tg\gamma\, \cos\varphi_n \sin\theta_n'\, \cos\theta_n' \right]^{1/2}$$

where ξ_i and ξ_j are projections of the unity vector directed along the n-th strut, prior to deformation:

$$\xi_1 = \cos\varphi_n \sin\theta_n' \qquad \xi_2 = \sin\varphi_n \sin\theta_n' \qquad \xi_3 = \cos\theta_n'$$

Due to shear deformation the model cell comprising N struts accumulates energy, which can be found similar to that in Paragraph 3.1.2:

$$W(\theta_E,\varphi_E,\psi_E) = \sum_{n=1}^{N} W_n(\theta_E,\varphi_E,\psi_E);$$

$$W_n(\theta_E,\varphi_E,\psi_E) = \frac{1}{2} E_0 F \frac{[\varrho_n(\theta_E,\varphi_E\psi_E) - \varrho_{n0}(\theta_E,\varphi_E)]^2}{\varrho_{n0}(\theta_E,\varphi_E)} \qquad (6.4)$$

Then energy W in every microsituation is expressed in the following way

$$W(\theta_E,\varphi_E,\psi_E) = \frac{1}{2} E_0 F \sum_{n=1}^{N} [\lambda_{n7}(\theta_E,\varphi_E,\psi_E) - 1] \varrho_{n0}(\theta_E,\varphi_E). \quad (6.5)$$

According to Eq.(6.4), the deformation energy depends on all the three Euler's angles. In the result, no simplification can be made in the calculation expression (6.1) of $<\sigma_{13}>$

When the model cell of local structure with a knot is considered, a relative length change of the n-th strut λ_{n7} can be calculated using the coordinate method, Eq.(3.15), Fig.3.2 (for a greater clearness the *oxyz* frame of reference is considered in Paragraph 6.1.2.). Using Fig.3.2 it can be proved that

$$\begin{cases} x_{n1} & x_{n0}(1 \quad 1/\beta_n) \\ y_{n1} & y_{n0}(1 \quad 1/\beta_n) \\ z_{n1} & z_{n0}(1 + 1/\beta_n) \end{cases}$$

where $\beta_n = D/(2\varrho_{n0})$

Since in pure shear the following relationships can be written for every surface point of the deformed model cell:

$$\begin{cases} x_{n2} = x_{n2}(x_{n1}) \\ y_{n2} = x_{n1} = const. \\ z_{n2} = z_{n1} = const. \end{cases}$$

and $x_{n0}^2 + y_{n0}^2 + z_{n0}^2 = (D/2)^2$, then:

$$\lambda_{nc} \quad \frac{(x_{n2}-x_{n0})^2+y_{n0}^2[(1+1/\beta_n)-1]^2+z_{n0}^2[(1+1/\beta_n)-1]^2}{x_{n0}^2[(1+1/\beta_n)-1]^2+y_{n0}^2[(1+1/\beta_n)-1]^2+z_{n0}^2[(1+1/\beta_n)-1]^2}$$

$$= (2/D)^2 \left[\beta_n^2 (x_{n2} - x_{n0})^2 + y_{n0}^2 + z_{n0}^2 \right]$$

Besides, considering radius vectors r_n and r_{n0}, it can be written that

$$r_n = \lambda_{nT} r_{n0} = (x_{n2}^2 + y_{n2}^2 + z_{n2}^2)^{1/2} \quad \text{where}$$

λ_{nT} is derived from Eq.(3.13) and r_{n0} from Eq.(3.11). Then:

$$x_{n2} = \left[\lambda_{nT}^2 r_{n0}^2 - (y_{n1}^2 + z_{n1}^2) \right]^{1/2}$$

Using Fig.3.2, it can be proved that

$$\begin{cases} x_{n0} = D/2 \cos\varphi_n \sin\theta_n' \\ y_{n0} = D/2 \sin\varphi_n \sin\theta_n' \\ z_{n0} = D/2 \cos\theta_n' \end{cases}$$

After several transformations, we obtain:

$$\lambda_{nc} = \left[1/\varrho_{n0}(x_{n2} - D/2 \cos\varphi_n \sin\theta_n')^2 + \right.$$
$$\left. + \sin^2\varphi_n \sin^2\theta_n' + \cos^2\theta_n' \right]^{1/2}$$

$$x_{n2} = \left[\lambda_{nT}^2 r_{n0}^2 - (\beta_n + 1)^2 (r_{n0} - D/2)^2 \times \right.$$
$$\left. \times (\sin^2\varphi_n \sin^2\theta_n' + \cos^2\theta_n') \right]^{1/2}$$

where $\varrho_{n0} = r_{n0} - D/2$ If there is no knot then:

$$D = 0 \quad \beta_n = 0 \text{ and } \lambda_{nc} \equiv \lambda_{nT}$$

The deformation energy W in every microsituation can be expressed as:

$$W(\theta_E, \varphi_E, \psi_E) \qquad \frac{E_0 F}{2} \sum_{n=1}^{N} (\lambda_{nc} - 1)^2 (r_{n0} \quad D/2) \qquad (6.6)$$

The stress $<\sigma_{13}>$ is calculated using Eqs.(6.1), (6.2), (6.5) or (6.6).

Table 6.1 Agreement of theoretical results of independent constants with experimental data in terms of the deformation energy calculation scheme (monotropic plastic foams).

Material	The deformation energy calculation scheme	Independent constants		Agreement of theoretical results with experimental data
Monotropic plastic foams	$\Delta\rho_n$ - scheme	E_3^*, ν_{31}^*	Semiaxis hypoth. (Chapter 3)	Poor
			Volume deform. hypoth.(Chapter 4)	Poor
		ν_{21}^*, ν_{23}^*	(Chapter 5)	Poor
		G_{13}^*	(Chapter 6)	–
	λ_n - scheme	E_3^*, ν_{31}^*	Semiaxis hypoth. (Chapter 3)	Good
			Volume deform. hypoth.(Chapter 4)	
		ν_{21}^*, ν_{23}^*	(Chapter 5)	
		G_{13}^*	(Chapter 6)	

Calculation schemes' evaluation (poor, good) criterions:

Agreement with experimental results of:

1)Functional dependence **mode** between physical quantities considered,

2)**Order** of calculated numerical values of physical quantities considered.

6.2 Numerical Calculations

The boundary deformations of linear proportionality of isotropic plastic foams determined experimentally in shear are the following [20,52]:

a) rigid PUR plastic foams $\gamma = 0.02$,
b) rigid PVC plastic foams $\gamma = 0.04$,
c) elastic PUR plastic foams $\gamma = 0.10$

Therefore, for the versatility sake of mathematical model the numerical value of deformation ε_{13} applied to the model cell has been restricted:

$$\gamma \leq 0.02 \qquad \varepsilon_{13} = 1/2\,\gamma \leq 0.01$$

Calculations are carried out according to the programmes depicted in Figs.3.4 and 6.2. In conformity with control calculations, numerical integration steps $\Delta\theta_E = \Delta\varphi_E = \Delta\psi_E = 10°$ provide a satisfactorial accuracy of results. Analysis of variational series has been carried out for selection σ_{13n} n 1,2,...,NN of stress σ_{13}. Since no minimization of energy function is made in shear modulus G_{13}^* calculations , errors of results are caused only by the numerical integration.

6.3 Analysis of Results and Conclusions

a) Variational analysis

The histograms of variational series for stress σ_{13} of selection σ_{13n} n 1, 2,... NN are depicted in Fig.6.3. Since in various microsituations stresses σ_{13n} differ mutually by several orders, it can be stated that the averaging (6.1) of stress σ_{13} is physically substantial when $N < 10$ Elements of the selection σ_{13} are not subjected to a normal distribution: AS $\neq 0$, EX $\neq 0$.

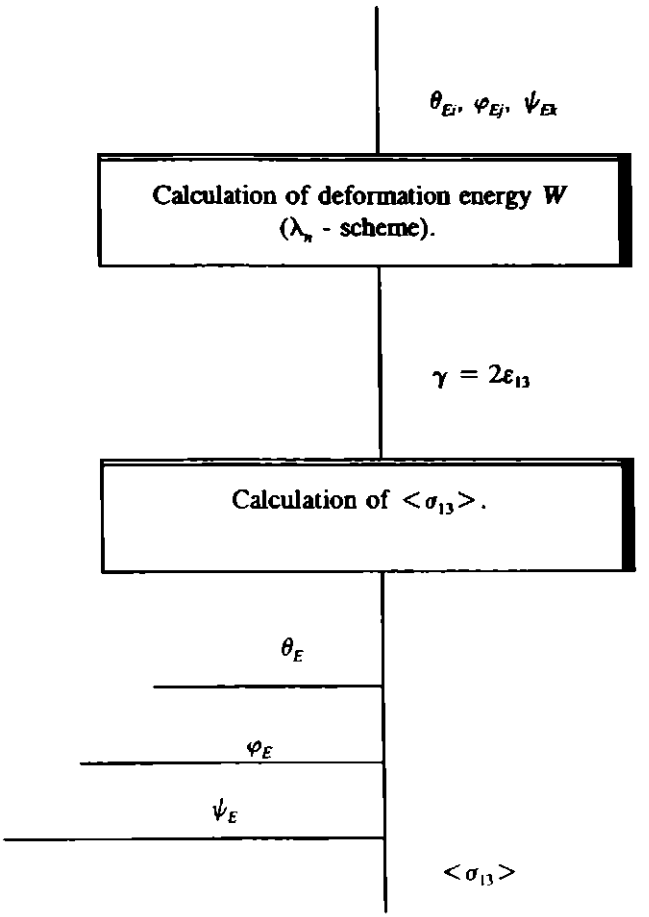

Fig.6.2 Calculation blocks corresponding to deformation ε_{13} in the programme "Constants", Fig.3.4.

b) Elastic Constants, Isotropic Plastic Foams

Shear modulus $G^* = G^*(P1)$ increases, when the space filling coefficient $P1$ grows (Figs.6.4 and 6.5). When PUR foams are considered, the best agreement of theoretical results with experimental data can be observed for the knot parameter $k = 0.1$ There are no experimental data available to the author for shear modulus G^* of PVC plastic foams. A good compatibility (Paragraph 3.1.5) can be observed between mathematical models of uniaxial compression/tension (Chapters 3 and 4) and shear deformation (Chapter 6): the values of modulus G^* calculated according to these models are practically equal (Fig.6.4, curves 1,2 and 4,5).

Dependence of shear modulus G^* on the knot parameter k is depicted in Fig.6.6. The modulus G^* reaches its greatest values when a half of the knot surface is covered with struts: $k = 0.5$. The same theoretical results was obtained in [15]. No experimental data are available to the author for relationship $G^* = G^*(k)$.

c) Elastic Constants, Monotropic Plastic Foams

Relationship $G_{13}^* = G_{13}^*(P1)$ depicted in Figs.6.7 and 6.8 is given together with shear moduli G_{23}^* and G_{12}^* calculated in Chapter 7 Assuming $k = 0.1$; $A = 1.05$ for PUR and $k = 0.5$; $A = 1.50$ for PVC plastic foams a good agreement of theoretical results and experimental data [20,52] can be observed. For both values of degree of monotropy A ($A = 1.05$ and A 1.50) modulus G_{13}^* differs very slightly from modulus G^* of isotropic foams. It can be concluded that

$$G_{12}^* = G_{23}^* \geq G_{12}^* \quad \text{when } A \geq 1$$

Relationship $G_{13}^* = G_{13}^*(A)$ for PUR plastic foams depicted in Fig.6.9 is given together with moduli G_{23}^* and G_{12}^* calculated in Chapter 7 After a slight maximum at A 1.5 G_{13}^* decreases. No experimental data are known to the author for these relationships.

Conclusions

1. Conclusions about the effect of strut systems state on calculation results are similar to those described in Paragraph 3.3.2. No singular orientations are observed in the model cell under shear deformation ε_{13} , because the post-deformation form of model cell is defined uniquely by transformation T_{ij} , Eq.(6.3).

2. Mathematical models of uniaxial compression/tension and shear deformation are mutually compatible.

3. Since the theoretical results concerning the shear moduli G_{13}^{*} agree satisfactorily with available experimental data, it can be concluded that the mathematical model proposed describes the shear deformation ε_{13} adequately.

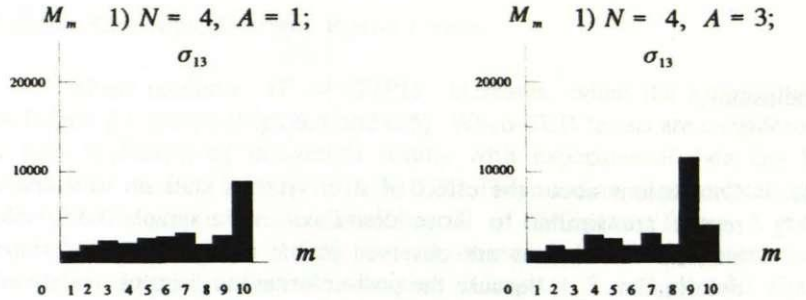

$\acute{I}_{13min} = 8231$ N/m²;
$\sigma_{13max} = 330000$ N/m²;
$\bar{\sigma}_{13,10} = 342242$ N/m².

$\sigma_{13min} = 33000$ N/m²;
$\sigma_{13min} = 240000$ N/m²;
$\bar{\sigma}_{13,9} = 210977$ N/m².

Fig.6.3 Histograms of variational series of selection σ_{13m}.

Initial calculation data: $N = 4$, $k = 0.1$, $\gamma = 0.02$, λ_n - scheme, $\Delta\theta_E = \Delta\varphi_E = \Delta\psi_E = 10°$

Fig.6.4 Dependence of shear modulus G^* on the space filling coefficient $P1$. Isotropic, rigid PUR plastic foams (see the next page for graph).

Theoretical results:

1 $k = 0.5$;
2 - $k = 0.5$, 1.0, semiaxes hypothesis assumed;
3 no knot model cell;
4 - $k = 0.1$;
5 - $k = 0.1$, semiaxes hypothesis assumed.

Experimental data:

● [52].

Initial calculation data: $G_0 = 870$MPA, $N = 4$, $A = 1$, $\gamma = 0.02$, λ_n scheme, $\Delta\theta_E = \Delta\varphi_E = \Delta\psi_E = 10°$.

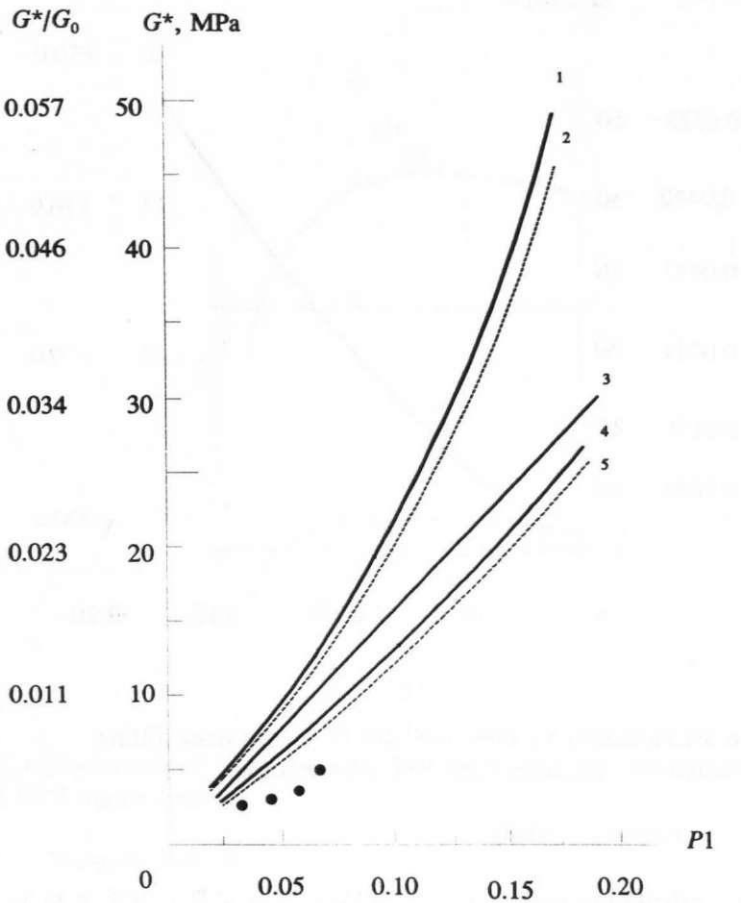

Fig.6.4 Dependence of shear modulus G^* on the space filling coefficient $P1$. Isotropic, rigid PUR plastic foams (see the previous page for initial calculation data).

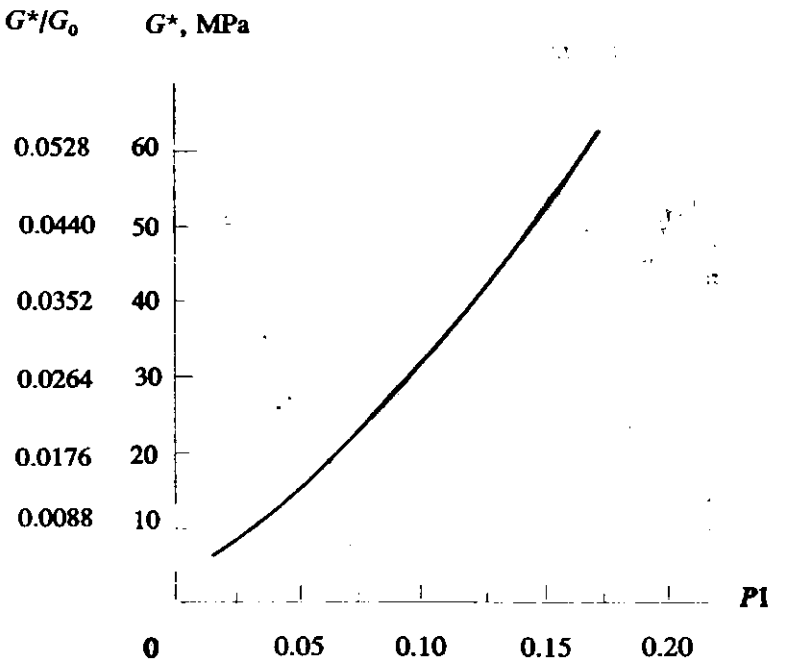

Fig.6.5 Dependence of shear modulus G^* on the space filling coefficient $P1$. Isotropic, rigid PVC plastic foams.

Theoretical results.

Initial calculation data: G_0 = 1136MPa, N = 4, k = 0.5, A = 1, γ = 0.02, λ_n - scheme, $\Delta\theta_E = \Delta\varphi_E = \Delta\psi_E = 10°$.

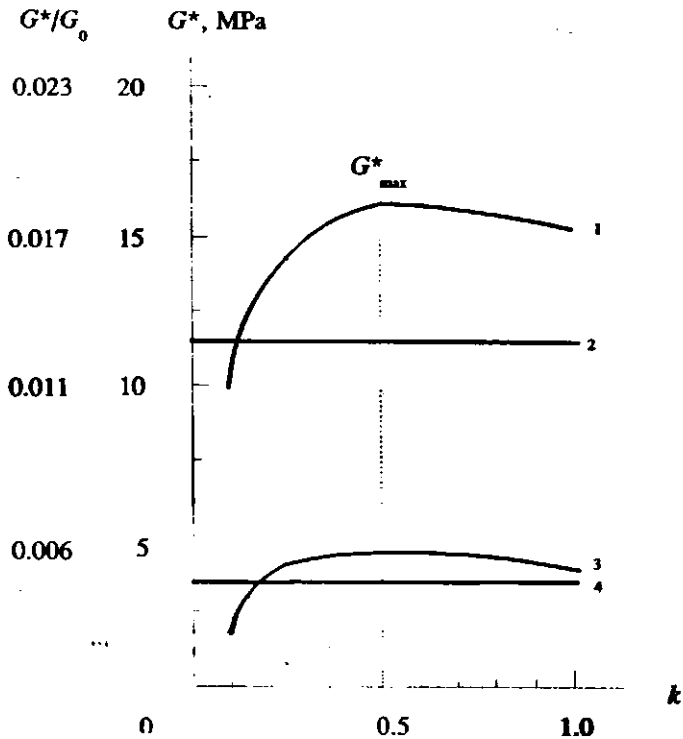

Fig.6.6 Dependence of shear modulus G^* on the knot parameter k Isotropic, rigid PUR plastic foams.

Theoretical results:

1 $P1 = 0.075$;
2 no knot model cell, $P1 = 0.075$;
3 $P1 = 0.025$;
4 no knot model cell, $P1 = 0.025$.

Initial calculation data: $G_0 = 870$MPa, $A = 1$, $N = 4$, $\gamma = 0.02$, λ_n - scheme, $\Delta\theta_E = \Delta\varphi_E = \Delta\psi_E = 10°$.

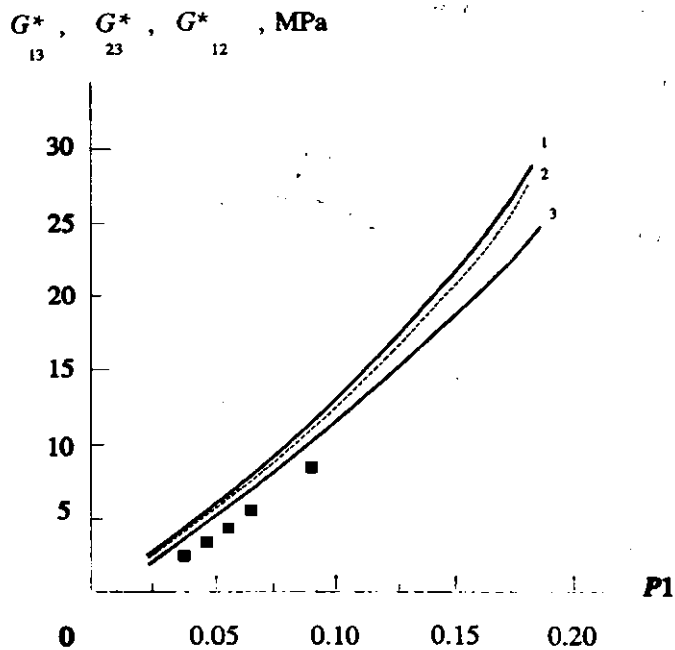

Fig.6.7 Dependence of shear moduli G_{13}^*, G_{23}^* and G_{12}^* on the space filling coefficient $P1$. Monotropic, rigid PUR plastic foams.

Theoretical results:

1 G_{13}^*, G_{23}^*;
2 - G^* (isotropic foams);
3 G_{12}^*

Experimental data:

■ G^* [52].

Initial calculation data: G_0 = 870MPa, N = 4, k = 0.1, A = 1.05, γ = 0.02, λ_n - schemes, $\Delta\theta_E = \Delta\varphi_E = 10°$.

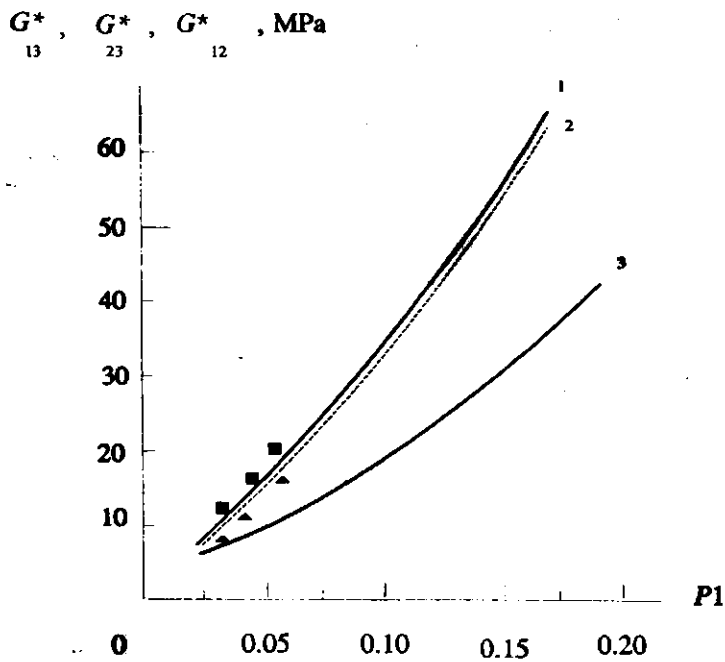

Fig.6.8 Dependence of shear moduli G_{13}^*, G_{23}^* and G_{12}^* on the space filling coefficient $P1$. Monotropic, rigid PVC plastic foams.

Theoretical results:

1 G_{13}^*, G_{23}^*;
2 - G^* (isotropic foams);
3 G_{12}^*

Experimental data:

■, ▲ G_{13}^*, G_{12}^*, [52].

Initial calculation data: G_0 = 1136MPa, N = 4, k = 0.5, A = 1.5, γ = 0.02, λ_n schemes, $\Delta\theta_E = \Delta\varphi_E = 10°$.

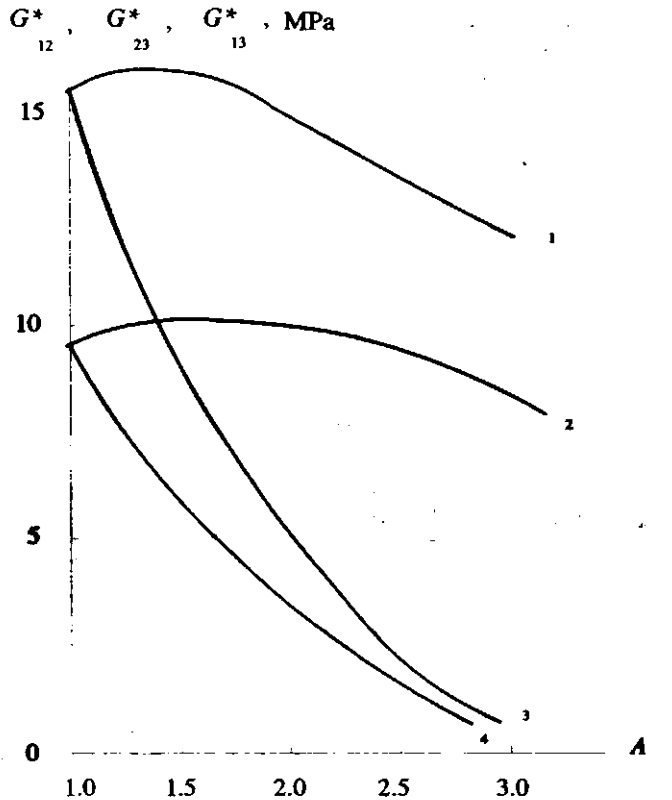

Fig.6.9 Dependence of shear moduli G_{13}^{*}, G_{23}^{*} and G_{12}^{*} on the extension degree A Monotropic, rigid PUR plastic foams.

Theoretical results:

1 G_{13}^{*}, G_{23}^{*}, $k = 1.0$;
2 - G_{13}^{*}, G_{23}^{*}, $k = 0.1$;
3 - G_{12}^{*}, $k = 1.0$;
4 - G_{12}^{*}, $k = 0.1$.

Initial calculation data: $G_0 = 870$ MPa, $P1 = 0.075$, $N = 4$, $\gamma = 0.02$, λ_n - schemes, $\Delta\theta_E = \Delta\varphi_E = \Delta\psi_E = 10°$.

7 Calculation of Dependent Elastic Constants. Analysis of the Results and Conclusions

In Section 2.1 it has been proved that seven dependent effective elastic constants can be derived from Eq.(2.5) using the five independent ones calculated previously:

$$\nu_{12}^{*} = \nu_{21}^{*} \qquad \nu_{13}^{*} = \nu_{23}^{*} \qquad \nu_{32}^{*} = \nu_{31}^{*}$$

$$E_1^{*} = E_2^{*} = \frac{\nu_{23}^{*}}{\nu_{31}^{*}} E_3^{*} \tag{7.1}$$

$$G_{23}^{*} = G_{13}^{*} \qquad G_{12}^{*} = \frac{\nu_{23}^{*}}{2\nu_{31}^{*}(1 + \nu_{21}^{*})} E_3^{*}$$

For derivation of dependent constants (7.1) only those previous theoretical results are used, which have been obtained by the λ_n - scheme. The following conclusions can be made about the dependent constants calculated.

According to conclusions made in Paragraph 3.3.3 about ν_{23}^{*}, ν_{21}^{*} and ν_{31}^{*}, the Poisson's coefficients ν_{32}^{*}, ν_{12}^{*} and ν_{13}^{*} are independent of such model cell characteristics as E_0 and $P1$. Dependence on the strut number N and the knot parameter k is very slight. For all extension degrees A of the modell cell

$$\nu_{32}^{*} \geq \nu_{12}^{*} \geq \nu_{13}^{*}$$

A sufficient agreement between theoretical results and experimental data was observed (Paragraph 3.3.3).

Relationship $E_1^{*} = E_2^{*} = f(P1)$ for PUR and PVC plastic foams depicted in Figs.3.21 and 3.22 is given together with Young's modulus $E_3^{*} = f(P1)$.

$$E_1^{*} = E_2^{*} < E_3^{*} \quad \text{for all } P1 \text{ considered and } A > 1$$

When $P1$ increases, E_1^{*} and E_2^{*} grow, too. The theoretical results agree well with experimental data (Paragraph 3.3.3).

Dependence of E_1^* and E_2^* on the extension degree A of model cell for PUR plastic foams depicted in Fig.3.23 is given together with modulus $E_3^* = E_3^*(A)$ calculated in Chapter 3. When A increases, moduli E_1^* and E_2^* decrease. Direct experimental data of dependence $E_1^* = E_2^* = f(A)$ are not available to the author. However, E_1^* and E_2^* can be calculated from Eq.(7.1) $E_1^* = E_2^* = \nu_{23}^*/\nu_{31}^* E_3^*$ Therefore the comparison with experimental data is made separately for modulus $E_3^* = f(A)$ (Paragraph 3.3.3) and relation $\nu_{23}^*/\nu_{31}^* = f(A)$ (Section 5.3). In both cases the agreement has been proved to be well. Therefore, E_1^* and E_2^* should be in a good agreement, too.

Dependence of G_{23}^* and G_{12}^* on the space filling coefficient $P1$ of model cell for PUR and PVC plastic foams depicted in Figs.6.7 and 6.8 is presented together with modulus G_{13}^* calculated in Chapter 6. When $P1$ increases, G_{23}^* and G_{12}^* grow, too. A sufficient agreement was observed between theoretical results and experimental data for PVC plastic foams. Only the experimental data characterizing the isotropic materials shear modulus are known to the author, when PUR plastic foams are considered. It can be seen that the theoretical results of slightly anisotropic ($A = 1.05$) PUR plastic foams are almost equal with the experimental data for isotropic PUR plastic foams.

Relationship G_{23}^* , $G_{12}^* = f(A)$ for PUR plastic foams depicted in Fig.6.9 is given in Chapter 6 together with shear modulus G_{13}^* When the extension degree A of model cell increases, G_{23}^* enlarges and G_{12}^* decreases. It can be concluded that:

$$G_{23}^* = G_{13}^* \geq G_{12}^* \quad \text{for all } A \geq 1.$$

No experimental data are available to the author for this relationship.

Conclusions

Since the theoretical results concerning the dependent elastic constants agree well with available experimental data, it can be concluded that the mathematical model proposed describes the seven dependent constants (7.1) adequately.

8 Main Conclusions

I A mathematical model of deformative properties and structure of light-weight, monotropic (or isotropic in the boundary case) plastic foams with a pronounced strut-like structure has been elaborated in the linear deformation theory. All the twelve elastic constants have been determined when treating monotropic plastic foams in the axes of elastic symmetry. To achieve integral characterization of the deformative properties of plastic foams as micro-nonhomogeneous composite materials, the elastic constants have been introduced as effective ones.

II In order to describe the plastic foams structure a local model consisting of two parts has been proposed, i.e., a model of continuous medium for calculation of stresses and a local structure model. Both models are chosen shaped as rotational ellipsoids. When calculating stresses due to the lack of a precise solution for an ellipsoid the possibility to replace the latter by a cylinder has been shown. As the result of minimization of the aim function composed in a definite way, configurations of spatially uniformly distributed N struts have been found. Assuming that the nonuniform distribution of struts in monotropic plastic foams develops gradually from the uniform distribution, the way of introducing monotropy into the model cell has been proposed.

III Using methods of orientative averaging the possibility to avoid artificial regularization of plastic foams structure has been shown. Accordingly, turning the uniform struts configurations as one whole throughout all the spatial orientations defined by three Euler's angles, a cluster or an ensemble of plastic foams structure microsituations has been found. Thus, the infinitely numerous spatial orientations of struts as well as the essential polydispersity of plastic foams structure have been taken into account. In order to calculate the effective elastic constants connecting average stresses and strains the ergodic hypothesis has been assumed to take place. Hence, the possibility to replace the hard-to-realize averaging throughout the volume by an averaging throughout a set of one-type situations has been shown.

IV Basing on capabilities to elaborate the corresponding calculation models, the selection of five independent constants has been described. The usage of variational analysis of model cells post-deformation form and the

minimization of deformation potential energy as a criterion for determination of this form have been verified in mathematical models of uniaxial compression/tension. The necessity to connect the semiaxes to be calculated by some tie condition has been stated during numerical control calculations. Thus the mutual interaction of neighboring model cells has been taken into account. The tie condition has been proposed in two formulations. Similarly, the insufficiency of considering only the axial deformation of struts even in the region of small deformations has been shown with the help of control calculations. It is necessary to evaluate also the reorientation of struts during deformation. The mutual compatibility of mathematical models of uniaxial compression/tension has been proved by analysis of numerical results. The theoretical results of Young's modulus and Poisson's coefficients concerned are found to be equal both for tension and compression.

V Subjecting surface points of the model cell to a definite spatial transformation the possibility of adequate modelling of the plastic foams shear deformation has been proved. Control calculations have shown the independence of the shear modulus sought on the struts reorientation in the process of deformation. The mutual compatibility (realization of the isotropy relationship) of the mathematical models of shear and uniaxial deformation has been proved by comparing the numerical results.

VI In order to perform numerical calculations a complex of programmes has been developed.The numerical values of five + seven = twelve elastic constants have been determined using the Simpson's method for calculation of the triple integral and step-type unconditional minimization of one-argument function. The parameters of numerical calculation process providing the acceptable accuracy of results have been evaluated. The necessity to perform an orientative averaging to obtain the desired quantities has been verified with the help of variational series analysis.

VII The dependence of calculated elastic constants on the main characteristics of plastic foams structure (the space filling coefficient, the degree of anisotropy, the number of struts, the knot parameter) has been investigated. A satisfactorial agreement has been found to exist between the theoretical results and the experimental data of plastic foams of various rigidity. Hence, the mathematical model proposed can be used to project plastic foams with a preassigned set of properties.

List of References

1. Brāzma N., Brigmane A., Krastiņš A., Rāts J. Augstākā matemātika. 2.izd. "Zvaigzne", R., 1970., 544 lpp.

2. Gruziņš I. Putuplasti un to izmantošana. LPSR Zin.biedr., R., 1985, 42 lpp.

3. Ashby M.F. *The Mechanical Properties of Cellular Solids.* Metallurgical Transactions A. 1983, V.14^A, September, p.1755-1769.

4. Baxter S. and Jones T.T. *The Physical Properties of Foamed Plastics and Their Dependence on Structure.* Plast. and Polymer. 1972, April, p.69-76.

5. Beverte I.V *Deformative Properties of Monotropic Plastic Foams with a Pronounced Strut-Like Structure.* A report on the 9-th Intern.Conf. on Mech. of Comp.Mat. Oct. 17-20, 1995, Riga, Latvia.

6. Beverte I.V and Krēgers A.F. *Young's Modulus of Monotropic Foam Plastics Subjected to Deformation Parallel to Rise Direction.* Mechanics of Composite Materials. 1993, V.29, N°1, p.19-26.

7 Chan R. and Nakamura M. *Mechanical Properties of Plastic Foams.* J.Cell.Plast. 1969, March/April, p.112-118.

8. Cunningham A. *Modulus Anisotropy of Low-Density Cellular Plastics: an Aggregate Model.* Polymer. 1981, V.22, July, p.882-885.

9. Gent A.N. and Thomas A.G. *The Deformation of Foamed Elastic Materials.* J.Appl.Polym.Sci. 1959, V.1, N°1, p.107-113.

10. Gent A.N. and Thomas A.G. *Mechanics of Foamed Elastic Materials.* Rubber Chem.Techn. 1963, V.36, N°3, p.597-610.

11. Kanakkanatt S.V. *Mechanical Anisotropy of Open-Cell Foams.* J.Cell.Plast. 1973, Jan./Febr., p.50-53.

12. Ko W.L. *Deformations of Foamed Elastomers.* J.Cell.Plast. 1965, January, p.45-50.

13. Handbook of Polymeric Foams and Foam Technology. Ed. by Klempner D. and Frisch K.C. Munich; Vienna; New York; Barcelona: Hanser Publ., 1991, 442p.

14. Kurek K. and Bledzki A. *Mechanical Behaviour of Polyurethane - and Epoxy Foams and Their Glass Fibre Composites.* Mechanics of Composite Materials. 1994, V.30, N°2, p.155-161.

15. Lederman J.M. *The Prediction of the Tensile Properties of Flexible Foams.* J.Appl.Polym.Sci. 1971, V.15, N°3, p.693-703.

16. Menges G. and Knipschild F. *Estimation of Mechanical Properties for Rigid Polyurethane Foams.* Polym.Eng. and Sci. 1975, V.15, N°8, p.623-627.

17. Phillips P.J. and Waterman N.R. *The Mechanical Properties of High-Density Rigid Polyurethane Foams in Compression: I.Modulus.* Polym.Eng. and Sci. 1974, V.14, N°1, p.67-70.

18. Rinde J.A. *Poisson's Ratio for Rigid Plastic Foams.* J.Appl.Polym.Sci. 1970, V.14, p.1913-1926.

19. Rusch K.C. *Load Compression Behavior of Brittle Foams.* J.Appl.Polym.Sci. 1970, V.14, N°5, p.1263-1276.

20. Renz R. *Zum zügigen und zyklischen Verformungs - verhalten Polymerer Hartschaumstoffe.* Dissertation zur Erlangung des akad. Grades eines Doktor-Ingenieurs. Karlsruhe, 1977, 139S.

21. Беверте И.В. *Теоретическое исследование деформационных свойств легких пенопластов.* Тез. докл. XII конф. молод. уч. и спец. Прибалт. и Белорус. по пробл. строй. матер. и констр. 31 янв.-2 февр. 1984 г. - Рига, с.102-103.

22. Беверте И.В. *Структурный подход в определении деформативных свойств легких открытопористых пенопластов.* Тез. докл. XIII обл. науч.-техн. конф. молод. уч. и спец. 27-28 марта 1984 г. - Гомель, с.18.

23. Беверте И.В., Крегерс А.Ф. *Жесткость легких открытопористых пенопластов.* Механика композит. материалов. 1987, N°1, с.30-37.

24. Беверте И.В. *Коэффициент Пуассона легких трансверсально-изотропных пенопластов.* Механика композит. материалов. 1989, N°6, с.980-986.

25. Беверте И.В. *Коэффициенты Пуассона легких трансверсально изотропных пенопластов при деформировании перпендикулярно направлению вспенивания.* Механика композит.материалов. 1991, N°4, с.703-711.

26. Берлин А.А., Шутов Ф.А. Химия и технология газонаполненных высокополимеров. М., 1980, 504с.

27 Валуйских В.П., Маврина С.А., Прокофьев В.Ю. *Имитационные модели конструкционных пенопластов открытой полиэдрической структуры.* Механика композит. материалов. 1987, N°5, с.808-812.

28. Валуйских В.П., Есипов Ю.Л. *Исследование физико-механических характеристик жестких пенополиуретанов.* Механика композит. материалов. 1989, N°3, с.414-418.

29. Валуйских В.П. *Статистические методы и задачи оптимального проектирования конструкций.* Автореферат диссертации на соиск. уч.ст. докт.техн.наук. М., 1990, 41с.

30. Вольмир А.С. Устойчивость деформируемых систем. М., 1967, 984с.

31. Дементьев А.Г. *Исследование влияния ячеистой структуры на механический свойства и стабильность пенопластов.* Автореферат диссертации на соиск. уч. ст. канд.наук. М., 1971, 22с.

32. Дементьев А.Г., Селивестров П.И., Тараканов О.Г. *Коэффициент Пуассона пенопластов.* Механика полимеров. 1973, N°1, 45-49с.

33. Дементьев А.Г., Тараканов О.Г. *Влияние ячеистой структуры пены на механические свойства пенопластов.* Механика полимеров. 1970, N°4, 594-602с.

34. Дементьев А.Г. Тараканов О.Г. *Моделирование и расчет ячеистой структуры пенопластов типа пенополиуретана.* Механика полимеров. 1970, N°5, 859-865с.

35. Дементьев А.Г. Тараканов О.Г. *Растяжение пенопластов.* Механика полимеров. 1971, N°4, 670-675с.

36. Дементьев А.Г., Тараканов О.Г. Структура и свойства пенопластов. М., 1983, 176с.

37. Дементьев А.Г., Тараканов О.Г. *Пенопласты с взаимопроникающими ячеистыми структурами.* Механика композит. материалов. 1985, N°2, 360-362с.

38. Зилауц А.Ф., Лагздинь А.Ж. *Одностержневая модель ячеистых сред при больших упругих деформациях.* Механика композит.материалов. 1992, N°1, 3-10с.

39. Кильчевский Н.А. Курс теоретической механики. т.1, изд.2-е, М., 1977, 480с.

40. Корн Г., Корн Т. Справочник по математике для научных работников и инженеров. М., 1974, 832с.

41. Крегерс А.Ф., Беверте И.В. *Оценка деформативности легких открытопористых пенопластов.* Тез.докл. XV обл. науч.-техн. конф. молод. уч. и спец. 8-9 апр.1986 г.- Гомель, с.21.

42. Крегерс А.Ф., Беверте И.В.*Оценка деформативности легких открытопористых пенопластов.* Тез.докл. VI всесоюзн. конф. по мех. полим. и комп. мат. 18-20 ноября 1986 г.- Рига , с.77-78.

43. Лагздыньш А.Ж., Тамуж В.П. *Тензоры упругости высших порядков.* Механика полимеров. 1965, N°6, 40-48с.

44. Лагздинь А.Ж., Тамуж В.П., Тетерс Г.А., Крегерс А.Ф. Метод ориентационного усреднения в механике полимеров. Р., 1989, 190с.

45. Лехницкий С.Г Теория упругости анизотропного тела. Изд.2-е, М., 1977, 415с.

46. Лурье А.И. Пространственные задачи теории упругости. М., 1955, 491с.

47. Маврина С.А. Математическое моделирование прочности пенопластов как пространственных стержневых систем. Автореферат диссертации на соиск.уч.степ. канд.техн.наук. Воронеж, 1991, 15с.

48. Мак-Кракен Д., Дорн У. Численные методы и программирование на Фортране. Изд. 2-е, М., 1977, 584с.

49. Малмейстер А.К., Тамуж В.П., Тетерс Г.А. Сопротивление полимерных и комп. материалов. Изд. 3-е, Р., 1980, 572с.

50. Романенков И.Г. *Оценка рассеяния физико - механических характеристик пенопластов.* Пластические массы. 1967, N°3, 69-71с.

51. Степин П.А. Сопротивление материалов. Изд. 6-е М., 1979, 312с.

52. Прикладная механика ячеистых пластмасс. Под.ред. Хильярда Н.К. М., 1985, 360с.

53. Цируле К.И., Путниньш Э.А. *Оценка газопроницаемости и ее связь с макроструктурой жесткого пенополиуретана.* Механика композит. материалов. 1988, N°5, 932-934с.

54. Шермергор Т.Д. Теория упругости микронеоднородных сред. М., 1977, 400с.